

# **Università della Calabria**

---

---

**Dottorato di Ricerca in  
“Metodologie per lo sviluppo di molecole di  
interesse farmacologico” XIX Ciclo**

***SYNTHESIS AND BIOLOGICAL EVALUATION OF  
POLYHETEROCYCLIC DERIVATIVES ENDOWED  
WITH ANTIVIRAL OR ANTICANCER ACTIVITY***

**COORDINATORE  
Prof. Giovanni Sindona**

**SUPERVISORE  
Prof. Antonio Garofalo**

**DOTTORANDA  
Dr Fedora Grande**

---

**Anno Accademico 2005-2006**

# CONTENTS

<b>PREFACE</b>	<b>1</b>
<b>INTRODUCTION</b>	<b>2</b>
<b>PART 1 - ANTIRETROVIRAL DRUGS</b>	<b>3</b>
<b>INTRODUCTION</b>	<b>4</b>
<b>CHAPTER 1 - HUMAN IMMUNODEFICIENCY VIRUS (HIV): PHYSICAL STRUCTURE, GENOME AND REPLICATION CYCLE</b>	<b>6</b>
1.1 HUMAN IMMUNODEFICIENCY VIRUS (HIV)	7
1.2 HIV PHYSICAL STRUCTURE AND GENOME	8
1.3 HIV GENOME ORGANIZATION	9
1.4 HIV REPLICATION CYCLE	10
<b>CHAPTER 2 - HIV-1 INTEGRASE: STRUCTURAL FEATURES, BIOLOGICAL ACTIVITY AND FIRST GENERATION INHIBITORS</b>	<b>15</b>
2.1 HIV-1 INTEGRASE	16
2.2 INTEGRASE STRUCTURAL FEATURES	16
2.3 BIOCHEMICAL MECHANISM OF INTEGRATION	20
2.4 HIV-INTEGRASE INHIBITORS	23
<b>CHAPTER 3 - SYNTHESIS AND BIOLOGICAL EVALUATION OF NOVEL HIV-1 INTEGRASE INHIBITORS</b>	<b>30</b>
3.1 PRELIMINARY STUDIES	31
3.2 SYNTHESIS OF NOVEL HIV-1 INTEGRASE INHIBITORS	35
3.3 CHEMISTRY	37
3.4 PHARMACOLOGICAL STUDIES	42

3.5 INTEGRASE ASSAYS	48
3.6 CONCLUSIONS	49
<b>PART 2 - ANTICANCER DRUGS</b>	<b>50</b>
<b>INTRODUCTION</b>	<b>51</b>
<b>CHAPTER 4 - ANTICANCER DRUGS AND NOVEL TRIALS IN DEVELOPMENT OF NEW COMPOUNDS</b>	<b>52</b>
4.1 ANTICANCER DRUGS	53
4.2 NOVEL TRIALS IN DESIGN AND DEVELOPMENT OF NEW ANTICANCER DRUGS	57
<b>CHAPTER 5 - SYNTHESIS AND BIOLOGICAL EVALUATION OF NOVEL ANTICANCER COMPOUNDS</b>	<b>60</b>
5.1 PRELIMINARY STUDIES	61
5.2 CHEMISTRY	64
5.3 PHARMACOLOGICAL STUDIES	69
5.3a Cytotoxicity assays	69
5.3b Flow cytometry studies	74
5.3c Preliminary <i>In Vivo</i> Studies	76
5.4 CONCLUSION	78
<b>GENERAL EXPERIMENTAL CHEMISTRY</b>	<b>79</b>
<b>GENERAL EXPERIMENTAL BIOLOGY</b>	<b>102</b>
<b>REFERENCES</b>	<b>108</b>

## **PREFACE**

One major hurdle to overcome in a drug discovery program is the identification of a suitable lead compound having the desired biological activity. Despite the remarkable progress made during the past decade in almost all the areas concerning with drug design and discovery, there is still a clear need to develop new effective drugs for the treatment of serious diseases such as cancer and AIDS.

The overall goals of the herein reported research work have been the design, synthesis and biological evaluation of small molecules endowed with pharmacologic activity. The project has resulted in the synergy of synthetic chemistry, computational chemistry and molecular biology. Thus, the first two years of the doctorate course has focused on the development of simple and innovative methods for the synthesis of heterocyclic derivatives, potentially active as antiretroviral and anticancer agents. The related experimental work was carried out to the Dipartimento di Scienze Farmaceutiche, Universita' della Calabria. The third final year of the doctorate has aimed to the evaluation of the biological properties of the previously synthesized compounds and was spent to the University of Southern California, Los Angeles, USA.

Following the results of earlier studies, different series of small molecules have been synthesized and some of them have been selected as potential lead compounds to be included in the anti-AIDS and anticancer programs of our research group.

## **INTRODUCTION**

Collaborative, multidisciplinary research has resulted in new approaches to design pharmaceutical agents with higher potency and fewer side effects.

Although remarkable progress have been made in the analytical techniques of biology, chemistry and pharmacology during the past 10 years, there is still need of effective therapeutic for the treatment of serious diseases, for which there are no useful therapies available. Two notable examples are cancer and AIDS.

Treating HIV infection or cancer has the same disadvantage due to the similarity of healthy cells with virus infected or cancer cells. Thus, drugs that can inhibit cellular protein or DNA macromolecules could also damage normal cells.

Consequently, there is a significant need to develop novel agents selectively targeting specific enzymes or cell cycle processes in unhealthy cells.

## **PART 1**

# **ANTIRETROVIRAL DRUGS**

## INTRODUCTION

Human immunodeficiency virus (HIV) causes Acquired Immunodeficiency Syndrome (AIDS), a condition in which the immune system begins to fail, leading to life-threatening opportunistic infections [1].

In the approximately 25 years since AIDS emerged, it is estimated that more than 65 million people worldwide have been infected with HIV and 25 million have already died [2].

In 2005 AIDS claimed an estimated 2.4-3.3 million lives, of which more than 570,000 were children (**Figure 1**). A third of these deaths are occurred in sub-Saharan Africa retarding economic growth and increasing poverty [3].

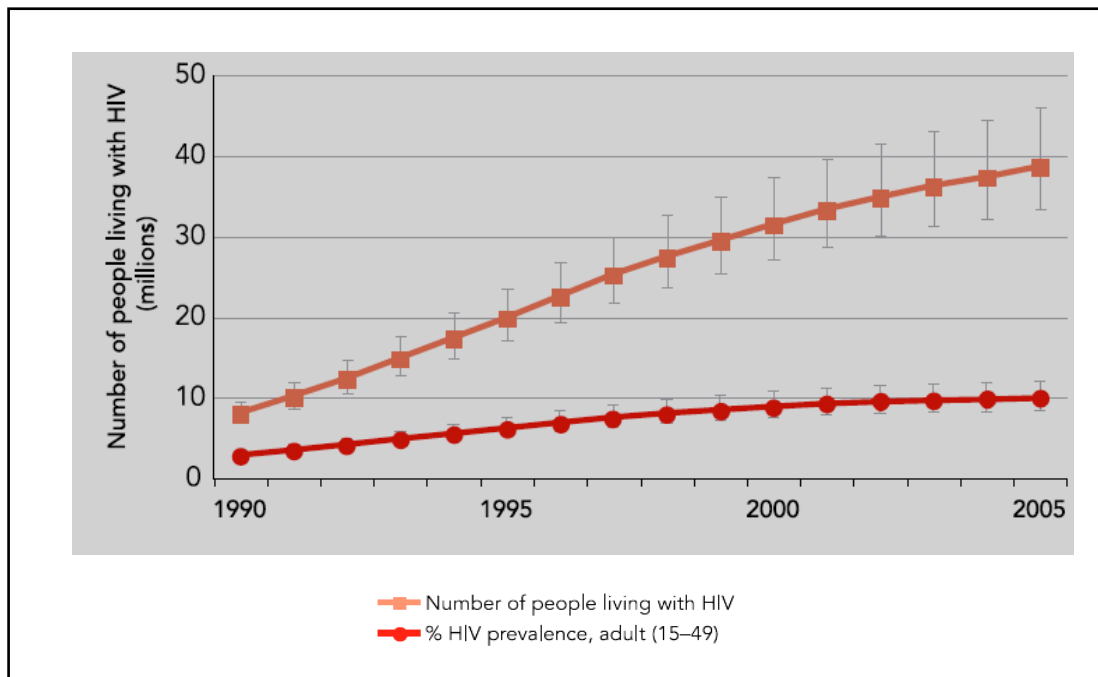


**Fig. 1** Diagram of HIV epidemic from 1990 to the end of 2005

The available antiretroviral treatment reduces both the mortality and the morbidity of HIV infection, but cannot completely exacerbate the virus infection. At present several anti-HIV

drugs have been developed and the majority of them targets two viral enzymes: reverse transcriptase and protease. The treatment with a combination of three or more protease and reverse transcriptase inhibitors, known as HAART (Highly Active Antiretroviral Therapy), has promoted a significant decrease of viral replication in HIV-infected individuals. Although the success of this approach, the virus remains in a quiescent form in infected cells and could not be completely eradicated [4].

Moreover HAART is limited by cumulative toxicity of drugs due to the long-term treatment and the rapid emergence of drug resistant HIV-1 strains [5]. Consequently, there has been considerable interest in the development of novel agents targeting different steps of viral replication cycle. Integration of viral genome into host cell chromosomal DNA is an essential step in the viral life cycle and is mediated by the virally encoded enzyme, integrase (IN).

Inhibition of this process provides an attractive strategy for antiretroviral drug design because the reactions catalyzed by IN are unique. Moreover, there are no functionally equivalent enzymes existing within human cell, which drastically reduces the potential for drug cytotoxicity issues [6].





## **CHAPTER 1**

***HUMAN IMMUNODEFICIENCY VIRUS (HIV):  
PHYSICAL STRUCTURE, GENOME  
AND REPLICATION CYCLE***

## 1.1 HUMAN IMMUNODEFICIENCY VIRUS (HIV)

Human immunodeficiency virus (**Figure 2**) is a retrovirus whose genetic content consists into two single-strands of positive RNA. Infection with HIV occurs by the transfer of blood, semen, vaginal fluid and breast milk. Within these body fluids HIV is present as both free virus particles and virus within infected immune cells. HIV primarily infects vital cells in the human immune system such as helper T cells (specifically CD4<sup>+</sup> T cells), macrophages and dendritic cells. HIV infection leads to low levels of CD4<sup>+</sup> T cells through three main mechanisms: direct viral killing of infected cells, increasing rates of apoptosis in infected cells, or killing of infected CD4<sup>+</sup> T cells by CD8 cytotoxic lymphocytes that recognize infected cells. When CD4<sup>+</sup> T cell numbers decline below a critical level, cell-mediated immunity is lost, and the body becomes progressively more susceptible to opportunistic infections. Eventually, HIV-infected individuals develop AIDS and die; however about one in ten remain healthy for many years, with no noticeable symptoms [7].



**Fig. 2** HIV virus

## 1.2 HIV PHYSICAL STRUCTURE AND GENOME

Human Immunodeficiency Virus (HIV) is a retrovirus, which belongs to *lentivirus* subclass. Like all viruses, HIV cannot grow and replicate on its own, thus in order to reproduce itself it must infect the cells of a living organism. It is around 120 nm in diameter and roughly spherical. The physical structure of HIV (**Figure 3**) is characterized by a lipid membrane (envelope) that surrounds the protein capsule. The envelope derives from the host cell plasma membrane and is acquired when the virus buds through the infected cell. It contains the lipid and protein constituents of the membrane from which it is derived. The envelope also includes the viral glycoproteins gp120 and gp41 [8].

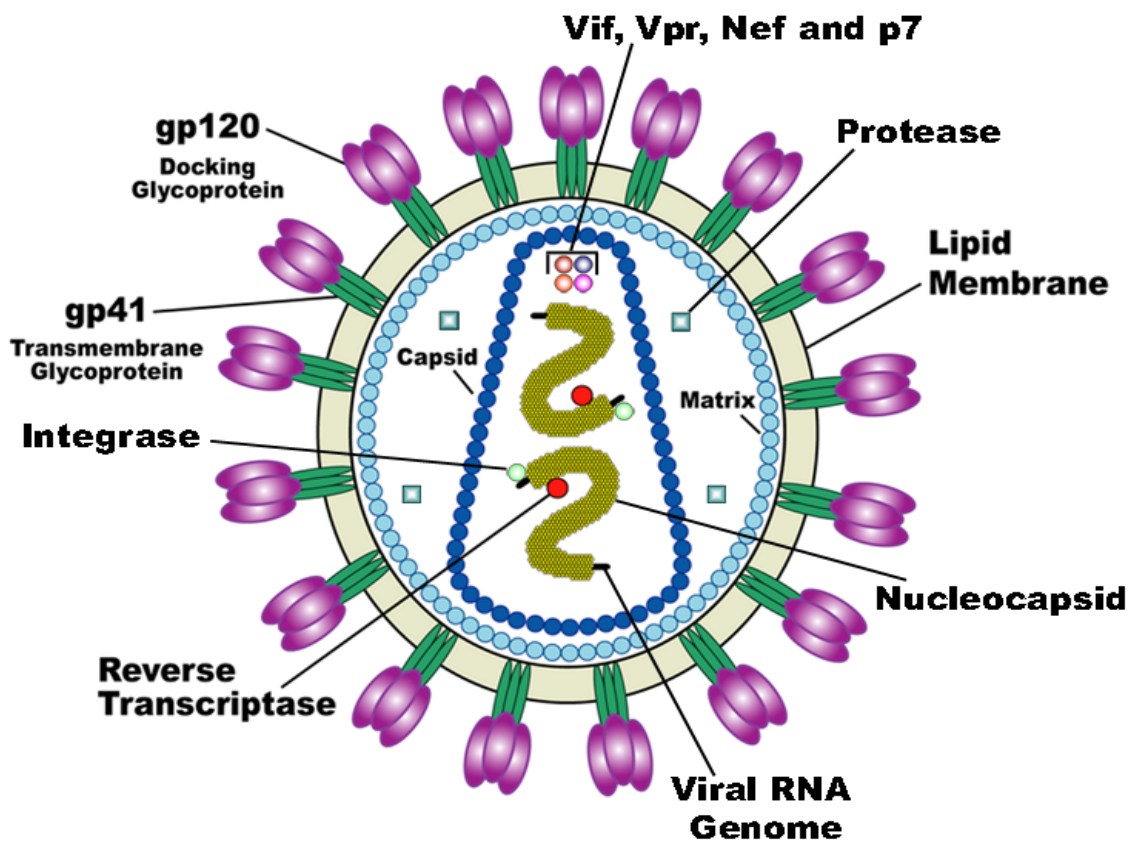


Fig. 3 Schematic illustration of HIV structure

In general, three gp41 glycoproteins are capped with three gp120 glycoproteins and together make up the spikes that project from HIV particles. Gp120/41 functions as the viral receptor or attachment protein: gp41 traverses the envelope, whereas gp120 is present on the outer surface and is noncovalently attached to gp41. The precursor of gp120/41, gp160, is synthesized in the endoplasmic reticulum and is transported via the Golgi body to the cell surface. Just below the viral envelope there is a layer of matrix protein (MA), which is made from the protein p17. The matrix surrounds the bullet-shaped nucleocapsid (*core*) of the virus, which is composed of proteins (p24). Also enclosed within the matrix are Vif, Vpr, Nef, p7 and viral protease enzyme. Inside the core are viral enzymes required for HIV replication such as reverse transcriptase and integrase. Also held within the core is HIV's genetic material, which consists of two identical single-strands of RNA.

### 1.3 HIV GENOME ORGANIZATION

The HIV genome consists in two identical copies of a positive sense single-stranded RNA, about 9,500 nucleotides long. These may be linked to each other to form a genomic RNA dimer. Both ends of the provirus are flanked by a repeated sequence known as the long terminal repeats (LTRs). The genes of HIV are located in the central region of the proviral DNA and encode at least nine proteins (**Figure 4**). Three of the HIV genes, known as gag, pol and env, contain information coding for structural proteins for new virus particles. The other genes (tat, rev, nef, vif, vpr and vpu) code for proteins that control the ability of HIV to infect a cell and the viral replication.

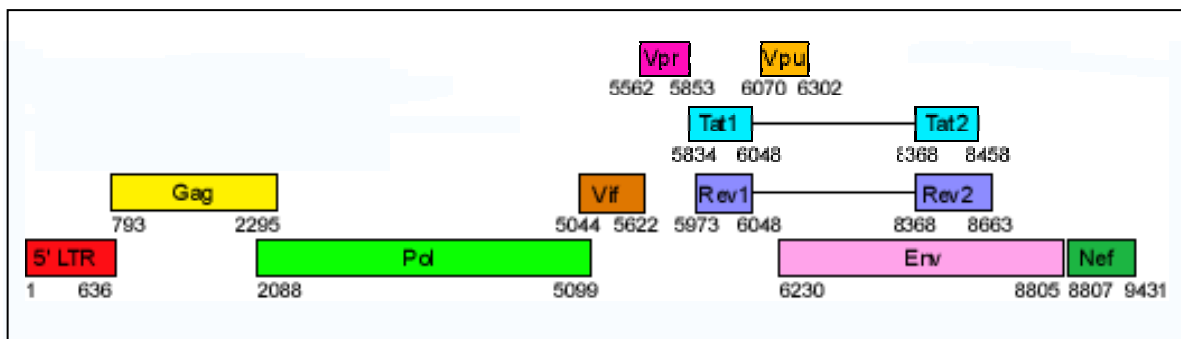
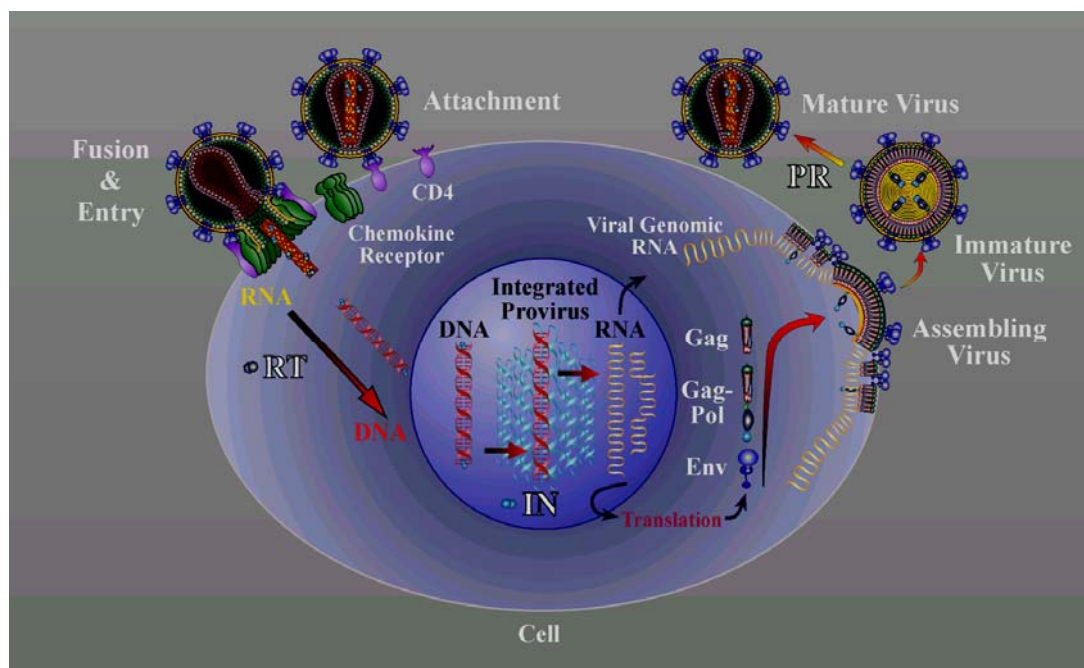


Fig. 4 Diagram of the HIV genome

- *gag* (Group-specific Antigen): codes for the matrix protein (p17) and the nucleocapsid proteins (p6, p7 and p24)
- *pol*: codes for viral enzymes (reverse transcriptase, integrase, and protease)
- *env* (for "envelope"): codes for the precursor of gp120 and gp41, proteins embedded in the viral envelope
- *tat*, *rev*, *nef*, *vif*, *vpr*, *vpu*: each of these genes codes for a single accessory protein with the same corresponding name (Tat, Rev, Nef, Vif, Vpr, Vpu)
- *tev*: this gene is only present in a few HIV-1 isolates. It is a fusion of parts of the *tat*, *env*, and *rev* genes

## 1.4 HIV REPLICATION CYCLE

The replication cycle of human immunodeficiency virus is a complex process, which could be divided into different phases (**Figure 5**). Each step may be taken advantage of in developing antiretroviral therapies.



**Fig. 5** Schematic representation of HIV replication cycle

- **Binding and entry**

HIV entry is a multistep process that involves a viral envelope glycoprotein (gp120) and a host cellular receptor (CD4). However viral penetration does not occur in all CD4<sup>+</sup> cells. Moreover, CD4 deficient cells can be infected with HIV, indicating that additional cellular factors are required to allow the fusion between HIV and target cells. Several studies over the last 10 years have demonstrated that HIV-entry is mediated by members of the chemokine receptor family [9-12]. Although many chemokine receptors have been reported to act as co-receptors in *in vitro* assays, only two of them, CC-chemokine receptor 5 (CCR5) and CXCR4, exhibit a significant physiological role [13]. The initial attachment of gp120 to the CD4 receptor induces a conformational change in the viral envelope protein, allowing the exposure of a previously hidden binding-site for co-receptors. Subsequently the interaction mediated by CCR5 or CXCR4 promotes a further conformational modification of the viral trans-membrane protein, gp41, essential to complete the fusion of the viral and cellular membranes [14-16]. Once HIV has bound to the target cell, the virus core is injected into the cytoplasm leaving the viral membrane and envelope proteins behind on the outer surface of the cell. Inside the cell the core protein is digested by host cell enzymes, releasing viral RNA and viral enzymes reverse transcriptase, integrase and protease.

- **Replication and transcription**

For HIV genes to get into the host cell's DNA, the viral RNA has first to be converted to DNA. The viral enzyme, reverse transcriptase (RT), produces a single strand of DNA from the viral RNA, while RNase-H breaks down the RNA once it has been copied. Reverse transcriptase also acts as a DNA polymerase, producing a partner strand of DNA to match the initial single strand. The result is a double-stranded DNA replica of the original RNA template which is successively transported into the cell nucleus. This process of reverse transcription is extremely error-prone and it is during this step that mutations may occur, promoting drug resistance.

- **Integration**

After entering the host cell nucleus, through pores in the nuclear membrane, the double-stranded viral DNA has to be integrated into the human genome. This process is carried out by another viral enzyme, integrase (IN). The viral DNA, integrated into the human DNA, turning the host cell into a "machinery" for manufacturing more viruses. A cell infected with HIV contains both viral and human DNA that act as template to produce messenger RNA (mRNA). The mRNA leaves the nucleus and enters the cytoplasm, where it delivers its instructions for making proteins [17].

- **Viral replication**

The mRNA derived from the viral DNA utilizes the host's cellular apparatus to produce virus proteins (core proteins, envelope proteins, enzymes and regulatory proteins, such as essential for HIV replication). For viral replication some cellular transcriptional factors, such as NF- $\kappa$ B, are required [18]. The core proteins are produced as a single multi-protein molecule, which later requires cutting into smaller proteins during viral maturation. These are transported to the cell membrane with viral RNA in preparation for assembly and viral budding. These small pieces produced include the regulatory proteins Tat and Rev. As Rev accumulates it gradually starts to inhibit mRNA splicing. At this stage, the structural proteins Gag and Env are produced from the full-length mRNA. The full-length RNA is actually the virus genome; it binds to the Gag protein and is packaged into new virus particles. HIV-1 and HIV-2 viral subtypes appear to package their RNA differently: HIV-1 will bind to any appropriate RNA while HIV-2 will preferentially bind to the mRNA which was used to create the Gag protein itself. This may mean that HIV-1 is better able to mutate, consequently then HIV-1 infection progresses to AIDS faster than HIV-2 infection and is responsible for the majority of global infections [19].

- **Assembly and release**

The final step of the viral cycle, assembly of new HIV-1 virions, begins at the plasma membrane of the host cell. The Env polyprotein (gp160) goes through the endoplasmic reticulum and is transported to the Golgi complex where it is cleaved by protease and

processed into the two HIV envelope glycoproteins gp41 and gp120. These are transported to the plasma membrane of the host cell where gp41 anchors the gp120 to the membrane of the infected cell. The Gag (p55) and Gag-Pol (p160) polyproteins also associate with the inner surface of the plasma membrane along with the HIV genomic RNA are gathered at the cell membrane. Mini-bubbles begin to form and successively bud out of the cell taking with it all viral proteins and RNA needed to form a virus particle or 'virion'.

The newly assembled virions are still immature as they enter the bloodstream. At this stage they are unable to infect other cells. The virions must undergo a process of maturation in order to become infectious. CD4 cells do not usually survive invasion by HIV. Either they disintegrate because of the large number of viruses budding off, or the body's immune system will recognize the viral envelope proteins in the cell membrane and destroy the damaged cells. As CD4 cells themselves are an essential part of the immune system their destruction can cause profound immunodeficiency [20].

- **Viral maturation**

Once the new virus has left the cell another viral enzyme, protease, cuts the molecule containing the HIV core proteins. The released individual proteins are reassembled to form a structured, mature virus. This virus is now able to infect other cells.



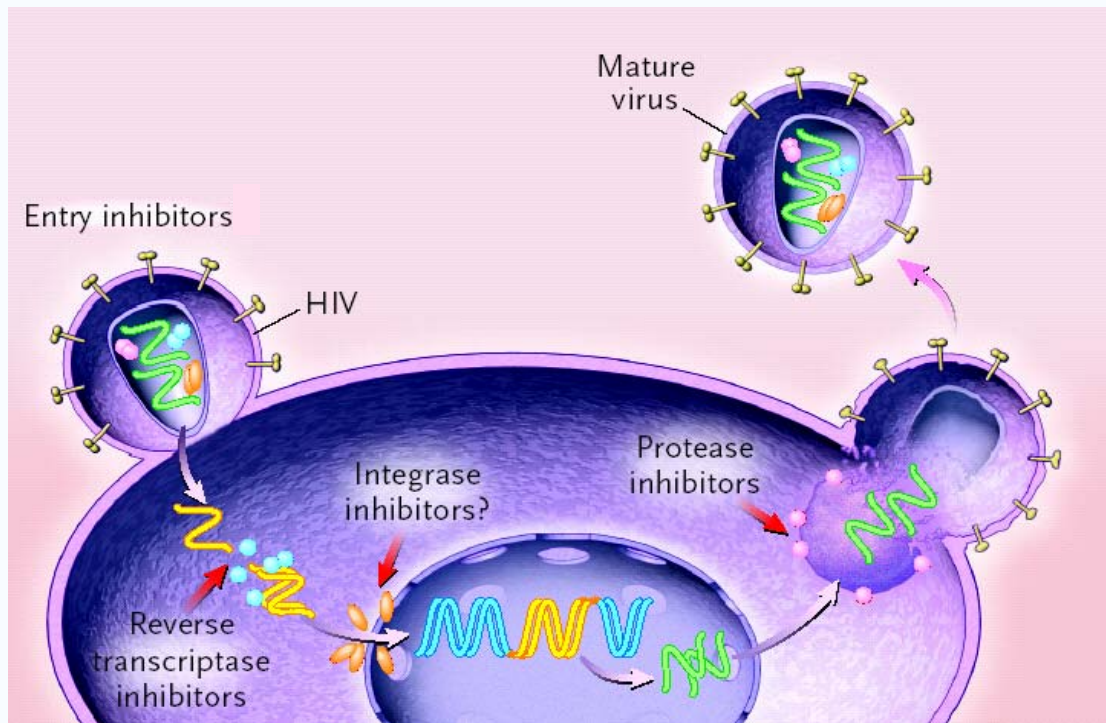


**Fig. 6** Replication cycle stages as possible therapeutic target

Although each of these steps could represent a therapeutic target (**Figure 6**), at present only 20 anti-HIV drugs targeting reverse transcriptase, protease and viral entry are available [15]. The introduction of highly active antiretroviral therapy (HAART), where a combination of drugs aimed at more than one retroviral drug target is used, has significantly reduced the morbidity and the mortality of HIV infection. Because the emergence of drug resistant viral strains and the side effects of current drugs, there is an important need to develop new anti-HIV drugs that specifically target alternative stages in the HIV replication cycle.

## **CHAPTER 2**

***HIV-1 INTEGRASE:  
STRUCTURAL FEATURES, BIOLOGICAL ACTIVITY AND  
FIRST GENERATION INHIBITORS***

## 2.1 HIV-1 INTEGRASE

HIV-1 integrase (IN) is an enzymatic protein utilized by HIV to incorporate its viral DNA into the host genome. Because of their essential role in the lifecycle of HIV, IN has recently become a major focus of attention as a new target for the development of novel drugs to prevent or slow the HIV infection.

Moreover, it is a multifunctional enzyme, which catalyzes various processes and exhibits some unique features. IN doesn't have any known counterparts in the host cell and uses the same active site to accommodate two different types of DNA substrates (viral and cellular), reducing the potential toxicity the develop of drug resistance [21].

However, HIV-1 integrase has been found to exhibit poor solubility and therefore is unsuitable for crystallization, an important step in the purification of any protein. Before a protein can be crystallized, it must be dissolved in an appropriate solvent and then teased until only the protein comes out of solution. Several methods have been utilized to help increase the solubility of the enzyme including the mutation of specific amino acid residues. Once the choice of mutation site has been decided, a wild type IN is generally abstracted from induced *E. coli* cells by incubation with lysozymes and is then followed by sonication. Finally, after ultrafiltration the protein could be crystallized [22]. Other methods of acquiring HIV IN included engineering a “copy cat” form. For example, DNA polymerase, which catalyzes the 3'-5' cleavage of DNA and possesses a similar active site to that of the integrase protein, has been used as a starting point for a model and various modifications have been made to make it as similar as possible to IN.

## 2.2 INTEGRASE STRUCTURAL FEATURES

HIV-1 IN belongs to the polynucleotidyltransferase superfamily, along with transposases, nucleases and recombinases [23]. IN is a 32 kDa protein (288 amino acids) produced from the C-terminal portion of the Pol gene product.

It consists of three discrete domains (**Figure 7**):

- N-terminal domain
- central catalytic domain (core)
- C-terminal domain

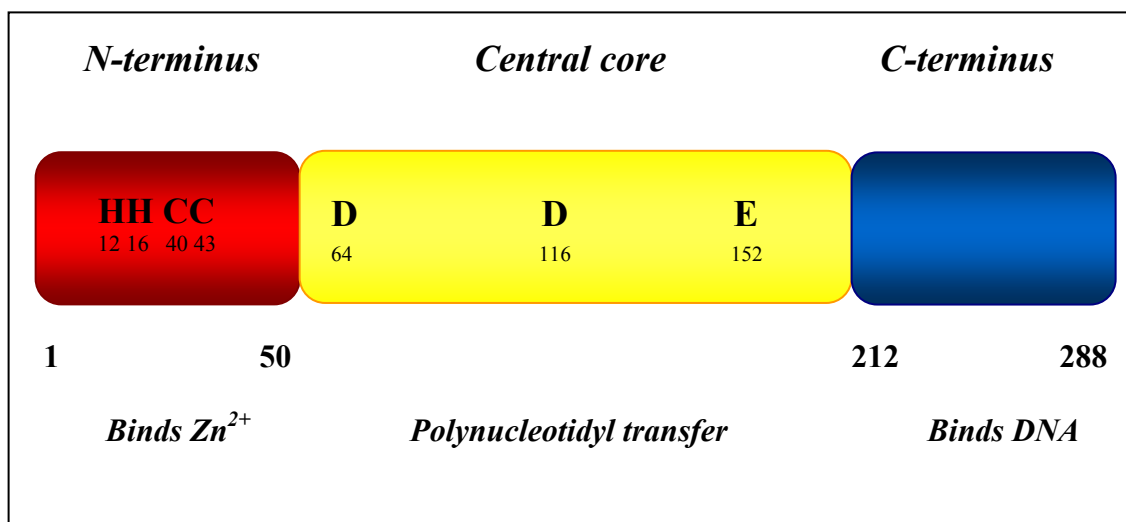


**Fig.7** Schematic representation of three IN domains

### **N-Terminal Domain (Residues 1-50)**

The N-terminal domain contains a conserved pair of histidine and cysteine residues, which together resemble the zinc-coordinating residues of the common transcription factor motifs, “zinc fingers”. This motif is highly conserved among retrovirus integrases and eukaryotic retrotransposons [24]. In general, the zinc finger motive is responsible for DNA binding. *In vitro* binding studies with the N-terminal part of IN failed to show affinity for LTR specific or nonspecific DNA. It has been shown that it can bind zinc and although the zinc finger is not responsible for DNA binding, it is required for IN catalytic activity [25]. Elucidation of the structure by NMR revealed the putative zinc finger of IN to be very different from the classical zinc finger. In contrast to the common zinc fingers, which are composed of  $\alpha$ -helices and  $\beta$ -sheets, the zinc finger of IN is composed of 3  $\alpha$ -helices. This structure is stabilized by the zinc-binding pocket through Zn<sup>2+</sup>-metal coordination [26]. The binding of

zinc ions to the N-terminal domain apparently also promotes polymerization of full-length integrase *in vitro* [27].

### **Catalytic Core (Residues 50-212)**

The active site of integrase consists of 5  $\beta$ -sheets surrounded by 6  $\alpha$ -helices. It contains the catalytic triad DD(35)E (Asp64, Asp161, and Glu152), which is conserved among all integrase proteins from retroviruses and retrotransposons [28].

The enzymatic core structure is flexible and may be involved in the changing of conformation upon substrate binding to allow catalysis to occur. The triad residues are required for catalysis by coordination of a divalent metal ion ( $Mg^{2+}$  or  $Mn^{2+}$ ), which undergoes octahedral coordination via the carboxyl groups of D64 and D116 and the oxygen atoms of four water molecules. The metal preference depends upon assay conditions,  $Mn^{2+}$  is generally preferred *in vitro assay*, while  $Mg^{2+}$  is the naturally preferred metal, due to the lower intracellular concentrations of  $Mn^{2+}$  [29]. This divalent metal is thought to have a double function: it acts as an electrophilic catalyst and contributes to orient the substrate in proper position for integration process [27].

Although the core is the unit in which all catalytic activity occurs, it cannot carry out the entire catalytic processes without its adjacent N and C-terminal domains. Moreover, the two active sites, in the core domain crystal structure of dimer IN, are too far apart to permit five base pair staggered cleavage of the target DNA, suggesting that either a very large conformational change occurs during catalysis or, more likely, that IN functions as a tetramer or another oligomeric form during some steps of the reaction [30].

### **C-Terminal Domain (Residues 212-288)**

The carboxy terminal domain of integrase is the domain that shows the least sequence conservation among integrases [31]. Since a polypeptide fragment of 50 amino acids (220-

270) is sufficient for DNA binding, the entire C-terminal domain is generally described as the DNA binding domain. The C-terminal domain binds nonspecifically to DNA and forms a dimer of parallel monomers [32]. The structure of each monomer consists of five anti-parallel  $\beta$  strands that fold into a  $\beta$ -barrel, strikingly similar to the SH3 domain (Src homology 3). It contains a saddle-shaped groove that might accommodate double-stranded DNA. K264, an important DNA-binding residue is located within this groove [28].

Although the structures of all three domains of integrase have been individually determined, their spatial arrangement in the active complex with DNA substrate and the individual positioning into a multimeric structure remain to be resolved.

Recent biochemical and structural data suggest that a dimer constitute the fundamental unit for integrase reactions, although a dimer of a dimer (a tetramer) is the more probably active form of IN (**Figure 8, 9**).

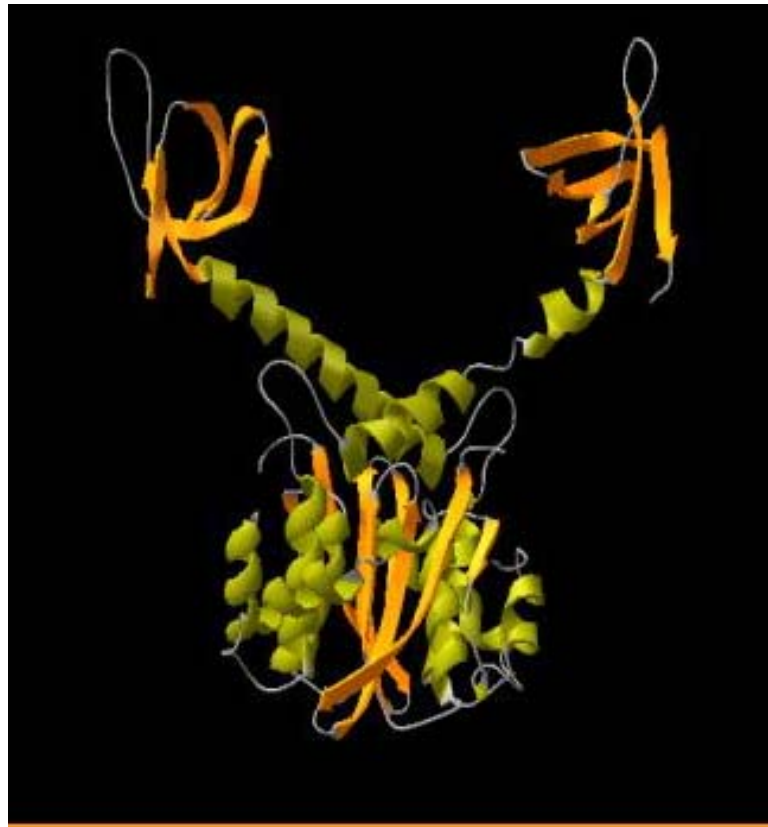


**Fig. 8** 3D Structure of the HIV Integrase Dimer

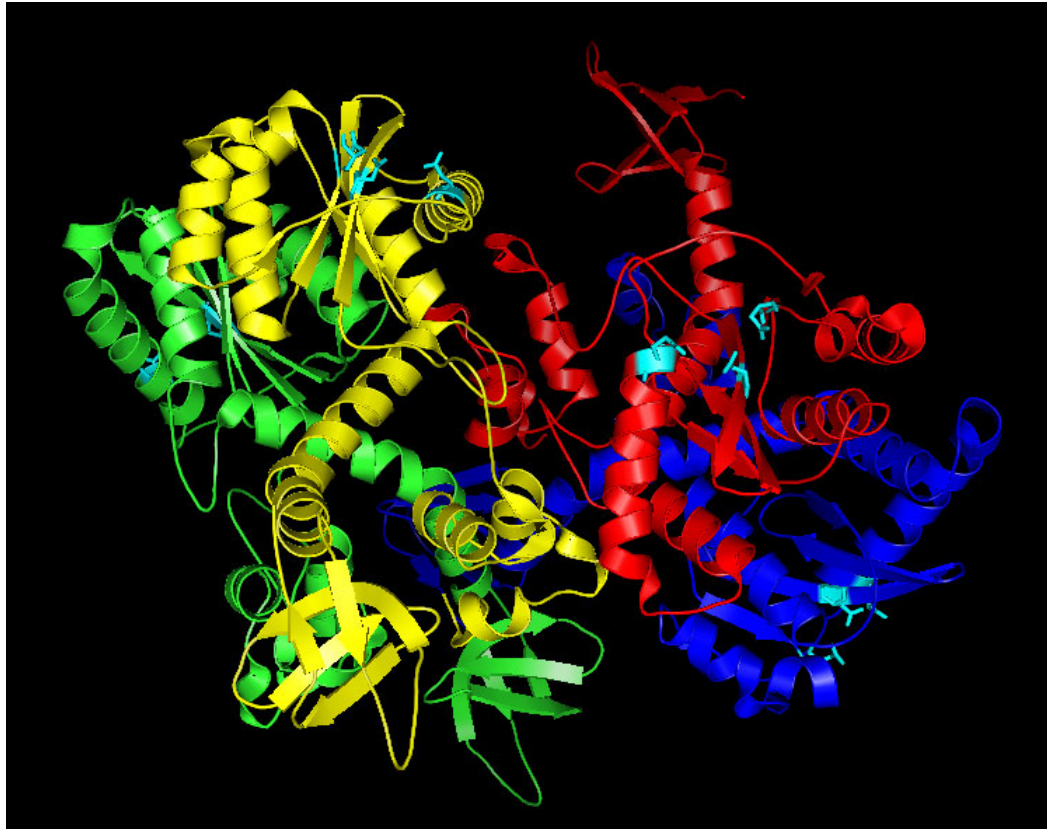


**Fig. 9** 3D Structure of the HIV Integrase Tetramer

### **2.3 BIOCHEMICAL MECHANISM OF INTEGRATION**

IN mediates the integration of proviral cDNA into the host genome, by catalyzing two reactions, namely, 3'-processing and strand transfer. This process starts when the enzyme recognizes an intact LTR end.

In the first step, the terminal GT dinucleotides, adjacent to a highly conserved CA dinucleotides, are removed from both 3'-end of the viral DNA which generates reactive nucleophilic hydroxyl groups. This site-specific endonucleolytic process physically takes place in cytoplasm of infected cells.

Successively, IN translocates to the cellular nucleus as a part of the pre-integration complex (PIC), still bound to the 3'-processed viral DNA and packaged together with several viral and cellular proteins. This completes insertion of both the 3'-ends of the viral DNA into the cellular genome. Chemically the “strand transfer” reaction involves a nucleophilic attack by the 3'-OH group generated after processing and a concomitant transesterification to the 5'-phosphate of the cleaved cellular DNA (**Figure 10**). The sites of integration in the two target DNA strands are separated by five nucleotides. The 3'-ends of the target DNA remain unjoined after the strand transfer. The integration reaction is completed by the removal of the two unpaired nucleotides at the 5'-end of the viral DNA and the repair of the single stranded gaps created between the viral and target DNA. This step is likely carried out by cellular DNA repair enzymes [33].

Another reaction, known as disintegration (**Figure 11**) can be carried out by the core domain independently of the N and C-terminal domains. Disintegration is basically the reverse of the integration reaction where the 3'-OH of the target DNA attacks the phosphodiester bond joining the viral and host DNA and ultimately releasing the model viral DNA end and restoring continuity with the target DNA [23]. The final product is left with single strand gaps in the target along the 5' ends of viral DNA that is filled and overhanging viral DNA successively removed by a separate HIV enzyme [29].

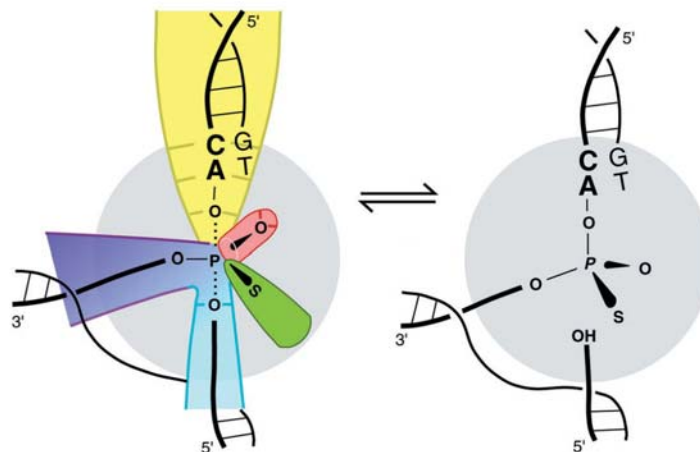


**Fig. 11** Disintegration reaction



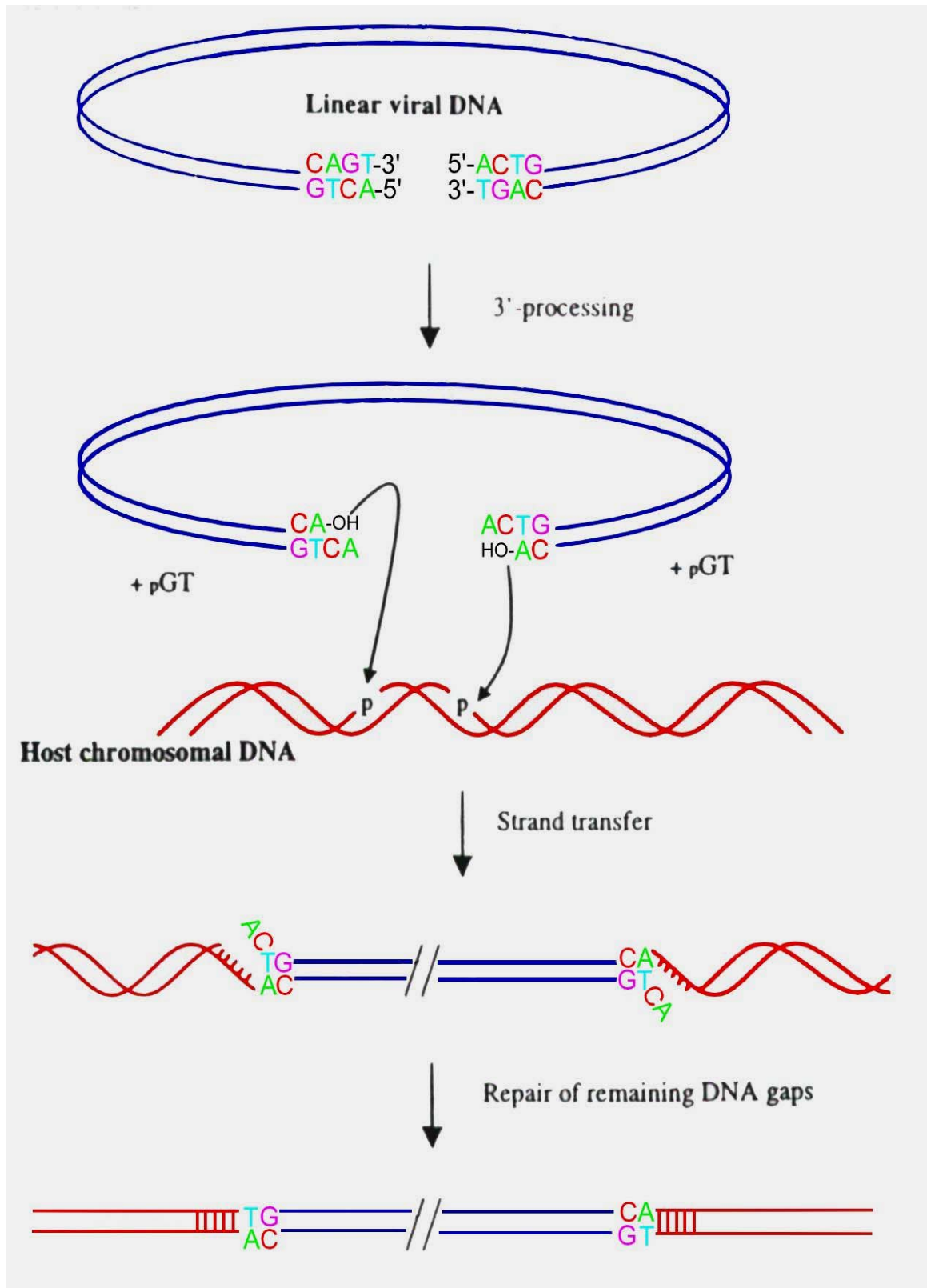
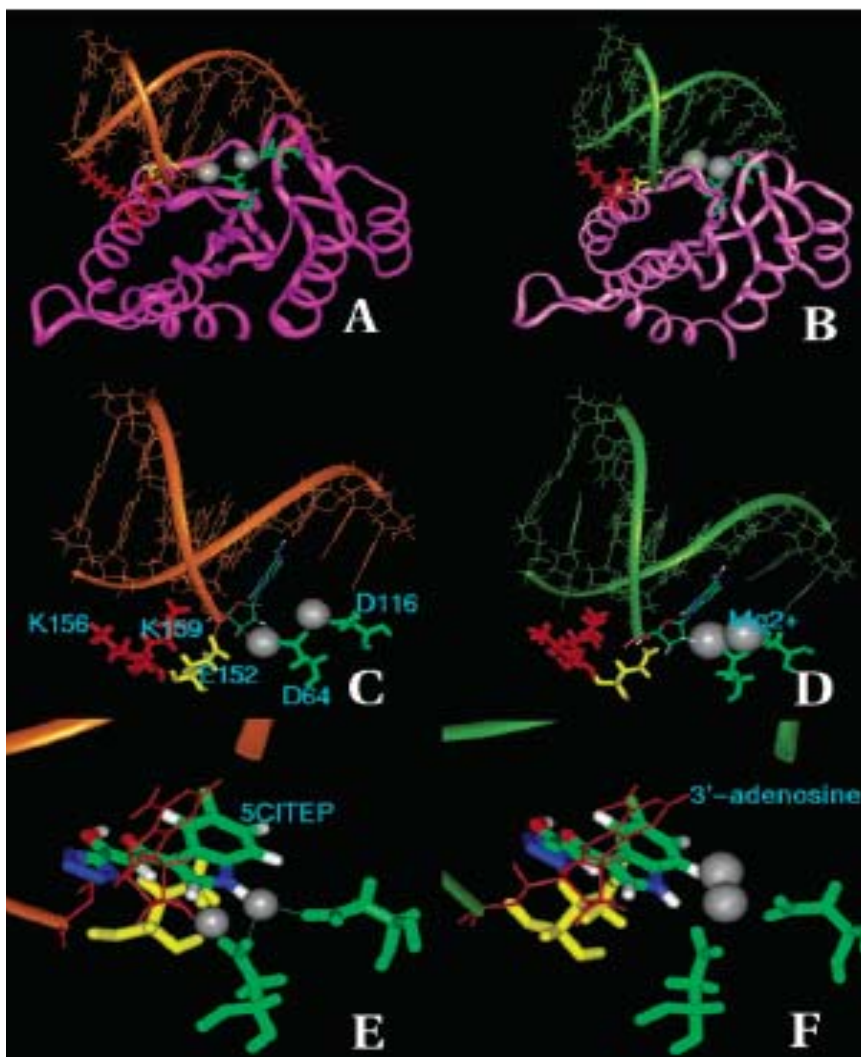


Fig.10 Mechanism of integration reactions

## 2.4 HIV-INTEGRASE INHIBITORS

Unlike RT and PR, the lack of detailed structural information has hampered structure-based discovery of selective inhibitors targeted to IN. Several structures of the *core* domain alone or together with either a C-terminal or an N-terminal domain and the *core* domain of IN in complex with a  $\beta$ -diketoacid derivative, 5CITEP, are available (**Figure 12**) [34].



**Fig. 12** (A) Docked IN/viral DNA complex featuring the IN active site residues. (B) Energy-minimized model of docked IN/viral DNA complex. (C) Detailed representation of docked viral DNA in relation to the IN active site residues. (D) Energy-minimized docked viral DNA in relation to the active site residues of IN. (E) Detailed view of the docked viral DNA superimposed on a MD simulation of the IN/5CITEP complex. (F) View of 5CITEP overlapping with the energy-minimized, docked processed viral DNA [34].

However, no X-ray structure of full-length IN, with or without the DNA substrate is available.

Despite the deficiency of full-length structural information of IN, several inhibitors, of a variety of chemical classes, have been discovered. The structures of some representative molecules of HIV-IN inhibitors are shown in **Figure 13**.

After a decade of research some compounds, belonging to the first-generation IN inhibitors, such as S-1360 and L-870, 810, have entered clinical trials, confirming IN as a rational retroviral drug target (**Figure 14**).

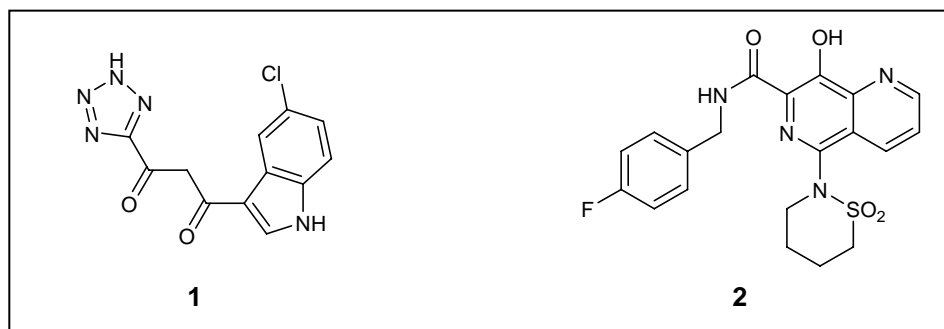


**Fig. 14** Structures of the clinical candidates S-1360 (1) and L-870,810 (2).

However, their continuous viral exposure in cell-based assays has resulted in HIV strains that show resistance. This observation emphasizes the need for the discovery of second and third generation IN inhibitors of novel structure and inhibition mechanisms [35].

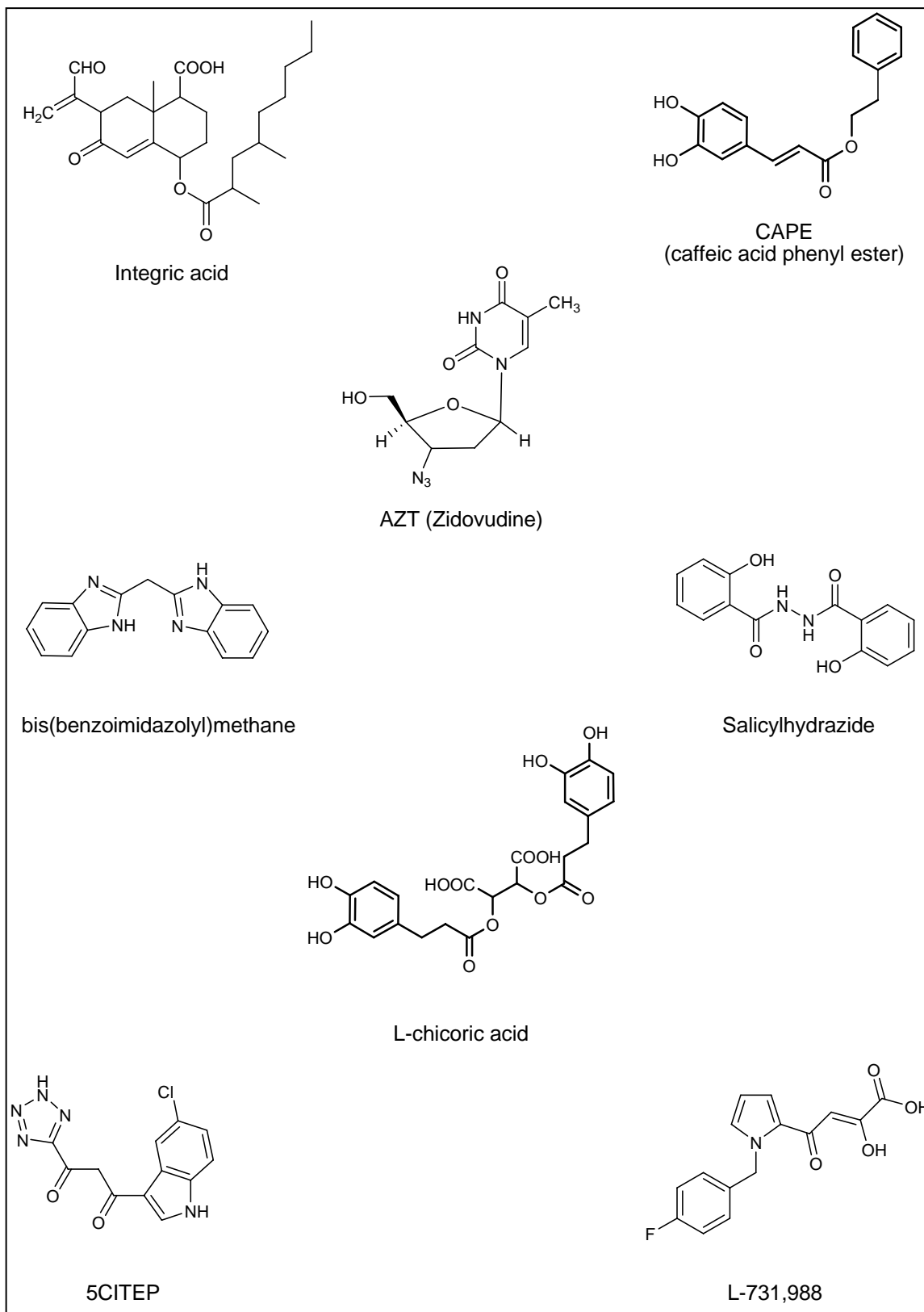


Fig. 13 Representative examples of HIV-IN inhibitors

The known IN inhibitors can be grouped into different categories according to their origin and chemical structure.

### **Small-Molecule Natural Product Inhibitors**

Nature has been a rich source for molecules containing remarkably diverse chemical scaffolds. Many valuable leads for a variety of therapeutic targets are traced back to natural products. Recent crucial breakthroughs in separation and structure determination technologies have allowed the screening of natural product mixtures of structurally diverse molecules [36].

Over the past several years numerous natural product IN inhibitors have been discovered by the screening of the extracts derived from microbial, plant, and marine organisms, such as integric acid, equisetin, trichosanthin, complestatin, integracins, integrastatins [37, 38].

### **Nucleotides and Nucleotide Analogues**

Nucleotide analogues, dinucleotides and oligonucleotides have shown activity against HIV-1 IN. They all seem to compete with the DNA substrate [39]. Nucleotides based on 3'-azido-3'-deoxythymidine (AZT) have been among the first inhibitors of HIV IN reported. In the 3'-processing reaction, IN excises the dinucleotide 5'-pGT after recognition of the adjacent dinucleotide 5'-pCA. Therefore, several dinucleotides were tested against IN and found to inhibit the enzyme more potently than mononucleotide analogues [40]. Interestingly, the 5'-pCA dinucleotide is more selective for inhibition of strand transfer than 3'-processing. Tri- or tetra-nucleotides are not distinctly more active than the dinucleotides.

## **Guanosine Quartet-Forming Oligonucleotides (GQuartets)**

G-quartets are oligonucleotides that can form a highly stable intramolecular four-stranded DNA structure containing two stacked guanosine-quartets (G-quartets). Although G-quartets inhibit HIV IN activity in the nanomolar range, it has been clearly shown by selecting and sequencing drug resistant HIV-1 strains that the antiviral activity in cell culture is due to the inhibition of viral entry [39, 41].

## **DNA Interacting Agents**

Many DNA binding agents were found to inhibit HIV-1 IN, probably due to interference with the interaction of the DNA substrate with the DNA binding domain of the enzyme. Intercalators and DNA groove binding compounds, such as netropsin, belong to this category. It is obvious that the value of intercalators as drugs is limited by their toxicity and relative lack of specificity [42].

## **Peptides derivatives**

Previously, a hexapeptide (HCKFWW) selective IN inhibitor was discovered through the screening of a synthetic peptide combinatorial library. Successively, monomeric, dimeric, and tetrameric analogs have been synthesized and their corresponding anti-IN activity was evaluated. The proposed mechanism of action is based upon interference with integrase binding and activity through the binding of these proteins to DNA [43].

## **Hydroxylated Aromatic Compounds**

Many polyhydroxylated aromatic compounds have been reported as inhibitors of HIV-1 IN *in vitro*. Flavones, tyrophostins, lignans, anthraquinones and bis-catechols are all

characterized by two vicinal hydroxyl groups positioned on an aromatic ring (catechol). Two possible mechanisms of action have been proposed:

- catechols may interfere with the coordination of the metal ions, required for the phosphoryl transfer reactions in the active site;
- the hydroxyls of catechols may function as hydrogen bond donors for interaction with the enzyme.

Moreover, hydroxylated aromatics that do not contain ortho-hydroxyls such as Curcumin, coumermycin A1 and bis-coumarins have been demonstrated to inhibit IN activity [44, 45].

### **$\beta$ -Diketo Acids**

$\beta$ -Diketoacid derivatives (ADKs) inhibit HIV-1 replication at micromolar concentrations through a specific inhibition of the DNA strand transfer step. Selected resistant HIV strains carried mutations in the integrase gene. When these mutations were introduced in integrase, they conferred partial resistance to the drugs. A diketo derivative (5-CITEP) was co-crystallized with the HIV-1 integrase core domain (**Figure 15**). The inhibitor bound to a site panning both the DDE motif and the mononucleotide-binding site. It has been demonstrated that diketo acids only bind to integrase after the enzyme has bound to its target DNA [33]. The ADKs have confirmed to be authentic integrase inhibitors, owing their antiviral effect to an inhibition of the integration process during viral replication. Several analogue derivatives have been synthesized in order to improve their antiviral activity.

Some representatives of this class (for example S-1369 and DFC 33) have shown strand transfer specific inhibition in the nanomolar range, thus these compounds are one of the most promising class of anti-IN compounds [46-48].

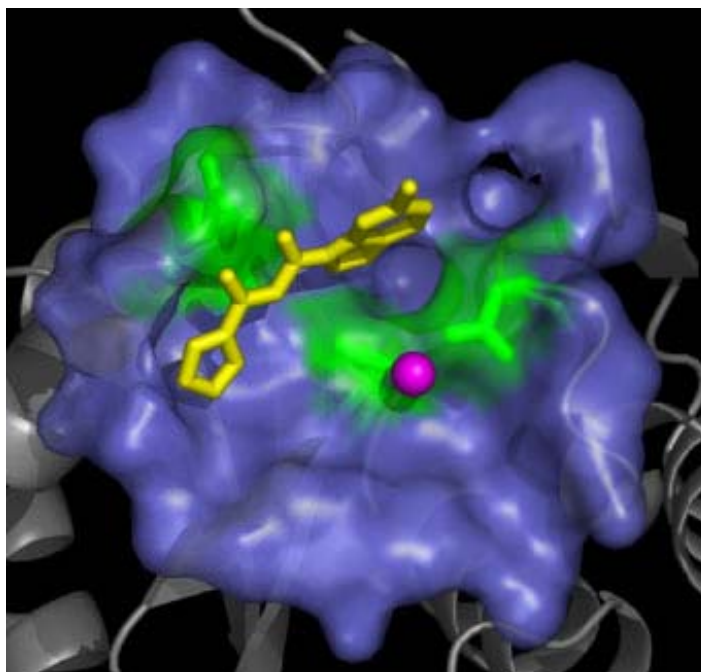


**Fig. 15** 5CITEP occupies a cavity between catalytically vital amino acid residues E152, and D64, D116 in the crystal structure of the HIV-1 integrase-5CITEP complex. The integrase active site region including the highly conserved DD(35)E motif is shown as a surface mode. The sphere represents  $Mg^{2+}$ .

In conclusion, considering its critical role in the HIV life cycle, the addition of IN inhibitors to current HAART combination regimens could enhance retroviral inhibition. Although the first-generation IN inhibitors have entered clinical studies, viral strains resistant to these inhibitors have been isolated in *in vitro* assay. Thus, there is an important need to develop new generation drugs with high activity against resistant virus and with improved pharmacokinetic properties.



## **CHAPTER 3**

### ***SYNTHESIS AND BIOLOGICAL EVALUATION OF NOVEL HIV-1 INTEGRASE INHIBITORS***

### 3.1 PRELIMINARY STUDIES

There are a number of characteristics in the biochemistry and molecular biology of integration that makes it a process that is not easy amenable to classical drugs. Although it has been demonstrated that integrase can turnover as a normal enzyme, the turnover rate is very low [49].

Although both reactions are temporally and spatially separated, the catalytic events take place in a pre-integration complex that may limit accessibility of drugs to the catalytic sites. Moreover, the inhibitors discovered in the enzymatic tests may target biochemical interactions (e.g.  $Mg^{2+}$  chelation) shared by many other enzymes, which would make it difficult to dissociate activity and toxicity of the compounds.

However, remarkable progress has been achieved since IN was recognized as an important antiretroviral target. Through high throughput screening of large collections of compounds and analogue-based drug design methods, a variety of chemical classes of IN inhibitor has been identified. The results from preclinical and clinical studies on the first generation IN inhibitors require a demand for new generation of drugs with improved pharmacokinetic and metabolic properties.

Pharmacophore-based drug design techniques facilitate the discovery of novel compounds on the basis of validated lead compounds specific for a drug target. A pharmacophore is commonly defined as an arrangement of molecular features of a molecule responsible for its biological activity (**Figure 16**). A three-dimensional (3-D) pharmacophore is defined by a critical geometric arrangement of such feature. The availability of even more powerful computers and commercially available databases has effectively improved the discovery of new therapeutic leads.

Generally, pharmacophore models can be generated using either a set of known inhibitors for an enzyme or the active site of the enzyme. Analogue-based pharmacophore models are generated by utilizing a set of known inhibitors for a drug target. These pharmacophore models are useful to discover novel compounds that contain the desired pharmacophoric features, but also have diverse structural and chemical features. These compounds are

expected to bind the drug target in a similar manner as the known inhibitors and exert an analogous biological response.

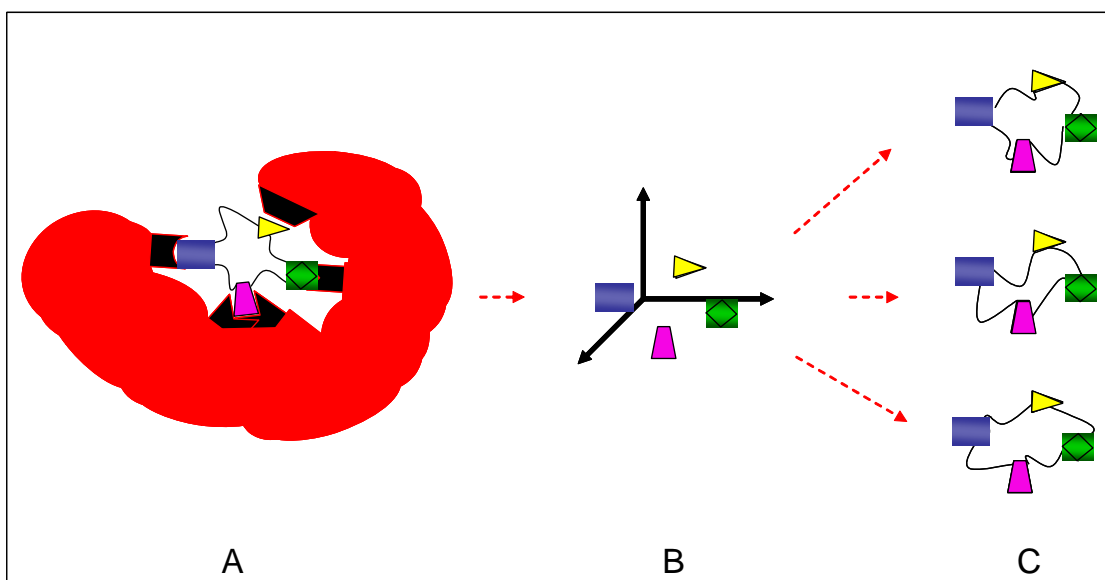


**Fig. 16** Schematic representation of application of pharmacophore-based technology in discovery of novel compounds containing diverse structural scaffolds: A) Hypothetical drug-target binding mode; B) 3D arrangement of pharmacophore features; C) novel lead compounds possess different chemical structures but the same pharmacophore features.

In addition, compounds bearing diverse structural features could show different pharmacokinetic properties than the inhibitors used to derive the model. Structure-based pharmacophore models are generated on the basis of key chemical features in the active site of target enzyme. These models are used to find out compounds containing complementary pharmacophoric features and shape.

The first generation of pharmacophore models in the field of IN inhibitor discovery was referred to as a 3-point, and shortly there after 4-point pharmacophore models, using early stage lead compounds as starting templates (i.e. CAPE, S-1360, 5-CITEP) [50-53]. However earlier pharmacophore model concentrated only on one part of the binding surface

defined by D64 and D116, while E152 was not considered because of a lack of crystal structure with fully resolved residues.

Recently, dynamic pharmacophore models have developed. Molecular dynamics (MD) simulations are used to evaluate the flexibility of target molecules under the influence of explicit solvents, and many conformational models of the protein are saved from the MD simulations and used in a series of “multi-unit search for interacting conformers” (MUSIC) simulations. These models take into account the key residues in the active site, including  $Mg^{2+}$ , D, D(35)E, and nearby K156, K159, critical to DNA binding as supported by photo-crosslinking studies and potential H-bond donor or acceptor (**Figure 17**)[54].

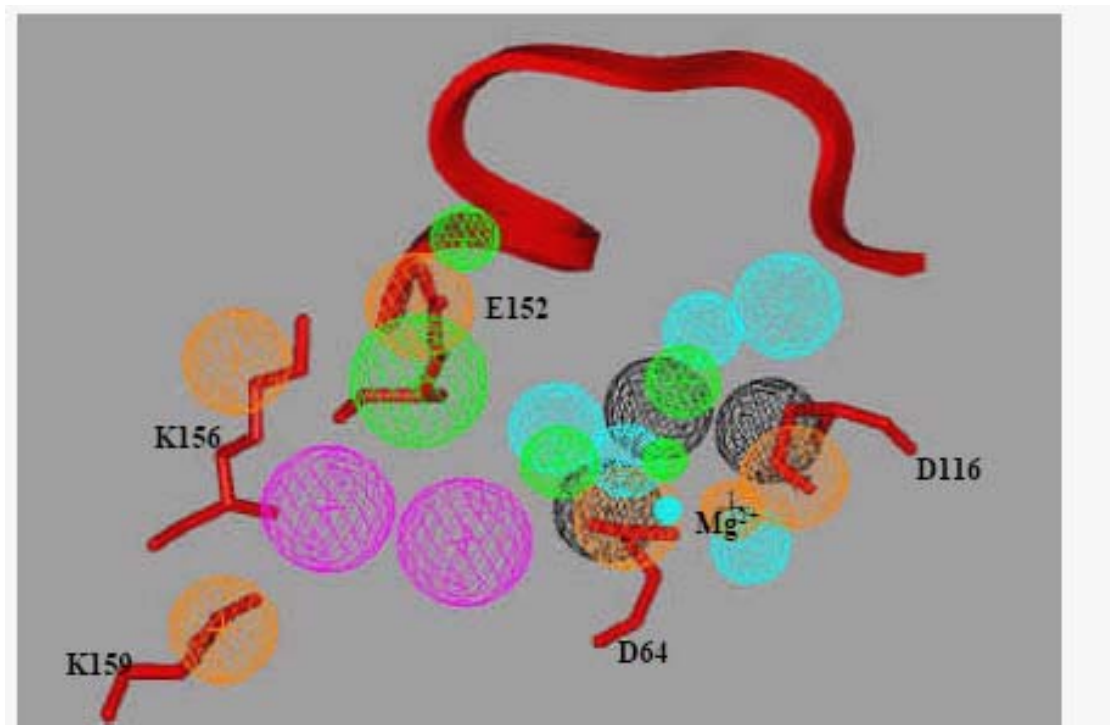


**Fig. 17** Schematic representation of structure-based dynamic pharmacophore models. Six H-bond donor features from 1st dynamic pharmacophore model are shown as cyan spheres and the black spheres represent excluded volume. H-bond donor (magenta spheres) and H-bond acceptor (green spheres) are shown from 2nd dynamic model. The brown spheres represent excluded volume defined by 2nd dynamic model. The stick and ribbon models represent the prominent amino acid residues and the flexible loop in the IN active site, respectively.

For example, Monte Carlo sampling method was applied as a docking procedure to identify the favorable functional features in the IN active site area. In a recent study, methanol was

used as an H-bond probe because it could represent an H-bond donor or H-bond acceptor depending on the protein environment. Ammonium was used as a positively charged probe and chloride as a negatively charged probe. The favorable probe binding locations were used to define the pharmacophore model (**Figure 18A**).

Successively, surface analysis was generated according to the values of calculated  $pK_a$  (by UHBD and GRASP software packages) indicating the negative and positive potential in the binding area (**Figure 18B**) [54].

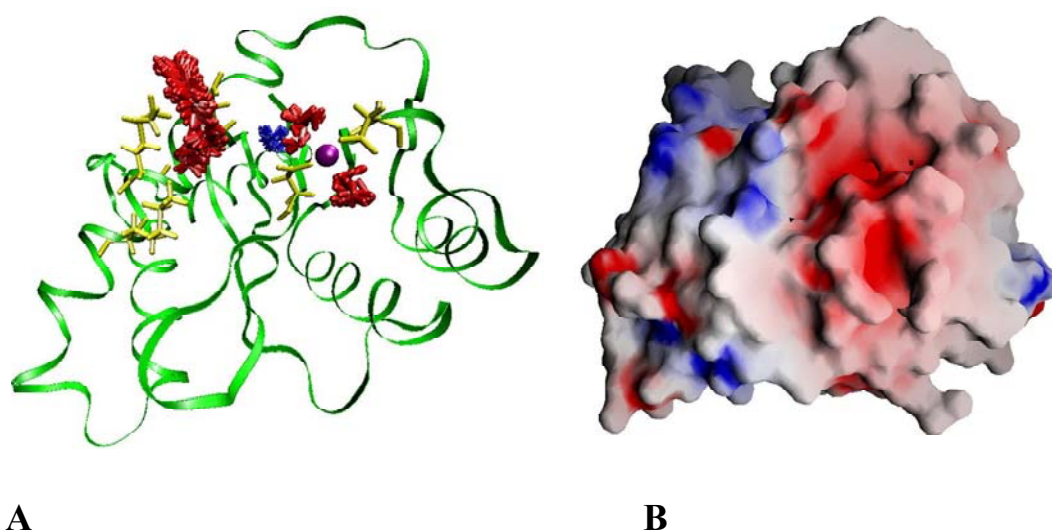


**Fig. 18** Structure-Based Dynamic Pharmacophore Model. A)Favorable sites defined by  $CH_3OH$  (red) and  $NH_4^+$  (blue); B) Potential surface of IN: red= negative potential, blue= positive potential.

### 3.2 SYNTHESIS OF NOVEL HIV-1 INTEGRASE INHIBITORS

One objective of this project has been the combination of novel computer-aided methods and the experimental techniques to discover new generation of selective IN inhibitors. As a first approach, according to the structure-based and dynamic receptor-based pharmacophore models previously reported, a series of easily synthesizable analogs of thiazolothiazepines were synthesized and evaluated for their IN inhibitory activity.

Previously, several thiazolothiazepine based compounds with antiviral activity in cell-based assays were identified by our research group [55]. Among all the reported IN inhibitors, thiazolothiazepines have the smallest and most constrained structures.

Moreover, unlike many other classes of inhibitors, which result active only in the presence of  $Mn^{2+}$  as a cofactor, these compounds retain activity also in the presence of  $Mg^{2+}$ . Because magnesium is more abundant than manganese in cells, it is thought that the  $Mg^{2+}$  is the biological metal in catalysis. However, in *in vitro* assays  $Mn^{2+}$  is a more efficient cofactor and has been routinely substituted for  $Mg^{2+}$ .

The structural motif common to these molecules consists of a central thiazepinedione moiety fused to a carbocyclic aromatic system (benzo or naphtho) and a pent-atomic ring as depicted in **Figure 19**.

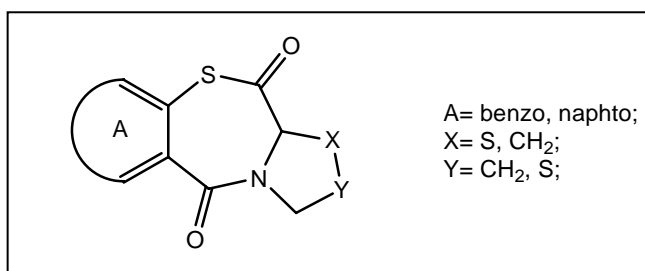


**Fig. 19** Common structural compounds of thiazolothiazepine derivatives.

Due to their low cytotoxicity, low molecular weight, drug-like properties, and structural novelty, these compounds appeared as a new promising class of IN inhibitors. Therefore, a

study to perform structural optimization of previous reported agents was realized by designing and synthesizing a new series of analogs.

Several structural modifications on the reference compounds have been planned in an attempt to identify more active compounds:

- the replacement of sulfur atom(s) by oxygen;
- the introduction of a methyl group on position 1 of the polycyclic system;
- a combination of both features, while maintaining a fused benzo- or naphtho-moiety with diverse geometries.

Such alterations cause variation in both lipophilicity and overall topology of rings, and modify the potential to coordinate a metal cofactor on the IN active site.

Furthermore, a new synthetic route aimed at avoiding racemization was successively undertaken. Along with other structural modifications, the development of stereoselective synthetic procedures represents an additional opportunity for the production of even more active compounds.

The initial synthetic pathways allowed the preparation of final compounds through two subsequent condensation steps between a benzo- or naphtho-carboxylic acid and a proper cyclic amino acid. However, the final cyclization step required a fairly harsh condition (i.e.: prolonged reaction time and high temperature). Under this condition a racemic mixture was always obtained, even though optically active aminoacids have been used as starting materials. This could be probably due to the rigidity caused by the preformed amide moiety that hindered the closure of the seven-membered ring.

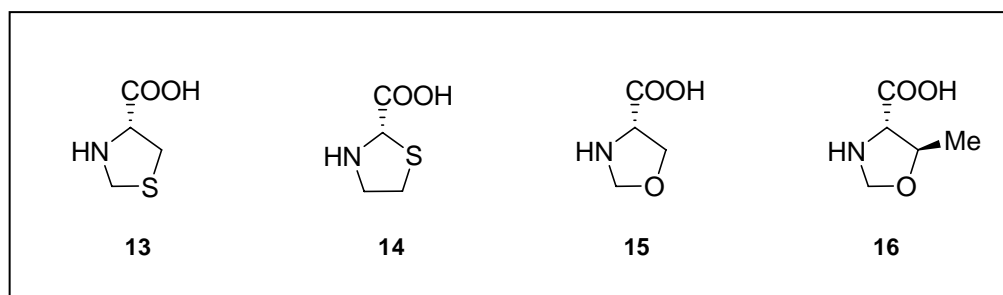
Therefore, the formation of the ester bond was firstly realized in a milder condition so that the chiral center would not be affected. In this case, the seven-membered ring closure reaction by the subsequent formation of the lactam moiety led to the desired homochiral compounds.

### 3.3 CHEMISTRY

The synthesis of thiazepinedione derivatives **1-5** (Table 1) has been accomplished following the general method outlined in Scheme 1. A modification of the above procedure was developed for the synthesis of oxazepinedione derivatives **6-12** (Table 1 and Scheme 2) [55, 56].

2,2'-Dithiodibenzoic acid **17** or 3,3'-dithio-2,2-dinaphthoic acid **18** were chosen as starting materials and reacted with the proper cyclic amino acid (Chart 1), according to the Schotten-Baumann procedure, to give the corresponding disulfides.

#### CHART 1

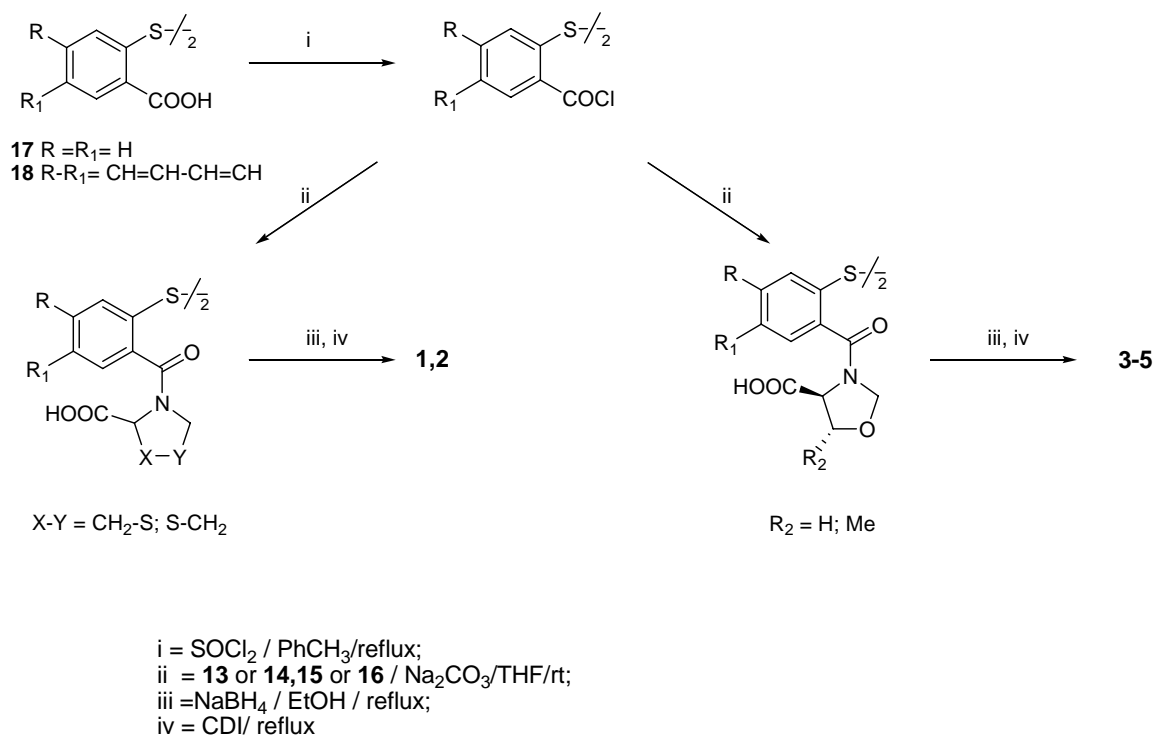


(R)-(-)-Thiazolidine-4-carboxylic acid **13** and (±)-thiazolidine-2-carboxylic acid **14** are commercially available, while oxazolidine-4-carboxylic acid **15** and (4S,5R)-oxazolidine-5-methyl-4-carboxylic acid **16** were prepared by reaction of formaldehyde with L-serine or L-threonine, respectively, in an *in situ* N-acylation reaction [57].

The crude disulfide intermediates were treated with NaBH<sub>4</sub> to give the corresponding thiophenols.



## SCHEME 1

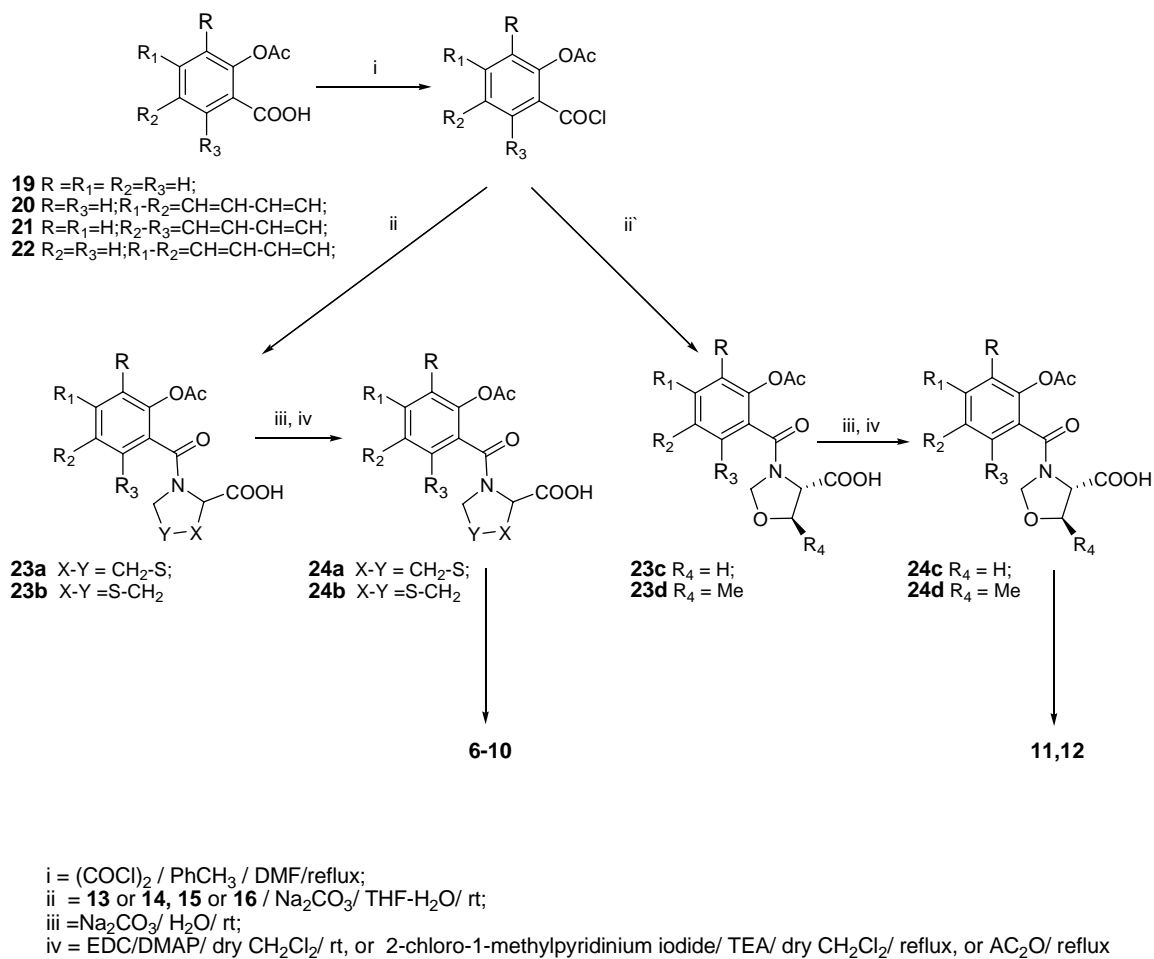


The final cyclization reaction was carried out using *N,N'*-carbonyldiimidazole (CDI) as condensation reagent to give the final compounds in good yield.

2-Acetoxybenzoic acid **19** or the proper acetoxyphthalic acid **20–22** was converted to the corresponding acid chloride [58], which was in turn added to cyclic amino acids **13–16**, giving the corresponding amides **23**, in good yields.

The hydroxyacids **24**, in turn obtained by controlled hydrolysis of amide intermediates, were subjected to lactonization using 1-(3-dimethylaminopropyl)-3-ethylcarbodiimide hydrochloride (EDC) and 4-(dimethylamino)pyridine (DMAP) [59] (method A) or 2-chloro-1-methylpyridinium iodide and triethylamine (TEA) [60] (method B), or acetic anhydride (method C) as dehydrating agents, leading to polycyclic compounds **4–10** (Scheme 2).

## SCHEME 2



The final compounds were obtained as enantiomeric mixtures. Only in the case of L-threonine, optically active final compounds were obtained, because racemization was prevented by the presence of the methyl group adjacent to the  $\alpha$ -carbon of the amino acid. Subsequently, a new synthetic strategy aimed at avoiding racemization was designed. In this case, several synthetic challenges have to be resolved. For example, appropriate protections for the secondary amino group of the amino acid as well as the aromatic carboxylic group were required prior to the carboxylic ester bond formation.

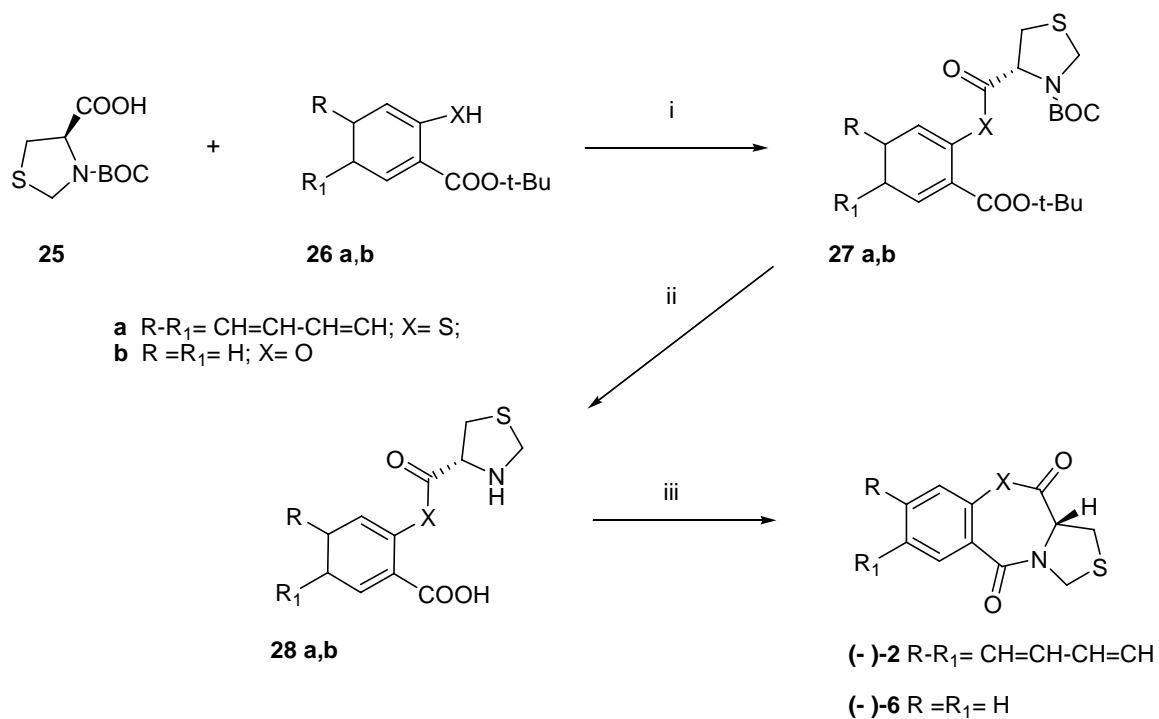
*N*-Boc-L-4-thiazolidinecarboxylic acid **25** and the *tert*-butyl 3-mercapto-2-naphthoate **26a** both bearing a protective group easily removable in mild hydrolytic conditions were selected as ideal precursors.

Their condensation to form the corresponding *N*-Boc-D-4-{[2-(*tert*-butoxycarbonyl)naphthalen-3-ylthio]carbonyl}-1,3-thiazolidine **27a** was accomplished with BOP/DIEA in DCM [61]. The fully protected intermediate was purified by column chromatography on silica gel and then amino and carboxylic groups were deprotected simultaneously by trifluoroacetic acid and excess anisole at room temperature. The thiophenol ester bond was not affected under this condition. Because of easy removal of excess reagents no further purification of D-3-[(1,3-thiazolidin-4-ylcarbonyl)thio]-2-naphthoic acid **28a** was needed.

Compound (–)-**2** was obtained by a cyclization reaction attempted under different experimental conditions. The best result was achieved by using PyBOP/DIEA as an intramolecular coupling reagent in DMF (**Scheme 3**)[62]. Optical activity and purity measurements on the final compound confirmed the stereo-controlled synthesis:  $[\alpha]_{\text{D}}^{20} = -91$  (CHCl<sub>3</sub>, *c* = 0.8); ee = > 93%. Enantiomeric excesses were determined by <sup>1</sup>H NMR spectroscopy using europium tris[3-(heptafluoropropylhydroxy-methylene)-(+)-camphorate].

To investigate the generality of this method, we prepared a related benzoxazepine. In particular the synthesis of L-(–)-1,11 $\alpha$ -dihydro-5*H*,11*H*-[1,3]thiazolo[4,3-*c*][1,4]benzoxazepine-5,11-dione (–)-**6** was undertaken by only slight modifications in the above reaction sequence (**Scheme 3**). Condensation between *N*-Boc-L-4-thiazolidinecarboxylic **25** and *tert*-butyl salicylate **26b**, using the BOP/TEA system in DCM [63], gave the corresponding ester **27b**, which was deprotected in the above conditions, to give essentially pure L-2-[(1,3-thiazolidin-4-ylcarbonyl)oxy]benzoic acid **28b**. The final cyclization step was carried out with PyBOP/DIEA in DMF to give optically pure L-(–)-**6** in a 75% yield;  $[\alpha]_{\text{D}}^{20} = -111$  (CHCl<sub>3</sub>, *c* = 1); ee = > 97%. The present procedure could therefore be used for the synthesis of homochiral compounds, when the starting cyclic amino acid is available in a single enantiomeric form.

**SCHEME 3**



i = BOP/ DCM/ rt  
 ii = TFA/ anisole/ rt  
 iii = PyBOP/ DIEA/ DMF/ rt

### 3.4 PHARMACOLOGICAL STUDIES

Thiazolothiazepines (**1** and **2**) have been identified as representative compounds of this novel class of potential HIV-1 IN inhibitors.

In order to understand their mode of interactions with IN active site, both compounds have been docked onto a previously reported X-ray crystal structure of IN active site, so showing the occupation of an area close to D64 and Mg<sup>2+</sup> and surrounded by key aminoacid residues such as K159 and K156 (**Figure 20**).

These first results suggest that the potential antiretroviral activity of thiazolothiazepine derivative is due to their capability to bind selectively to the enzymatic *core*, inhibiting in this way the catalytic process.

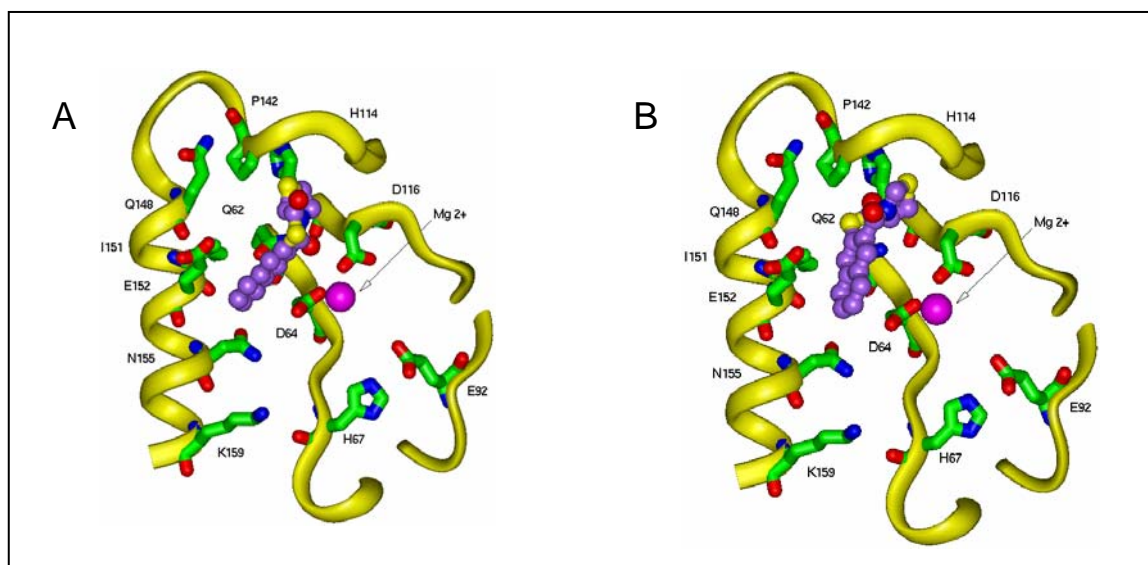


**Fig. 20** Bound conformation of molecules **1** (A) and **2** (B) inside IN active site.

In an attempt to establish a coherent structure–activity relationship, the replacement of the sulfur atom by an oxygen atom has been realized. It has been also evaluated whether a naphthalene ring could be replaced by fused rings. Furthermore, molecular modeling

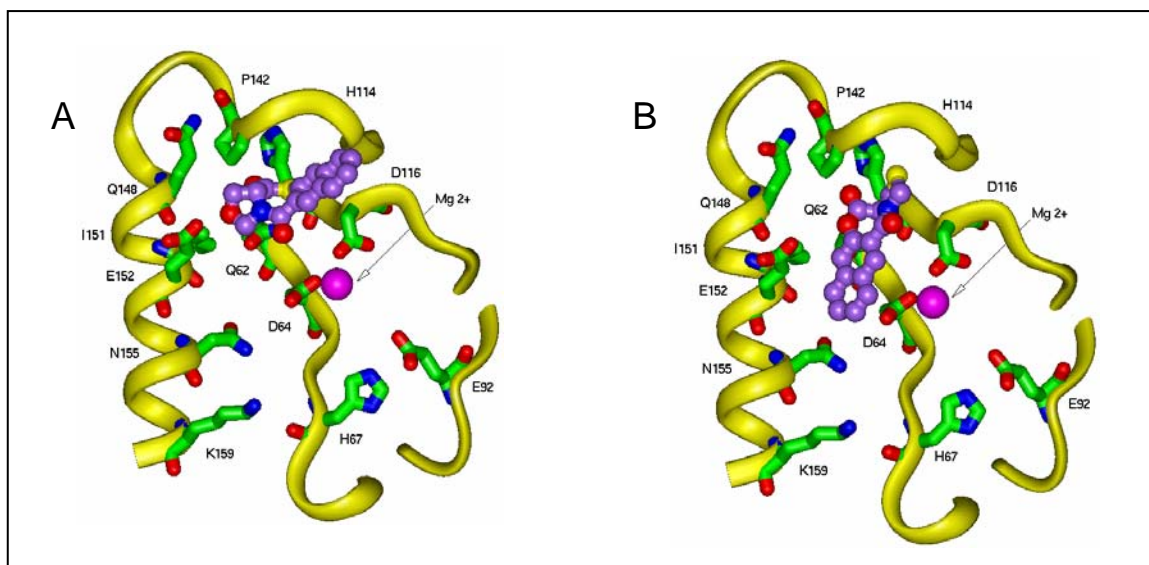
studies have been realized to determine the amino acid residues on the active site of IN that are important for ligand binding [64].

The structures of all the compounds were built and minimized using Catalyst software. The poling algorithm implemented within Catalyst was used to generate conformations for all the compounds. For each compound all feasible unique conformations were generated over a 20 kcal/mol range of energies using the best flexible conformation generation method in Catalyst. The subunit B of the core domain X-ray structure of IN (PDB 1BIS) in which all the active site amino acid residues were resolved was chosen for docking purpose. A  $Mg^{2+}$  ion was placed in the active site between carboxylate oxygen atoms of amino acid residues D64 and D116 considering the geometry of the  $Mg^{2+}$  ion that was present in the crystallographic subunit A of the IN.

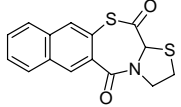
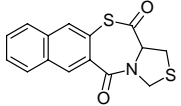
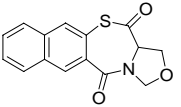
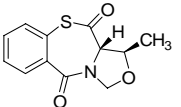
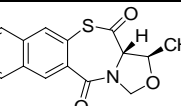
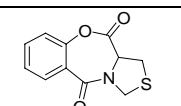
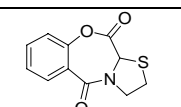
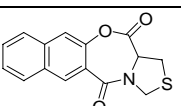
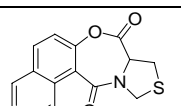
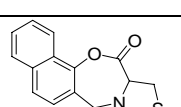
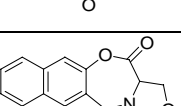
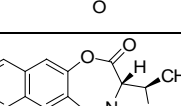
All the water molecules present in protein were removed and hydrogen atoms were added to the protein considering appropriate ionization states for both the acidic and basic amino acid residues.

In order to identify the biologically active conformation of the compounds **1–10**, all the compounds have been docked onto the active site of IN using GOLD (Genetic Optimization for Ligand Docking) software package.

The GOLD fitness scores along with structures are given in **Table 1**, while the active site amino acid residues that interact with compounds are given in **Table 2**. Compounds **1–8** and **10** occupied a wide cavity surrounded by the active site amino acid residues E152, I151, P142, I141, G140, F139, N117, D116, H114, D64, and Q62. The bound conformation of the compounds **3** and **8** inside the active site of IN is shown in **Figure 21**. Compounds **9,11,12** occupied an area close to D64 and  $Mg^{2+}$  surrounded by amino acid residues K159, K156, N155, E152, D116, H67, and T66. The oxygen atom of the oxazolidine ring of **11** and **12** formed a coordination bond with  $Mg^{2+}$ .



**Fig. 21** Bound conformation of molecules **3** (A) and **8** (B) inside IN active site

	Structure	Integrase assay IC <sub>50</sub> (μM)		GOLD Score
		<i>3'-processing</i>	<i>Strand transfer</i>	
1		40	47	34.18
2		92	100	35.28
3		95	90	31.60
4		910	900	36.24
5		800	700	37.78
6		904	873	33.85
7		450	400	32.21
8		100	90	37.17
9		350	300	32.23
10		300	300	34.42
11		150	100	35.30
12		200	200	34.07

**Table 1.** IN inhibitory catalytic activity and docking scores of thiazepinediones and oxazepinediones.



<b>Compound</b>	<b>Interacting amino acid residues</b>
<b>1</b>	K159, K156, N155, E152, D116, H67, T66
<b>2</b>	K159, K156, N155, E152, D116, H67, T66
<b>3</b>	E152, I151, P142, D116, H114, D64, Q62
<b>4</b>	E152, I151, P142, D116, H114, D64, Q62
<b>5</b>	I151, P142, I141, F139, N117, D116, H114, Q62
<b>6</b>	E152, I151, P142, F139, H114, D116
<b>7</b>	E152, I151, Q148, P142, P141, H114, D116, D64
<b>8</b>	E152, I151, P142, D116, D64, Q62
<b>9</b>	K159, K156, N155, T66, D64
<b>10</b>	K159, K156, N155, E152, D116, T66, D64
<b>11</b>	K159, K156, N155, E152, T66, D64
<b>12</b>	E152, I151, P142, G140, D116, H114, D64, Q62

**Table 2.** Active site amino acids residues interact with compound **1- 12**.

In conclusion, as it is shown in **Tables 1 and 2**, none of the compounds where heterocyclic sulfur was replaced with oxygen(s) showed superior activity over the corresponding thio-derivative compounds. Moreover, naphthalene derivatives have shown a higher inhibition potency, confirming that a thiazepinedione fused to a naphthalene ring system is the best combination for the molecule to accommodate into the IN active site. In particular, a 2,3 annelation of the naphtho system to the central thiazepinedione ring, seems to confer the optimal geometry for the molecules to interact with enzyme. On the other hand, the addition of a methyl group at position 1 markedly lowers potency.

In addition, further studies have been done to prove that chirality should be a crucial feature to be taken into consideration for optimizing interaction of these derivatives inside the IN active site. In earlier experiments, ( $\pm$ )-**2** showed  $IC_{50}$  ( $\mu$ M) = 92 and 100 for the 3'-processing and strand transfer, respectively, in the inhibition of HIV-1 IN catalytic activity

[7]. In the same conditions, pure (-)-2 showed  $IC_{50}$  ( $\mu M$ ) = 65 and 88, respectively. Furthermore both racemic and pure (-)-2 have been docked inside the IN active site in order to observe any difference in target-binding (**Figure 22**).

These preliminary results proved that both enantiomers possess inhibitory activity, though a greater potency has to be ascribed to pure (-)-1. Thus (-)-1 may be considered the eutomer. The comparison of such values by purely theoretical conjectures, an eudismic ratio = 2.4 (-)/(+) could be then calculated in the inhibition of the 3'-processing step, assuming that both stereoisomers would act as inhibitors at the active site, each being independent from the other.

However, additional compounds must be tested to establish a more comprehensive quantitative structure–activity relationship and develop even more active compounds.

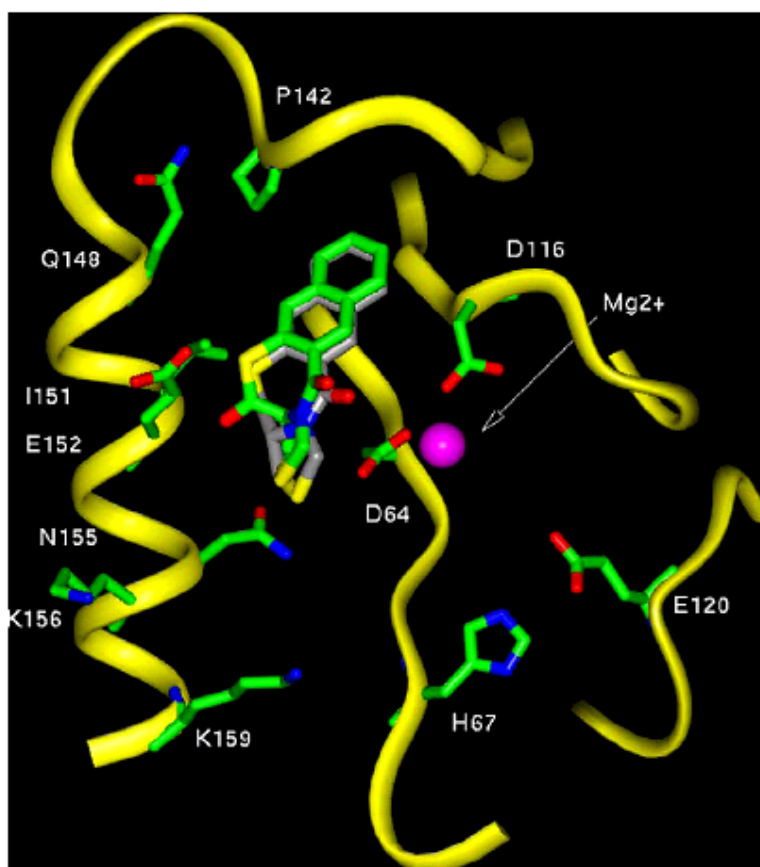


**Fig. 22.** The predicted bound conformation of S and R enantiomeric forms of compound 2 inside the HIV-1 IN active site. The two isomers are shown as stick models in green (S isomer), gray (R isomer). The yellow ribbon model represents active site region of the HIV-1 IN. The prominent active site amino acid residues are shown as stick models while magenta sphere represents  $Mg^{2+}$ .

### 3.5 INTEGRASE ASSAYS

In an attempt to evaluate the anti-IN activity sensitized compounds were tested according to the NCI Antiviral Drug Screening program using recombinant IN,  $^{32}\text{P}$ -labeled linear oligonucleotide, and metallic ions such as  $\text{Mn}^{2+}$  and  $\text{Mg}^{2+}$ .

A 21-mer oligonucleotide, labeled with  $^{32}\text{P}$  and corresponding to the U5-end of the HIV-1 proviral DNA, is allowed to react with purified HIV-1 IN together with a metallic ion. The initial step involves nucleolytic cleavage of two bases from the 3'-end, resulting in a 19-mer oligonucleotide. Subsequently, 3'-ends are then covalently joined to another identical oligonucleotide, which serves as the target DNA.

Gel electrophoresis technique allows to analyze and quantify the reaction products.

Percent inhibition (% I) was calculated using the following equation:

$$\% I = 100 [1 - (D - C) / (N - C)]$$

where C, N, and D are the fractions of 21-mer substrate converted to 19-mer (3'-processing product) or strand transfer products for DNA alone, DNA plus IN, and IN plus drug, respectively.

The  $\text{IC}_{50}$  values were determined by plotting the logarithm of drug concentration versus percent inhibition to obtain concentration that produced 50% inhibition. Synthesized compounds resulted equally potent in  $\text{Mg}^{2+}$ - and  $\text{Mn}^{2+}$ -based assays.

Moreover, these compounds were tested against other viral proteins (reverse transcriptase, protease, virus attachment, or nucleocapsid zinc fingers) none of them exhibited any detectable activities at 100  $\mu\text{M}$ , suggesting selectivity against IN.

### 3.6 CONCLUSIONS

In an attempt to identify new inhibitors of HIV-1 IN, we have synthesized and evaluated a series of thiazolothiazepines as novel leads for designing drugs against IN and HIV replication.

Docking studies demonstrated that these compounds interact with key residues as well as metal ion important for catalytic activity of IN. The fact that thiazolothiazepines are equally potent in  $Mg^{2+}$ - and  $Mn^{2+}$ -based assays suggests that the IN binding site by these compounds differs from previously reported inhibitors.

Moreover, the developed stereoselective synthetic procedure allowed the preparation of analogs in a single enantiomeric form, confirming that chirality is a crucial feature to be taken into consideration for optimizing compounds interaction into IN active site.

Another advantage of this class of compounds is that they are amenable for preparation of chemical libraries using recent advances in combinatorial chemistry.

In conclusion, the novel and straightforward preparation, the low cytotoxicity and the good selectivity against IN of synthesized compounds suggest that thiazolothiazepines have considerable promise as inhibitors of IN.

**PART 2**  
**ANTICANCER DRUGS**



## INTRODUCTION

Cancer is a word widely used to indicate a class of diseases characterized by uncontrolled division of cells and their ability to invade other tissues. These cells can proliferate either into adjacent tissue (invasion) or implant into distant sites where they can be transported through the bloodstream or lymphatic system (metastasis). Actually, cancer is responsible for about 25% of all deaths in the developed countries [65, 66].

Cancers are classified by the type of cancerous cells and, therefore, the tissue presumed to be the origin of the tumor.

Nowadays, most cancers can be treated. The choice of therapy depends on the site and character of the malignancy and whether there is metastasis. Once diagnosed, cancer is usually treated with a combination of surgery, radiotherapy and chemotherapy.

Theoretically, cancers can be cured if entirely removed by surgery, but this is not always possible. When cancer cells spread to other sites, by metastasis, prior to surgery, complete surgical excision is impossible. Instead, the effectiveness of radiotherapy is often limited by toxicity in normal tissues in the body. Treatment with chemotherapy drugs aims to target specific type of cancers, arresting the growth or killing the cancer cells.

Despite advances in technology and anticancer chemotherapy, there is still need to develop highly active, well-tolerated, and ideally orally active drugs, which exploit the increased understanding of tumor biology.

The available anticancer drugs have distinct mechanisms of action which may differ in their effects on different types of normal and cancer cells. Since there are several types of cancer and only very few demonstrable biochemical differences between cancerous cells and normal cells, the effectiveness of many anticancer drugs is limited by their toxicity to healthy cells. Because the common approach of chemotherapy is to kill or to decrease the growth rate (cell division) of cancer cells, the side effects are seen in bodily systems that naturally have a rapid turnover of cells including skin, hair, gastrointestinal, and bone marrow. Moreover, cancerous cells, which are initially suppressed by a specific drug, could easily develop resistance to that drug. For this reason cancer chemotherapy might consist of using several drugs in combination, for various lengths of time.

## **CHAPTER 4**

### ***ANTICANCER DRUGS AND NOVEL TRIALS IN DEVELOPMENT OF NEW COMPOUNDS***

## 4.1 ANTICANCER DRUGS

In general, chemotherapy agents can be classified into different categories, according to their mechanism of action:

- XAlkylating Agents
- XAntimetabolites
- XPlant Alkaloids
- XAntitumor Antibiotics
- XHormones/Antihormones
- XMiscellaneous

The structures of some representative anticancer therapeutics are shown in **Figure 23**.

### **Alkylating Agents**

These agents chemically damage DNA and RNA. In general, these drugs contain bifunctional reactive groups which alkylate DNA nucleotides resulting in strand breakage. Cyclophosphamide, cisplatin, nitrosoureas and some antibiotics, such as daunorubicin and doxorubicin, are examples of drugs belonging to this class.

### **Antimetabolites**

An antimetabolite is a chemical with a similar structure to a biological molecule (metabolite) required for normal biochemical reactions, but different enough to interfere with the normal functions of cells. Anti-metabolites (purine or pyrimidine analogs) become the building blocks of DNA, stopping normal cell division. They also affect RNA synthesis. Due to their efficiency, these drugs are the most widely used cytostatics. Examples of drugs



in this class are mercaptopurine and thioguanine (purine antagonists), 5-fluorouracil and cytarabine (pyrimidine antagonists). Methotrexate, a folic acid analogue, is also an antimetabolite. It prevents the formation of tetrahydrofolate, essential for purine and pyrimidine synthesis, by inhibiting dihydrofolate reductase and, consequently, the production of DNA, RNA and proteins.

### **Plant Alkaloids**

Most of the clinically useful agents in this class interfere with microtubule function. Some appear to be rather effective in select cancers, whereas others are used in a wide variety of tumors. For example, Vinca alkaloids, Vinblastine and Vincristine, bind to tubulin dimers and are incorporated into microtubules, blocking further assembly. This results in net depolymerization, which, in turn, arrests mitosis.

Taxol (Paclitaxel), a highly complex organic compound from bark of Pacific yew tree *Taxus brevifolia*, is one of most active of all anticancer drugs. It has the same net effect of Vinca alkaloids, but a completely different mode of action. Actually, it enhances microtubule polymerization.

### **Antibiotics**

Streptomycin derivatives are among the most useful and widely administered anticancer drugs available. These drugs act generally to block of DNA and/or RNA synthesis by intercalating into DNA and to induce DNA strand breaks. Examples of this class of drugs are Bleomycin, Mitomycin and Doxorubicin, which are perhaps the most important anticancer drugs in clinical use for treatment of a wide range of cancers (carcinomas, sarcomas, leukemias, lymphomas).

## **Hormones**

Synthetic glucocorticoids have been used to block growth of many different kinds of tumors, due to their strong anti-proliferative action. High doses of estrogens were previously used in breast and prostate cancers. Androgens and estrogen receptor antagonists have been successfully used as highly specific agents for cancers arising in the prostate and breast, respectively. Prednisone, Tamoxifen and Flutamide are some example of hormone based anticancer drugs.

Furthermore, there are various agents that don't belong to any of the above classes but are useful as anticancer drugs, such as monoclonal antibodies.

Recently, anticancer research has focused on development of compounds targeting physiological enzymes, often over-expressed in cancer cells, that modulate a wide variety of cellular functions, including cell differentiation, cell cycle progression, apoptosis, cytoskeletal modifications, and angiogenesis.

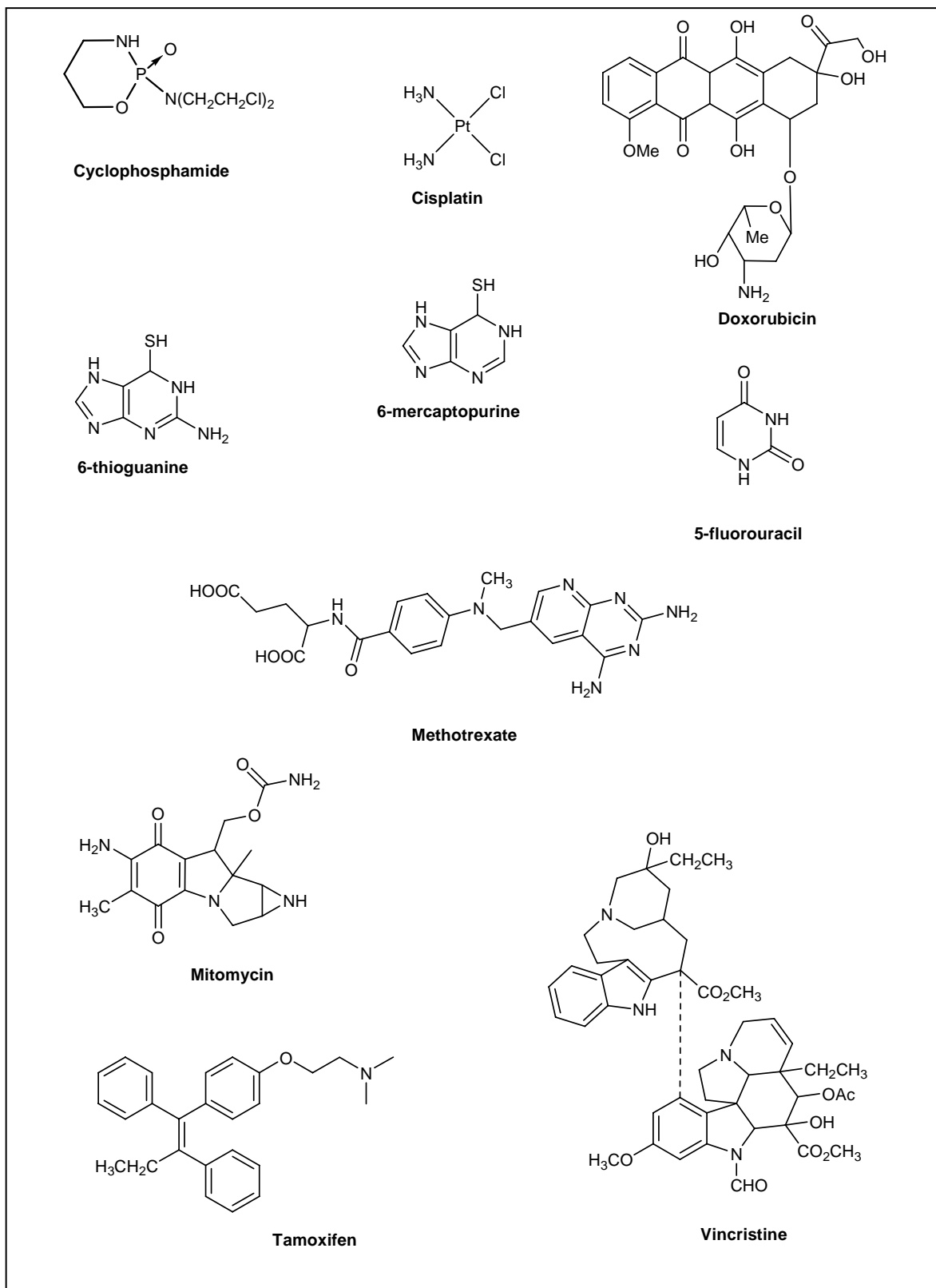


**Fig. 23** Representative examples of anticancer drugs

## 4.2 NOVEL TRIALS IN DESIGN AND DEVELOPMENT OF NEW ANTICANCER DRUGS

The improvement in diagnostic techniques as well as advances in synthesis and understanding of chemical principles accelerated enormously the discovery of new drug entities in the second half of the 20<sup>th</sup> century.

Unfortunately, despite the best advances in technology, cancer is at present most often diagnosed and treated when it is too late and metastasis has already occurred.

Consequently, there is a considerable interest in development of screening method to detect cancer diseases at earlier stages and discovery of new highly active, well-tolerated, and ideally orally active drugs.

Traditionally most anticancer drugs were discovered by high throughput screening with cytotoxicity as the end point measurement [67]. In general, most of these drugs have multiple mechanism of action and hence multiple mechanism of resistance, due to the abundance of sequence and structural homology into the biological systems [68]. Whatever the mechanism, one major hurdle to overcome, in any drug discovery program, is the identification of a suitable lead compound having desired biological activity on a validated target. Nowadays, genetic information is guiding the identification of single molecular target, since the knowledge that the genes of specific cell phenotypes encode proteins that may be involved in the pathogenesis of a particular disease state, such as a cancer disorder. Complementing the field of genomics, new proteomics technologies are under development to identify all the protein in a cell [69, 70].

Proteome has been defined as the protein complement expressed by a genome. By breaking proteins down into manageable pieces, researchers have been able to identify and quantify peptides using LC/MS and LC/MS/MS and correlate this information with the amount of protein expressed by the cell. Proteomics, through protein-protein association studies, could eventually provide a detailed map of all protein interactions in healthy and diseased cells and thus facilitate development of drugs that selectively target disease associated pathways while minimizing unwanted side effects [71].

Moreover, proteomic analysis allows the identification of proteins in response to drug treatment, resulting in a powerful approach to understand the mechanism of action of a drug.

Thus, in the near future, based on a combination of the genomic and proteomic portraits of the disease, an individualized selection of therapeutic combinations that best target the protein network could be selected and used.

Despite the considerable impact of these recent progresses, the discovery of novel therapeutics against cancer and their clinical application is still not straightforward.

Of over 100 FDA (Food and Drug Administration) approved anticancer drugs, fewer than 25 are widely used and only one-fifth of them have “drug-like” properties.

Drug-like properties usually refer to favorable absorption and good bioavailability that a drug must possess to enter clinical trials.

Preclinical evaluation of pharmacokinetic and pharmacodynamic properties and knowledge of drug metabolism are important in the drug development processes.

In the past, it was difficult to almost impossible to predict these characteristics for a specific compound. Recent technological advances in computer simulations have allowed absorption, distribution, metabolism, excretion, and toxicity (ADMET) prediction to become a reliable and rapid means of decreasing the time and resources needed to evaluate the therapeutic potential of a drug candidate [67].

Modern computers give the opportunity to organize and submit new compounds to a rigorous virtual screening to assess their “druggability” before resources are committed to additional research.

The progress in combinatorial chemistry and molecular genetic allowed automated synthesis of a large number of compounds for screening across in *in vitro* assay [72]. The valuation of the physico-chemical properties of the compounds being screened is the first filter in the modern High Throughput Screening (HTS) approach and the starting points for medicinal chemistry SAR (structure-activity-relationship) studies.

One of the most reliable computational methods in the early discovery setting is the “rule of five”. This approach allows the identification of compounds that possess acceptable range of calculate physico-chemical properties related to solubility, absorption and permeability.

This method is called the ‘rule of 5’ [73] because the cutoffs for each of the four parameters are all close to 5 or a multiple of 5.

The ‘rule of 5’ states that poor absorption or permeation is more likely when:

- The compound molecular weight is over 500;
- There are more than 5 H-bond donors;
- There are more than 10 H-bond acceptors;
- The logarithm of Partition Coefficient (Log P) [74] between a strongly hydrogen bonding solvents (like water) and a non polar solvent (like octanol) is over 5.

Based on these considerations and on previous studies results, we identified pyrroloquinoxalinyacylhydrazides derivatives as novel promising anticancer compounds with desirable ADMET properties.

Thus a novel and simple synthetic route has been developed to synthesize a series of derivative compounds, which satisfy ADMET computational calculations.

Successively these compounds have been evaluated in *in vitro* and *in vivo* assays against a range of human tumor cell type and some of them showed remarkable activity, confirming their potential application in clinical experimentation.

## **CHAPTER 5**

### ***SYNTHESIS AND BIOLOGICAL EVALUATION OF NOVEL ANTICANCER COMPOUNDS***

## 5.1 PRELIMINARY STUDIES

In previous studies, certain hydrazide-containing inhibitors of HIV-1 integrase exhibited significant cytotoxicity in cancer cell due to lack of selectivity for the viral enzyme [75].

Although HIV IN has no cellular homologue, its inhibitors may however inhibit other enzymes with similar active site chemistry. Because IN belongs to the large family of polynucleotidyltransferases [76], it is plausible that some of HIV IN inhibitors could target an unknown DNA-processing enzyme. Furthermore, several enzymes have a similar chemistry to IN of DNA binding, as well as DNA cleavage, and recombination [77]. Transposases, recombinases and other DNA processing enzymes are thought to share a common active site motif, including critical acidic amino acid residues, that require divalent metal such as  $Mn^{2+}$  and  $Mg^{2+}$  but not  $Ca^{2+}$  [78, 79].

For example, the similarities between retroviral integrases and topoisomerase prompted the evaluation of topoisomerase I and II poisons against integrase [80].

In a more recent study, even the most selective integrase inhibitors, DKAs, have also identified to inhibit bacterial recombinase enzymes, RAG1/2 [81].

Accordingly, we have been routinely using topoisomerases as a counter screen for integrase inhibitors [51, 53, 82, 83] and built a 10,000 compound database of reported and patented integrase inhibitors, which are in some instances likely to target additional DNA processing enzymes, possibly even more potently than integrase.

Using this database, we developed various pharmacophore models followed by toxicity prediction using ADMET Predictor software package (Simulations Plus, Inc., Lancaster, CA) and cluster analysis to separate a majority of antiviral compounds from cytotoxics [82].

On the basis of these pharmacophores, two compounds, **SC21** and **SC23** (**Figure 24**), belonging to the salicylhydrazide class, have been identified as potential leads with remarkably activity against a range of human derived cell lines [75].



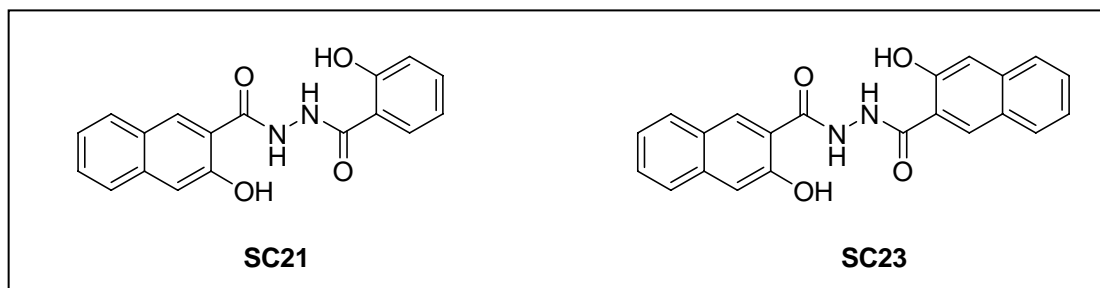


**Fig. 24** Previous HIV-IN leads with promising anticancer properties

Thus, in an effort to optimize the physicochemical properties of these compounds and assess a coherent mode of action, we have designed and synthesized several derivatives, taking also into consideration a different recent study, where pyrroloquinoxaline-based compounds has been identified as new class of small molecules possessing antiretroviral activity and promising pharmacokinetic properties [84].

In the light of these findings, a series of heterocyclic analogues were synthesized and SAR studies were conducted by appropriately varying the substituents on the benzo-fused ring of the quinoxaline system and by introducing different heteroacyl moieties. The tricyclic quinoxaline system resulted as a critical structural requirement for antiviral activity as well as a hydrazine linker between the two cyclic portions of the molecule.

The new antiviral compounds were showed to offer promising pharmacological and pharmacokinetic properties in terms of antiviral activity and oral bioavailability.

In the course of our research, aimed at identifying novel antiviral agents a series of pyrroloquinoxaliny compounds (**Figure 25**) has been prepared in order to establish structure-activity relationship and assess a coherent mode of action.

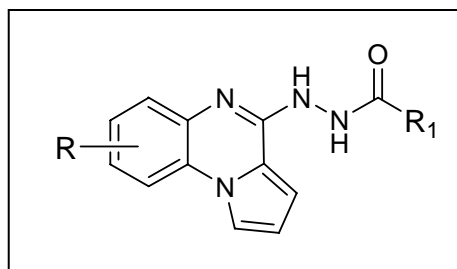


**Fig.25** Common structural features of new synthesized compounds.

Although these derivatives fitted in pharmacophore model of HIV IN, when subjected to *in vitro* IN assays, they showed to not satisfy the expectations. Therefore, pursuing the development of this class of compounds, we deeply searched I our in-house multiconformational database common structural features and pharmacophore fragments. Therefore, we tested the new compounds in initial cytotoxicity screens, showing remarkable activity in a panel of tumor cell lines.

Encouraged by these results, several new derivatives were synthesized and after *in silico* calculation of a host of parameters, including physicochemical, pharmacokinetic and drug-like properties for oral absorption (using ADMET Predictor software package), we selected compound **36** (Figure 26) for further evaluation.

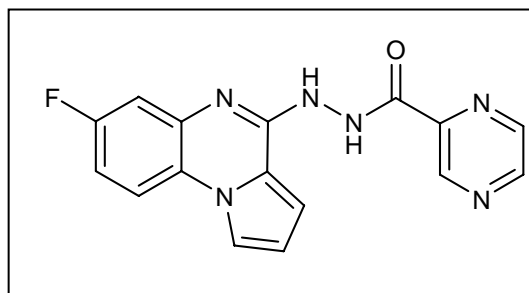


**Fig.26** Chemical Structure new lead: compound **36**

Actually, this compound showed superior potency in many cell lines when compared to many of its very close analogues and was successively chosen for preclinical studies, resulting in a very promising compound with desired drug-like properties.

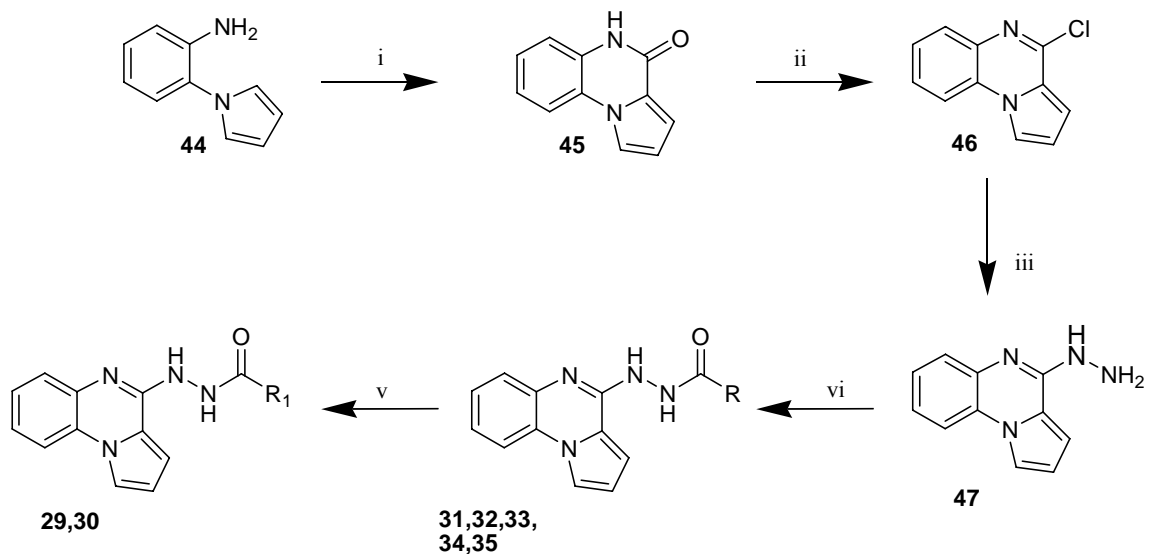
## 5.2 CHEMISTRY

The synthetic procedures for the preparation of compounds **29-35** and **36-43** (Tables 3) are shown in **Scheme 4** and **Scheme 5**, respectively.

COMPOUND	STRUCTURE	COMPOUND	STRUCTURE
29		36	
30		37	
31		38	
32		39	
33		40	
34		41	
35		42	
		43	

Table 3. Chemical Structure Compounds 29-43

## SCHEME 4



The synthesis of compounds **29-35** has been accomplished starting from the commercially available 1-(2-aminophenyl)pyrrole **44**. Compound **44** was treated with triphosgene in toluene under reflux to give **45** in quantitative yield. The lactam obtained was subsequently transformed into 4-chloro-1*H*-pyrrolo[1,2-*a*]quinoxaline **46** by treatment with phosphoryl chloride. Reaction of **46** with hydrazine monohydrate in DMF afforded 4-hydrazinopyrrolo[1,2-*a*]quinoxaline **47**.

The hydrazine derivative was reacted with the appropriate carboxylic acid to give compounds **31-35**. This condensation reaction was carried out under different experimental conditions and using several coupling reactants, such as DCC (dicyclohexylcarbodiimide),

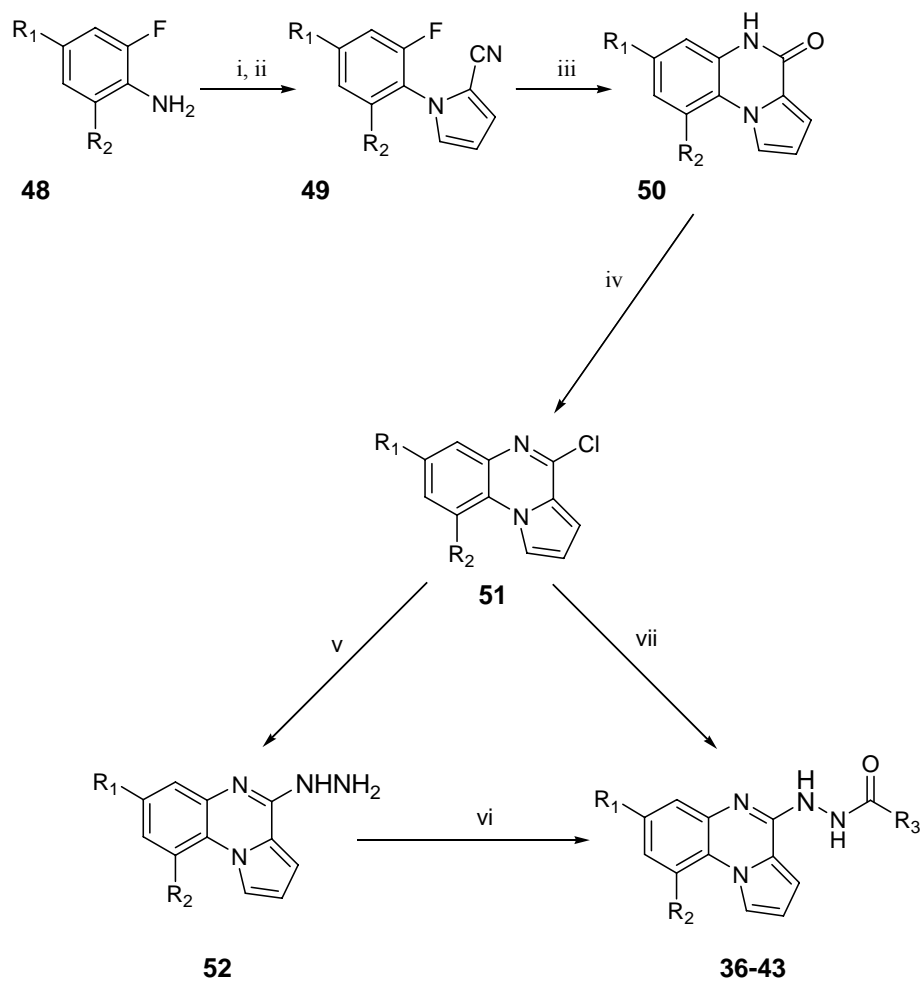
BOP, EDC or CDI. However, the best results were achieved by using EDC in the presence of DMAP.

The preparation of **29** and **30** was accomplished by a condensation step, using a procedure identical to that described for the preceding compounds but using the appropriate *N*-Boc-aminoacid, followed by a deprotection step using trifluoroacetic acid and anisole (**Scheme 4**).

Since the presence of a fluorine atom on pyrroloquinoxaline tricyclic ring seemed to be an important structural feature for the anticancer activity for these derivatives, a modification of the above procedure was developed for the synthesis of compounds **36-43**.

Commercially available difluoroanilines **48**, bearing a fluorine atom at position 2 as leaving group, were chosen as starting material. These were subjected to Clauson-Kaas reaction with 2,5-dimethoxytetrahydrofuran to give corresponding arylpyrroles, which were transformed into the corresponding 2-carbonitrile derivatives **49** after a one-pot modified Vilsmeier-Haack reaction. The nitriles were directly cyclized to tricyclic lactames by potassium hydroxide in boiling *tert*-butanol. The lactames obtained were subsequently transformed into corresponding chloro-derivatives by treatment with phosphoryl chloride. Chloro-derivatives **51** were finally converted into the desired hydrazine derivatives, which in turn were reacted with a proper carboxylic acid in presence of triphenylphosphine and 2,2'-dipyridyldisulfide to give the expected final compounds **36-43** [85].

**SCHEME 5**



i = 2,5-Dimethoxytetrahydrofuran / AcOH  
 ii = a) POCl<sub>3</sub> / DMF; b) NH<sub>2</sub>OH · HCl / AcONa ; c) Ac<sub>2</sub>O  
 iii = KOH / t-BuOH  
 iv = POCl<sub>3</sub>  
 v = NH<sub>2</sub>NH<sub>2</sub> · H<sub>2</sub>O / MeOH  
 vi = R<sub>3</sub>COOH / EtOH  
 vii = R<sub>3</sub>CONH<sub>2</sub> / EtOH  
 R<sub>1</sub>, R<sub>2</sub>, R<sub>3</sub> see **Table 5**

Despite the high yield gained for the preparation of all intermediates, the latter step furnished the final compound in very low yield. Therefore, an alternative method for the synthesis of the final product was planned. Accordingly, the chloro-derivative intermediates were directly reacted with a preformed acylhydrazides in ethanol under reflux. Acylhydrazides were in turn prepared by reaction of specific methyl carboxylates with hydrazine monohydrate [86].

This simple modification allowed to obtain compounds (as hydrochloride salts) in high yield and very good purity (**Scheme 5**) [87].

Moreover, the possibility to obtain final compounds directly as salts should promote an improved solubility in physiological fluids. This is a clear advantage that enhances the value of the entire synthetic pathway.

## 5.3 PHARMACOLOGICAL STUDIES

All synthesized compounds have been firstly subjected to ADMET computer simulations to evaluate their pharmacokinetic properties and all of them satisfy the Lipinski's "rule of five" as shown in **Tables 4** and **5**.

For example, the most active compound, namely derivative **38**, has a molecular weight of 322.3 (MW < 500), calculated Log P of 1.82 (cLog P < 5), number of hydrogen bond donor of 2 (HBD < 5), and number of hydrogen bond acceptor of 6 (HBA < 10). In addition, compound **38** with only three rotatable bonds is very compact. Successively, the new compound have been tested in different cancer cell lines to evaluate the antitumor activity.

### 5.3a Cytotoxicity assays

An initial cytotoxicity screen was carried out using 3-(4,5-dimethylthiazol-2-yl)-2,5-diphenyltetrazolium bromide (MTT) assay [88, 89]. MTT assay is based on the ability of a mitochondrial dehydrogenase enzyme from viable cells to cleave the tetrazolium ring of the pale yellow MTT and form dark blue formazan crystals (**Figure 27**) which is largely impermeable to cell membranes, thus resulting in its accumulation within healthy cells. Solubilisation of the cells, by the addition of a detergent, results in the liberation of the crystals which are solubilized. The number of surviving cells is directly proportional to the level of the formazan product created. The results can be easily read and processed on a multiwell scanning spectrophotometer.

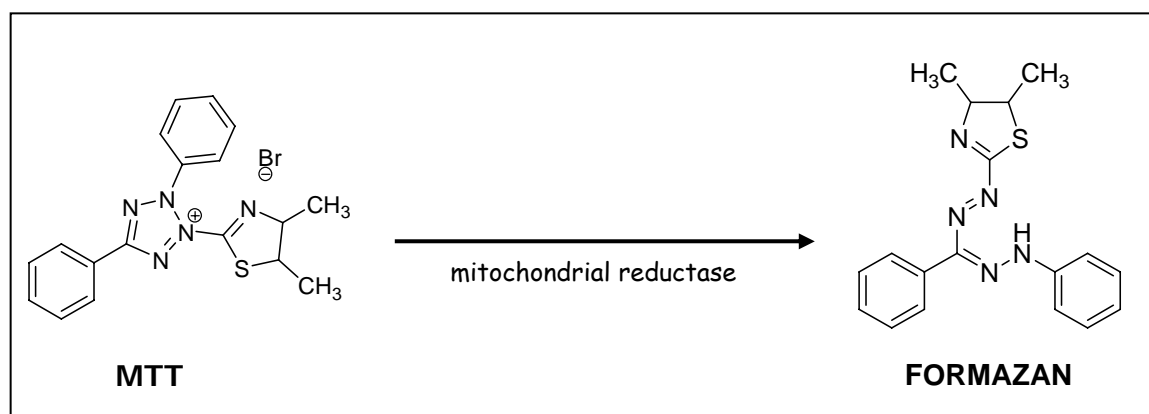


**Fig.27** MTT reaction in viable cells



Table 4

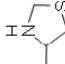
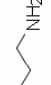
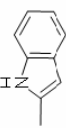
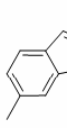
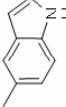
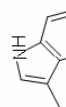
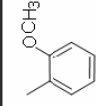
CMPD	R	R <sub>1</sub>	IC50 [μM]				Mol. Weight	Acid-pred pKa	Basic-pred pKa	S+logP	N_FrRotB	HDB	HBA
			MDA-MB 435	HCT 116 p53++	HCT 116 p53--	HT 29							
29			>20	15 ± 3	10 ± 2	14 ± 1	313.4	10.31	6.17; 3.71; -1.06; -3.85	1.21	4	3	5
30			>20	>20	>20	>20	268.3	10.4	8.54; 4.14; -0.81; -3.78	0.71	5	3	5
31			>20	>20	>20	>20	341.4	9.48; 11.93	4.15; 1.54; -1.19; -3.94	3.21	3	3	4
32			>20	>20	>20	>20	341.4	9.86; 14.18	4.13; 1.59; -0.69; -3.77	3.20	3	3	4
33			>20	>20	>20	>20	341.4	9.87; 14.50	4.17; 2.05; -0.59; -3.64	3.18	3	3	4
34			>20	>20	>20	>20	341.4	9.75; 12.75	4.21; 2.11; -0.90; -3.80	3.19	3	3	4
35			>20	>20	>20	>20	392.3	9.69	3.92; -1.10; -4.17	3.18	4	2	5

Table 5

CMPD	R <sub>1</sub>	R <sub>2</sub>	R <sub>3</sub>	IC50 [μM]											
				MDA-MB 435	HCT 116 p53++	HCT 116 p53--	HT 29	hLN- CAP	Mol. Weight	Acid- pred pKa	Basic-pred pKa	S+ logP	N_Fr RotB	HD B	HBA
36	F	H		4 ± 0.1	0.6 ± 0.07	0.9 ± 0.04	0.9 ± 0.06	0.4 ± 0.1	322.3	9.08	3.52; 0.97; -0.95; -2.79; -5.21	1.79	3	2	6
37	F	H		>20	>20	>20	17	>20	321.3	9.3	3.69; 0.66; -1.32; -3.58	2.50	3	2	5
38	H	F		3 ± 2	0.4 ± 0.01	0.3 ± 0.07	0.3 ± 0.06	0.4	322.3	9.08	3.31; 0.91; -0.97; -2.79; -5.20	1.82	3	2	6
39	F	H		>20	>20	>20	>20	NT	321.3	9.5	3.84; 2.37; -0.75; -3.13	2.16	3	2	5
40	F	H		>20	>20	>20	>20	NT	338.3	9.24	3.59; -1.28; -3.90	3.18	3	2	4
41	F	H		>20	>20	>20	>20	NT	326.3	9.52	3.65; -1.28; -3.85	3.10	3	2	4
42	F	H		>20	>20	>20	>20	NT	310.3	9.27	3.49; -1.43; -4.11	2.61	3	2	5
43	F	H		15 ± 1	8 ± 1	11 ± 1	13 ± 2	NT	372.3	8.9	3.55; 1.18; -0.93; -2.73; -4.88	2.83	3	2	6

Cytotoxic concentration (IC50) is defined as drug concentration causing a 50% decrease in cell population using MTT assay as described in the experimental section. MDA-MB-435: breast cancer cells, HCT and HT29: colon cancer cells, LnCap: prostate cancer cells. MW = molecular weight, S+LogP: logarithm of permeability (SimulationsPlus, Inc.), Rbond: number of rotatable bond, HBD: number of hydrogen-bond donor, HBA: number of hydrogen-bond acceptor.

To make comparative studies, compounds **29-43** were subjected to colony formation assay[90]. This is a clonogenic cell survival assay, which is based on the ability of a cell to proliferate indefinitely, thereby retaining its reproductive ability to form a large colony or a clone. This cell is then said to be clonogenic. In general, this assay is extensively used for research and clinical applications to assess the functional integrity of cells after in vitro manipulations. Thus, it is useful to predict the response of tumour cells to chemotherapeutic agents. Furthermore, this assay permits the differentiation of cytostatic effects of compounds, where the number of colonies and size remains constant, and cytotoxic effects where the size and number may be reduced.

Cell colony formation has been found to be a more sensitive parameter of toxicity than cell viability since it is assessed while the cells are in a state of proliferation, and more susceptible to toxic effects. Traditionally, enumeration of colonies has involved laborious counting by hand using a microscope. Recent advances have provided automatic number counting colonies using digital colour cameras which, with the accompanying software, allows a number of different colony colours to be distinguished.

In **Figure 28**, MTT and Colony Formation assays results for compounds **36** and **38** are shown as representative examples.

All compounds were tested in four human cancer cell lines, a breast cancer cell MDA-MB-435 and three colon cancer cells. Compound **29** was moderately active against colon cancer lines and inactive against the breast cancer line. All other indole analogues (**30-35**) were inactive at 20  $\mu\text{M}$  (**Table 4**). In the pyridino and pyrazino derivatives position of the nitrogen atom on the ring, as well as the fluorine substitute on the tricycle system appeared to be important for activity. For example, **37** and **39** were inactive, whereas **36** and **38** were highly active in all cell lines. In particular, compound **36** showed an excellent activity in a panel of cancer cell lines from different tumor origins with  $\text{IC}_{50}$  dose range of 0.5 to 4.0  $\mu\text{M}$  (**Table 5**).

Furthermore, in all tested cell lines, compound **38** with  $\text{IC}_{50}$  value ranges from 0.3 to 4  $\mu\text{M}$  was more potent than the selected **36**. Interestingly, in colony formation assay at doses above 1  $\mu\text{M}$ , both **36** and **38** completely abolished cell growth (**Figure 28**).

Among all synthesized compounds, **36** has been selected for further preliminary pharmacological studies on the basis of its potency against all cell lines and its desirable physicochemical and “drug-like” properties.

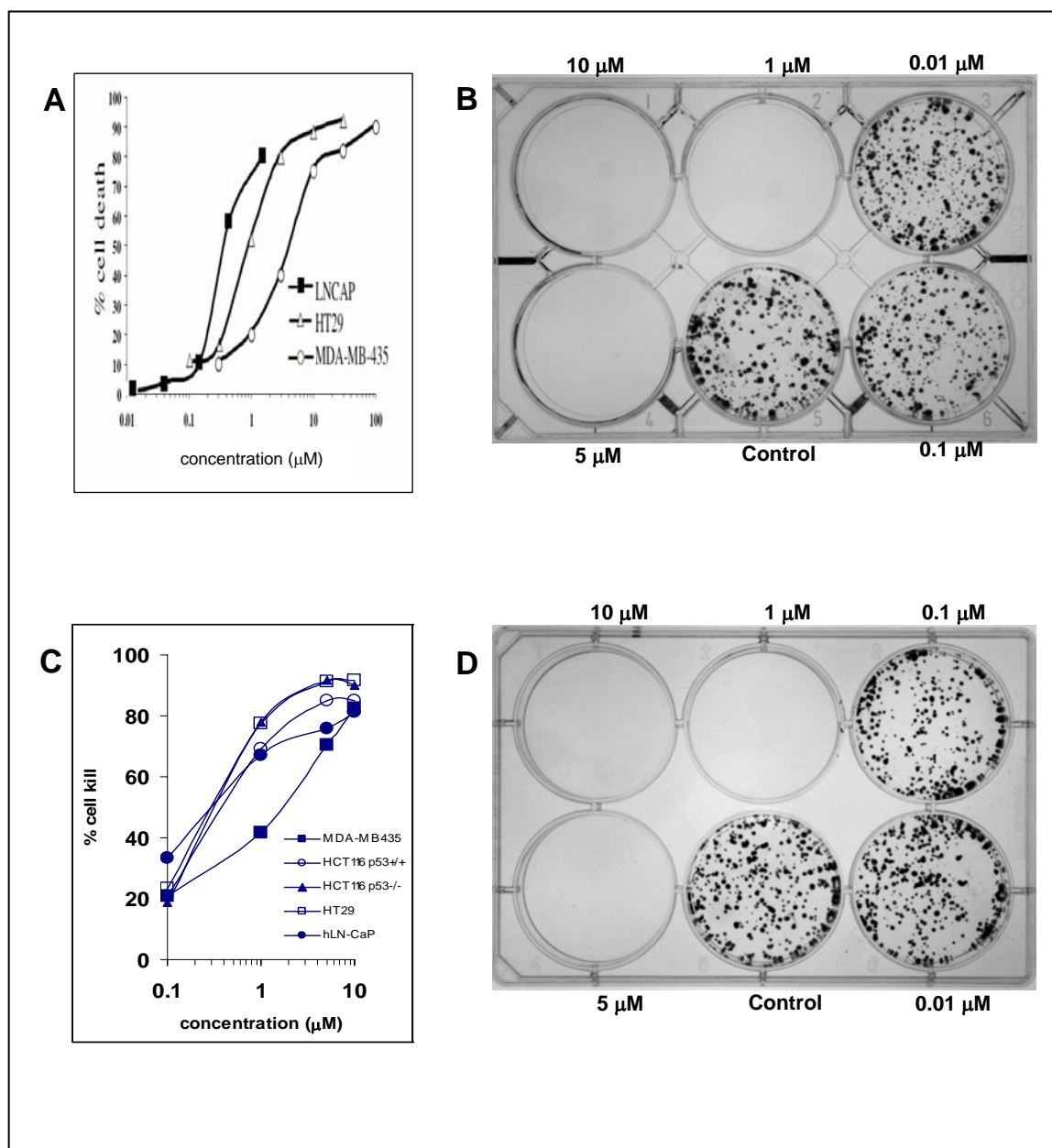


**Fig. 28** MTT and Colony formation results for compound **36** (A and B) and **38** (C and D)

### 5.3b Flow cytometry studies

Cell cycle perturbations induced by compound **36** were examined in HEY cells (cisplatin resistant cells). The analysis of DNA profiles by indicated that this compound induced S-phase. Nearly 80% of the cells were still retained in S-phase after 24 hours of treatment with **36** (3  $\mu$ M). The maximum arrest in HEY cells was observed at 24 hours of drug exposure, which was sustained up to 48 hours.

Furthermore, flow cytometry studies indicated that compound **36** induce apoptosis (**Figure 29**). At 10  $\mu$ M, **36** caused 15% apoptosis as indicated by sub-G<sub>0</sub>/G<sub>1</sub> population. An early event in apoptotic cell death is the translocation of the phosphatidyl-serine residues to the outer part of the cell membrane.

This event precedes nuclear breakdown, DNA fragmentation and the appearance of most apoptosis-associated molecules and is readily measured by annexin V binding assay. By this method, we compared compound **36** with camptothecin (CPT).

As shown in **Figure 29**, **36** induced early apoptosis comparable to that induced by CPT.

The percentage of early-apoptotic cells increased in treated cells reaching 37% and 34% at 48 hours for **36** and CPT, respectively. At 48 hours an increase in late-apoptosis/necrosis was also observed for both compounds (16% and 39% for **36** and CPT, respectively).

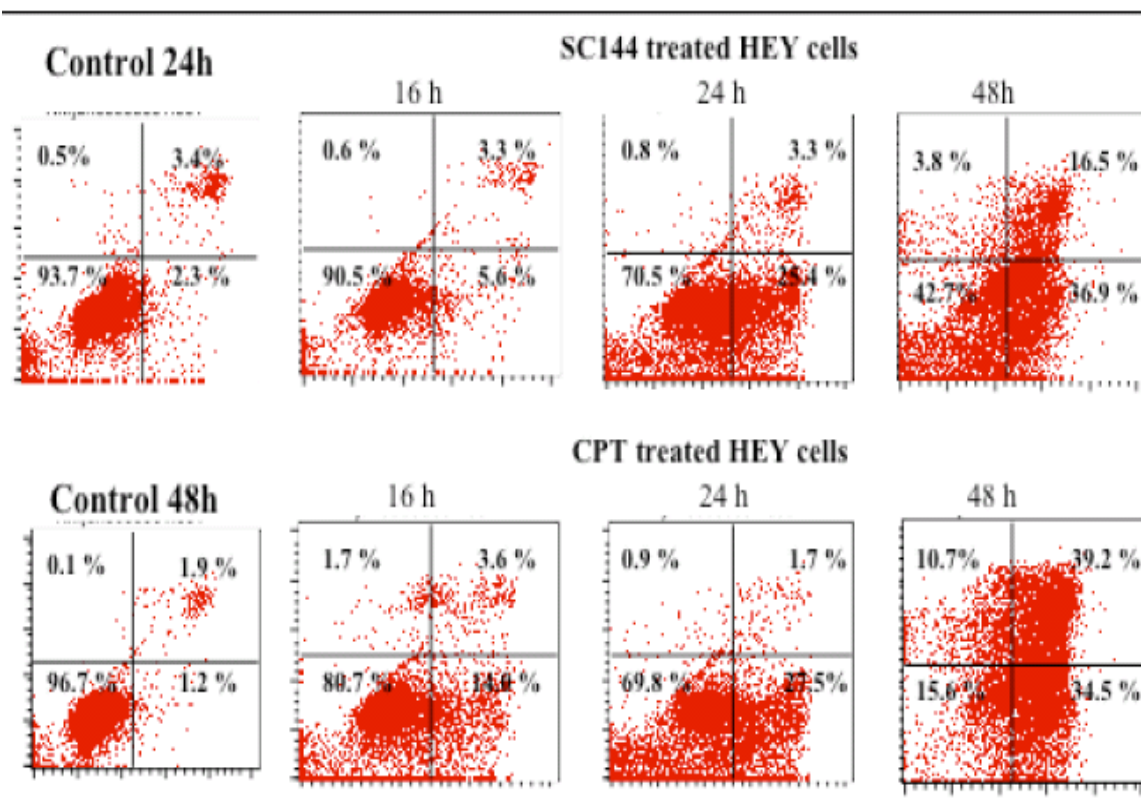


**Fig. 29** Apoptosis analysis of HEY cells treated with 36 and CPT (IC80). Cells were stained with annexin V/propidium iodide and analyzed by flow cytometry. Cells in the bottom left quadrant of each panel (Annexin V-negative, propidium iodide-negative) are viable, whereas cells in the bottom right quadrant (Annexin V-positive, propidium iodide-negative) are in the early stages of apoptosis, and cells in the top right quadrant (Annexin V-positive, propidium iodide-positive) are in later stages of apoptosis and necrosis.

### 5.3c Preliminary *In Vivo* Studies

The good results obtained in *in vitro* essays encouraged us to start preliminary in *in vivo* experimentation. The *in vivo* efficacy of compound **36** was evaluated in nude mice xenograft model of human breast MDA-MB-435 cells.

Animals were treated with a daily i.p. injections of saline (controls) and **36** at 0.3 mg/kg, 0.8 mg/kg and 4 mg/kg. After fifteen-days of dosing, the drug treatment was discontinued and the animals were monitored biweekly for five weeks.

For statistical analysis the %T/C value was calculated on day 31 of dosing and is plotted for all of the treatment groups. A moderate but significant reduction was observed at the lowest dose of compound **36** in breast cancer xenografts ( $p < 0.05$  at day 31).

Significant reduction in tumor growth was observed at higher doses.

The selected compound reduced tumor growth by 60% at 4 mg/Kg ( $p < 0.001$ ). Whereas in control mice, tumor mass became bulky, spread all around the chest cavity, and densely vascularized, the treated tumors were markedly decreased in size, poorly vascularized and remained localized.

Treatment with compound **36** was well tolerated and did not result in drug-related deaths. Furthermore, no changes in body weight compared to vehicle control were observed.

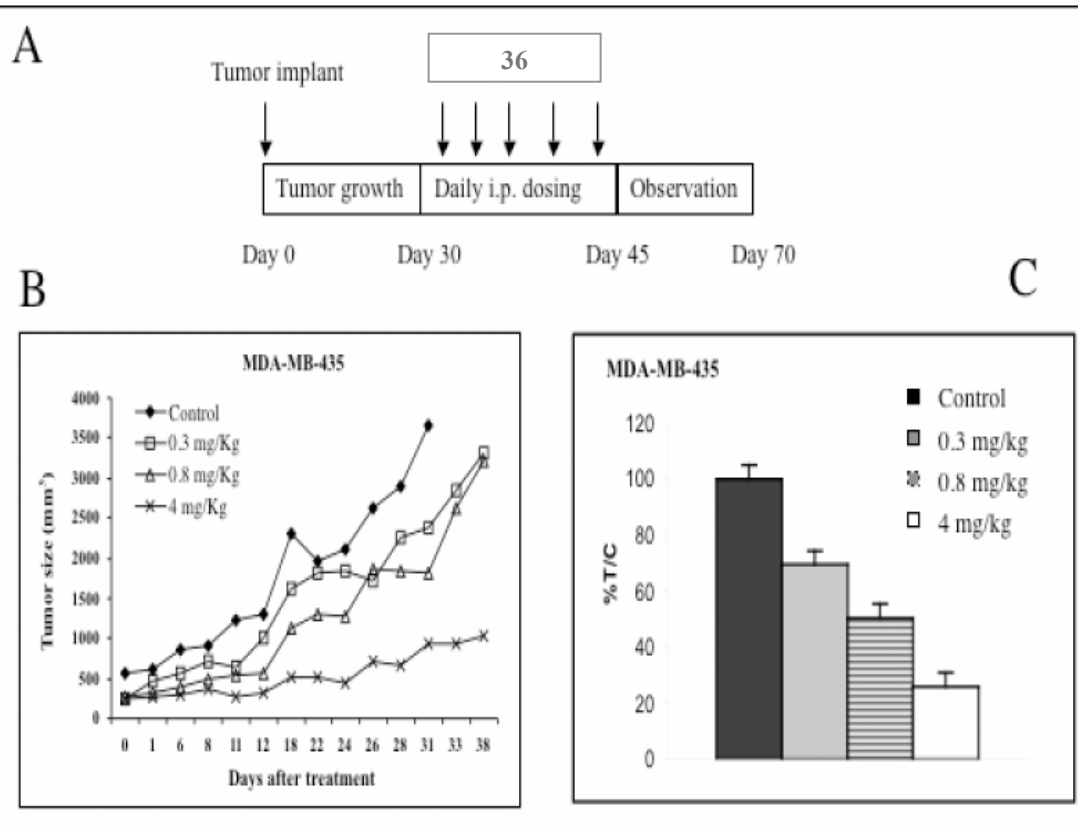


**Fig. 30** A) Schematic outline of tumor growth and dosing in xenograft models. Athymic nude mice ( $n = 10$ ) implanted with MDA-MB-435 cells were treated with the indicated doses of **36** compound by daily i.p. administration for 15 days. B) **36** reduced the size of human breast cancer xenografts at doses of 0.3, 0.8 and 4 mg/Kg. Tumor growth was monitored for five weeks. Values represent the median tumor weight for each group. C) The %T/C for each treatment group was calculated on day 31 of experiment (bars  $\pm$  SD).



## 5.4 CONCLUSION

In conclusion, considering their cytotoxicity profiles in a variety of in vitro systems and their favorable pharmacokinetic properties, pyrroloquinoxaliny derivatives seem to represent a novel class of anticancer drugs. Although the elucidation of the mechanism of action of these compounds is under active investigation, these agents showed promising therapeutic potential. A number of characteristics of synthesized compounds suggest that they have considerable potential as a possible anticancer chemotherapeutics.

Since they are small-molecules, thus readily cross membranes, and are stable under physiological conditions, unlike peptides or oligonucleotides, do not need significant chemical modification to enhance cell-permeability and stability.

The developed synthetic route is straightforward and simple. This results in a clear advantage over compounds that can only be prepared in low yield due to multiple synthetic steps.

Further studies are under investigation to developing a more comprehensive structure–activity relationship amongst these novel compounds. Whereas proteomic studies are in progress to better understand the mechanisms involved in the activity of pyrroloquinoxaliny derivatives in order to identify crucial features for the remarkable antitumor activity.

# **GENERAL EXPERIMENTAL CHEMISTRY**

## Experimental

All reactions were carried out under a nitrogen atmosphere. The reaction progress was monitored by TLC on silica gel plates (Merck 60, F254, 0.2 mm). Organic solutions were dried over MgSO<sub>4</sub>. Evaporation refers to removal of solvent on a rotary evaporator under reduced pressure. Melting points were measured using a Gallenkamp apparatus and are uncorrected. Specific rotations  $[\alpha]_D$  were determined to the stated temperature and conditions by a Perkin–Elmer 343 polarimeter. IR spectra were recorded as thin films on Perkin-Elmer 398 and FT 1600 spectrophotometers. <sup>1</sup>H NMR spectra were recorded on a Brüker 300-MHz spectrometer with TMS as an internal standard: chemical shifts are expressed in  $\delta$  values (ppm) and coupling constants (*J*) in Hz. Mass spectral data were determined by direct insertion at 70 eV with a VG70 spectrometer. Merck silica gel (Kieselgel 60/230-400 mesh) was used for flash chromatography columns. Elemental analyses were performed on a Perkin-Elmer 240C elemental analyzer, and the results are within  $\pm 0.4\%$  of the theoretical values. Yields refer to purified products and are not optimized.

## Thiazolothiazepine and Thiazoloxazepine derivatives

### (±)-2,3-Dihydro-5*H*,13*aH*-naphto[2,3-*c*][1,4]-thiazolo[2,3-*c*][1,4]thiazepine -5,13-dione (**1**)

A mixture of 3,3'-dithio-2,2'-dinaphthoic acid **18** (0.5 g, 1.3 mmol) and thionyl chloride (1.82 mL) was refluxed for 2 h. After cooling, the excess of thionyl chloride was removed under vacuum with the aid of dry benzene (2-5 mL). The resulting solid was dissolved in dry THF (20 mL), and the solution was added dropwise to a mixture of (±)-thiazolidine-2-carboxylic acid **14** (0.33 g, 2.46 mmol) and sodium carbonate (0.13 g, 1.23 mmol) in water. Additional sodium carbonate was added from time to time to maintain a weakly alkaline pH. The mixture was stirred overnight, then concentrated, and made acidic (pH 3-4) by adding concentrated HCl. The gummy solid was extracted into ethyl acetate, and the resulting solution was washed with water, dried, and evaporated to give a foam product. Column chromatography (ethyl acetate: toluene: methanol: formic acid, 10:10:1.5:0.5 as solvent) gave almost pure corresponding disulfide as an amorphous solid. Such a material (0.41 g, 0.64 mmol), was dissolved in 85% ethanol (10 mL) containing NaOH (50 mg) and to this was added a solution of NaBH<sub>4</sub> (1.14 g, 30 mmol) in ethanol (50 mL). The mixture was stirred overnight at room temperature, then concentrated, and diluted with chilled water. The cold solution was left at room temperature for 15 min before being filtered and made acidic (pH 3-4) by HCl 1N. The gummy solid was extracted into ethyl acetate and then thoroughly dried under vacuum before being subjected to the successive reaction without further manipulation. Crude thiophenol derivative (0.39 g, 95% yield) was dissolved into dry THF (10 mL), and *N,N*-carbonyldiimidazole (0.21 g, 1.30 mmol) was added in portions. The solution was stirred for 40h at room temperature. The solvent was evaporated, and the residue was partitioned between CHCl<sub>3</sub> and 0.5 N HCl. The organic solution was separated and washed with NaHCO<sub>3</sub>-saturated solution and water. After drying and evaporation of the solvent, a pasty residue was obtained and purified by flash chromatography (8% methanol in EtOAc) to give 0.12 g (36 % yield for the entire process from **14**) of **1** as a white powder: mp 196-198

°C (benzene); IR (KBr) 1720, 1660  $\text{cm}^{-1}$ ;  $^1\text{H}$  NMR ( $\text{CDCl}_3$ )  $\delta$  (ppm): 8.52 (s, 1H), 7.99 (s, 1H), 7.93 (m, 1H), 7.84 (m, 1H), 7.63 (m, 2H), 5.44 (s, 1H), 4.11 (m, 2H), 3.16 (m, 2H). MS (EI)  $m/z$  301 ( $\text{M}^+$ ) Anal. ( $\text{C}_{15}\text{H}_{11}\text{NO}_2\text{S}_2$ ) C, H, N.

**(±)-1,13a-Dihydro-3H5H,13H-naphto[2,3-f]-thiazolo[4,3-c][1,4]thiazepine -5,13-dione (2)**

Starting from **18** and the title compound **2** was obtained (0.18 g, 25% yield for the entire process) adopting the same procedure as for **1** but using (R)-(-)-Thiazolidine-4-carboxylic acid **13** instead of **14**: mp 200-202 °C (benzene); IR (KBr) 1720, 1650  $\text{cm}^{-1}$ ;  $^1\text{H}$  NMR ( $\text{CDCl}_3$ )  $\delta$  (ppm):  $^1\text{HNMR}(\text{CDCl}_3)$   $\delta$  (ppm): 8.51(s, 1H), 7.98 (s, 1H), 7.94 (m, 1H), 7.84 (m, 1H), 7.58 (m, 2H), 4.97 (0.5 di ABq, 2H,  $J = 10.6$  Hz), 4.73 (0.5 di ABq, 2H,  $J = 10.6$  Hz), 4.66 (dd, 1H,  $J = 6.9, 1.6$  Hz), 3.65 (dd, 1H,  $J = 11.8, 1.46$  Hz), 3.14 (dd, 1H,  $J = 12.0, 6.7$  Hz). MS (EI)  $m/z$  301 ( $\text{M}^+$ ) Anal. ( $\text{C}_{15}\text{H}_{11}\text{NO}_2\text{S}_2$ ) C, H, N.

**(±)-1,13a-Dihydro-3H,5H,13H-naphtho[2,3-f]oxazolo[4,3-c][1,4]thiazepine-5,13-dione (3)**

This compound was prepared starting from oxazolidine-4-carboxylic acid **15** and 3,3'-dithio-2,2'-dinaphthoic acid **18**, essentially as described for compound **1**. Compound **3** was obtained as a colorless solid (21% for the entire process from **15**): mp 154–156°C (dichloromethane/petroleum ether); IR (KBr) 1695, 1635  $\text{cm}^{-1}$ ;  $^1\text{H}$  NMR ( $\text{CDCl}_3$ )  $\delta$  (ppm): 8.57 (1H, s), 8.02 (1H, s), 7.97 (1H, m), 7.85 (1H, m), 7.63 (2H, m), 5.34 (1H, 0.5 of ABq,  $J = 5.4$  Hz), 5.23 (1H, 0.5 of ABq,  $J = 5.4$  Hz), 4.85 (1H, d,  $J = 8.6$  Hz), 4.34 (1H, d,  $J = 5.8$  Hz), 3.98 (1H, dd,  $J = 8.6$  and 5.8 Hz); MS (EI)  $m/z$  285 ( $\text{M}^+$ ). Anal. ( $\text{C}_{15}\text{H}_{11}\text{NO}_3\text{S}$ ) C, H, N.

**(1R,11aS)-1,11a-Dihydro-1-methyl-3H,5H,11H-oxazolo[4,3-c][1,4]benzothiazepin-5,11-dione (4)**

Starting from (4S,5R)-oxazolidine-5-methyl-4-carboxylic acid **16** and 2,2'-dithiodibenzoic acid **17**, compound **4** was obtained as colorless crystals (32% for the entire process from **11**): mp 94–96°C (diethyl ether/light petroleum);  $[\alpha]_d^{21}$  -95.5 (*c* 1, CHCl<sub>3</sub>); IR (KBr) 1705, 1645 cm<sup>-1</sup>; <sup>1</sup>H NMR (CDCl<sub>3</sub>)  $\delta$  (ppm): 8.01 (1H, m), 7.47 (3H, m), 5.51 (1H, 0.5 of ABq, *J* = 5.8 Hz), 5.02 (1H, 0.5 of ABq, *J* = 5.8 Hz), 4.95 (1H, m), 3.83 (1H, d, *J* = 3:7), 1.31 (3H, d, *J* = 6.2); MS (EI) *m/z* 249 (M<sup>+</sup>). Anal. (C<sub>12</sub>H<sub>11</sub>NO<sub>3</sub>S) C, H, N.

**(1R,13aS)-1,13a-Dihydro-1-methyl-3H,5H,13H-naphtho[2,3-f]oxazolo[4,3-c][1,4]thiazepine-5,13-dione (5)**

Starting from (4S,5R)-oxazolidine-5-methyl-4-carboxylic acid **16** and 3,3'-dithio-2,2'-dinaphthoic acid **17**, compound **5** was obtained as colorless needles (37% for the entire process from **17**): mp 163–165°C (diethyl ether/light petroleum);  $[\alpha]_d^{21}$  - 121.0 (*c* 1, CHCl<sub>3</sub>); IR (KBr) 1700, 1645 cm<sup>-1</sup>; <sup>1</sup>H NMR (CDCl<sub>3</sub>)  $\delta$  (ppm): 8.60 (1H, s), 8.12 (1H, s), 8.00 (1H, m), 7.80 (1H, m), 7.60 (2H, m), 5.56 and 5.09 (2H, ABq, *J* = 5.5 Hz), 4.99 (1H, dq, *J* = 6.5 and 3.4 Hz), 3.93 (1H, d, *J* = 3.4), 1.29 (3H, d, *J* = 6.5); MS (CI) *m/z* 300 (M<sup>+</sup>). Anal. (C<sub>16</sub>H<sub>13</sub>NO<sub>3</sub>S) C, H, N.

## General procedure for the synthesis of compounds 23

The preparation of compound **23c** is described as a representative example

### **N-(3-Acetoxy-2-naphthoyl)oxazolidin-4-carboxylic acid (23c)**

A mixture of formaldehyde (37% solution in water, 14.0 mmol, 1.0 mL), L-serine (1.4 g, 13.3mmol), and 2N NaOH (6.5 mL) was stirred overnight at 0°C. Sodium carbonate (0.7 g, 6.6mmol) was added in one portion to the cold solution. A solution of 3-acetoxy-2-naphthoic acid chloride (3.3 g, 13.3mmol) in dry THF (20 mL) was then added dropwise, while a weakly alkaline pH was maintained by the addition of solid sodium carbonate. The mixture was stirred overnight, then concentrated and made acidic (pH 3–4) by adding concentrated HCl. The solid formed was extracted into ethyl acetate, and the resulting solution was washed with water, dried, and evaporated. The resulting residue was purified by column chromatography on silica gel (CHCl<sub>3</sub>:CH<sub>3</sub>OH:HCO<sub>2</sub>H, 86:14:1) to give a yellow solid (3.0 g, 70%).

IR (KBr) 2700 (br), 1715, 1690, 1635cm<sup>-1</sup>; <sup>1</sup>H NMR (CDCl<sub>3</sub>) δ (ppm): 9.57 (1H, br, exch. with D<sub>2</sub>O), 7.78–7.65 (3H, m), 7.48 (1H, m), 7.32 (2H, m), 5.30 (2H, s), 5.01 (1H, t, *J*=6,7 Hz), 4.40 (1H, m), 4.09 (1H, m), 2.31 (3H, s); MS (EI) *m/z* 329 (M<sup>+</sup>). Anal. (C<sub>17</sub>H<sub>15</sub>NO<sub>6</sub>) C, H, N.

## General procedure for the synthesis of compounds 24

The preparation of compound **24c** is described as a representative example

### **N-(3-hydroxy-2-naphthoyl)oxazolidin-4-carboxylic acid (24c)**

N-(3-Acetoxy-2-naphthoyl)oxazolidin-4-carboxylic acid (2.0 g, 6.0 mmol) was dissolved in a solution of sodium carbonate (0.8 g, 7.5 mmol) in water (20 mL) and stirred overnight at room temperature, then made acidic (pH 3–4) by adding concentrated HCl at 0°C. The solid formed was extracted with ethyl acetate, and the resulting solution was washed with water, dried, and evaporated. The resulting residue was purified by crystallization to give a solid (1.5 g, 85%): mp 182–184°C (acetone/diethyl ether); IR (KBr) 2800 (br), 1695, 1635  $\text{cm}^{-1}$ ;  $^1\text{H}$  NMR ( $\text{CD}_3\text{OD}$ )  $\delta$  (ppm): 9.00 (2H, br), 7.82 (1H, s), 7.76 (1H, m), 7.64 (1H, m), 7.40 (1H, m), 7.28 (1H, m), 7.20 (1H, s), 5.21 (2H, s), 4.99 (1H, t,  $J = 6,7$  Hz), 4.47 (1H, m), 4.11 (1H, m); MS (EI)  $m/z$  287 ( $\text{M}^+$ ). Anal. ( $\text{C}_{15}\text{H}_{13}\text{NO}_5$ ) C, H, N.



## Cyclization reaction

### Method A

A mixture of the appropriate Hydroxyacid **24** (0.4 mmol), EDC (0.085 g, 0.44 mmol), and DMAP (cat.) in dry dichloromethane (20 mL) was stirred at room temperature for 40 h. The solution was then shaken with a saturated solution of NH<sub>4</sub>Cl and water, successively. After drying and solvent evaporation, a pale yellow oil was obtained and purified by column chromatography on a silica gel (15% ethyl acetate in hexanes).

### Method B

2-Chloro-1-methylpyridinium iodide (0.12 g, 0.48 mmol) and TEA (110  $\mu$ L, 0.8 mmol) were added to a suspension of the appropriate hydroxyacid **24** (0.4 mmol) in dry dichloromethane (15 mL). After heating overnight under reflux, the mixture was worked up as described for method A.

### Method C

A suspension of the appropriate compound **24** (0.4 mmol) in acetic anhydride (2 mL) was stirred overnight at room temperature. The resulting solution was then diluted with chilled water and left for several hours at 4 °C. The aqueous solution was extracted with chloroform and the organic layer was shaken successively with a 5% sodium bicarbonate solution and brine. A pure solid was obtained after evaporation of the solvent.

**(±)-1,11a-Dihydro-3*H*,5*H*,11*H*-thiazolo[4,3-*c*][1,4]benzoxazepin-5,11-dione (6)**

Compound **6** was prepared following the method A (33 mg, 35%); mp 143–145°C (diethyl ether/light petroleum); IR (KBr) 1695, 1635 cm<sup>-1</sup>; <sup>1</sup>H NMR (CDCl<sub>3</sub>) δ (ppm): 7.94–7.20 (4H, m), 4.86 and 4.72 (2H, ABq, *J* = 10.6 Hz), 4.46 (1H, dd, *J* = 6.8 and 3.3 Hz), 3.76 (1H, dd, *J* = 12.3 and 3.3 Hz), 3.32 (1H, dd, *J* = 12.3 and 6.8 Hz); MS (CI) *m/z* 236 (MH<sup>+</sup>). Anal. (C<sub>11</sub>H<sub>9</sub>NO<sub>3</sub>S) C, H, N.

**(±)-2,3-Dihydro-5*H*,11a*H*-thiazolo[2,3-*c*][1,4]benzoxazepin-5,11-dione (7)**

Compound **7** was prepared following the method B (13 mg, 14%); mp 154–156 °C (benzene); IR (KBr) 1700, 1635 cm<sup>-1</sup>; <sup>1</sup>H NMR (CDCl<sub>3</sub>) δ (ppm): 7.95–7.22 (4H, m), 5.27 (1H, s), 4.20 (1H, m), 3.88 (1H, m), 3.37 (1H, m), 3.16 (1H, m); MS (CI) *m/z* 236 (MH<sup>+</sup>). Anal. (C<sub>11</sub>H<sub>9</sub>NO<sub>3</sub>S) C, H, N.

**(±)-1,13a-Dihydro-3*H*,5*H*,13*H*-naphtho[2,3-*f*]thiazolo[4,3-*c*][1,4]oxazepine-5,13-dione (8)**

This compound was prepared following the method C (46 mg, 38%); mp 217 °C (dichloromethane/petroleum ether); IR (KBr) 1705, 1630 cm<sup>-1</sup>; <sup>1</sup>H NMR (CDCl<sub>3</sub>) δ (ppm): 8.55 (1H, m), 7.98 (1H, d, *J* = 8.3 Hz), 7.86 (1H, d, *J* = 8.3 Hz), 7.60 (3H, m), 4.91 (1H, 0.5 of ABq, *J* = 10.7 Hz), 4.56 (1H, 0.5 of ABq, *J* = 10.7 Hz), 4.55 (1H, dd, *J* = 6.8 and 3.4 Hz), 3.80 (1H, dd, *J* = 12.5 and 3.4 Hz), 3.34 (1H, dd, *J* = 12.5 and 6.8 Hz); MS (CI) *m/z* 286 (MH<sup>+</sup>). Anal. (C<sub>15</sub>H<sub>11</sub>NO<sub>3</sub>S) C, H, N.

**(±)-1,13a-Dihydro-3H,5H,13H-naphtho[2,3-f]oxazolo[4,3-c][1,4]oxazepine-5,13-dione (9)**

This compound was prepared following the method A (56 mg, 52%); mp 205 °C(ethyl ether); IR (KBr) 1695, 1635 cm<sup>-1</sup>; <sup>1</sup>H NMR (CDCl<sub>3</sub>) δ (ppm): 8.52 (1H, s), 7.95 (1H, d, *J* = 7.9 Hz), 7.83 (1H, d, *J* = 7.9 Hz), 7.60 (3H, m), 5.28 and 5.21 (2H, ABq, *J* = 5.3 Hz), 4.82 (1H, dd, *J* = 8.8 and 2.4 Hz), 4.28 (2H, m); MS (EI) *m/z* 269 (M<sup>+</sup>). Anal. (C<sub>15</sub>H<sub>11</sub>NO<sub>4</sub>) C, H, N.

**(1R,13aS)-1,13a-Dihydro-1-methyl-3H,5H,13H-naphtho[2,3-f]oxazolo[4,3-c][1,4]oxazepine-5,13-dione (10)**

Method C was followed for the preparation of compound **10** (49 mg, 43%); mp 198 °C (benzene); [α]<sub>D</sub><sup>21</sup> -197.0 (c 1, CHCl<sub>3</sub>); IR (KBr) 1700, 1640 cm<sup>-1</sup>; <sup>1</sup>H NMR (CDCl<sub>3</sub>) δ (ppm): 8.60 (1H, s), 7.98 (1H, d, *J* = 7.5 Hz), 7.86 (1H, d, *J* = 7.9 Hz), 7.70 (1H, s), 7.65 (2H, m), 5.62 and 5.03 (2H, ABq, *J* = 5.5 Hz), 4.88 (1H, m), 3.82 (1H, d, *J* = 6.9), 1.45 (3H, d, *J* = 6.0); MS (CI) *m/z* 284 (MH<sup>+</sup>). Anal. (C<sub>16</sub>H<sub>13</sub>NO<sub>4</sub>) C, H, N.

**(±)-1,13a-Dihydro-3H,5H,13H-naphtho[1,2-f]thiazolo[4,3-c][1,4]oxazepine-5,13-dione (11)**

This compound was prepared following the method C (52 mg, 43%); mp 237 °C (dichloromethane/light petroleum); IR (KBr) 1725, 1640 cm<sup>-1</sup>; <sup>1</sup>H NMR (CDCl<sub>3</sub>) δ (ppm): 8.64 (1H, d, *J* = 8.1 Hz), 8.03 (1H, d, *J* = 8.6 Hz), 7.91 (1H, d, *J* = 7.2 Hz), 7.65 (2H, m), 7.33 (1H, d, *J* = 8.6 Hz), 5.00 (1H, 0.5 of ABq, *J* = 10.5 Hz), 4.90 (1H, 0.5 of ABq, *J* = 10.5 Hz), 4.64 (1H, dd, *J* = 6.5 and 1.7 Hz), 3.79 (1H, dd, *J* = 12.0 and 1.7 Hz), 3.39 (1H, dd, *J* = 12.0 and 6.5 Hz); MS (CI) *m/z* 286 (MH<sup>+</sup>). Anal. (C<sub>15</sub>H<sub>11</sub>NO<sub>3</sub>S) C, H, N.

**(±)-1,13*a*-Dihydro-3*H*,5*H*,13*H*-naphtho[2,1-*f*]thiazolo[4,3-*c*][1,4]oxazepine-5,13-dione (12)**

This compound was prepared following the method C (26 mg, 23%); mp 200°C (dichloromethane/light petroleum); IR (KBr) 1740, 1645 cm<sup>-1</sup>; <sup>1</sup>H NMR (CDCl<sub>3</sub>) δ (ppm): 8.41 (1H, m), 7.90 (2H, m), 7.82 (1H, d, *J* = 8.4 Hz), 7.70 (2H, m), 4.95 (1H, 0.5 of ABq, *J* 10.6 Hz), 4.85 (1H, 0.5 of ABq, *J* = 10.6 Hz), 4.55 (1H, dd, *J* = 6.5 and 1.8 Hz), 3.82 (1H, dd, *J* = 11.8 and 1.8 Hz), 3.37 (1H, dd, *J* = 11.8 and 6.5 Hz); MS (CI) *m/z* 286 (MH<sup>+</sup>). Anal. (C<sub>15</sub>H<sub>11</sub>NO<sub>3</sub>S) C, H, N.

## Optical active compounds

A typical procedure is described for the synthesis of compound (–)-6.

### ***N*-Boc-L-[2-(*tert*-butoxycarbonyl)phenyl]-1,3-thiazolidine-4-carboxylate (27b)**

*N*-Boc-L-4-thiazolidinecarboxylic **25** (1.40 g, 6 mmol), *tert*-butyl salicylate **26b** (1.17 g, 6 mmol), triethylamine (1.21 g, 12 mmol) and BOP reagent (2.65 g, 6 mmol) were dissolved successively in dichloromethane (45 ml). The solution was kept at room temperature for 3 h. Saturated aqueous sodium chloride solution (100 ml) was added and the resultant mixture is extracted with ethyl acetate. The organic phase was separated, washed successively with 1 N hydrochloric acid, saturated sodium hydrogen carbonate solution and sodium chloride solution, dried on MgSO<sub>4</sub>, and evaporated in vacuo. Pure **27b** (1.60 g, 65% yield) was obtained as a white solid after column chromatography purification on silica gel (diethyl ether:light petroleum, 1:1 as eluent); mp 89.5 °C. <sup>1</sup>H NMR (CDCl<sub>3</sub>) δ (ppm): 7.2–7.9 (m, 4 H), 5.05 (d, 1 H, *J* = 6.5), 4.70 (dd, 1 H, *J* = 6.5, 1.7), 4.55 (t, 1 H, *J* = 1.7), 3.75 (m, 1 H), 3.48 (m, 1 H), 1.62 (s, 9 H), 1.51 (s, 9 H). Anal. C<sub>20</sub>H<sub>27</sub>NO<sub>6</sub>S (C, H, N).

### **(–)-2,3-Dihydro-5*H*,11*aH*-thiazolo[2,3-*c*][1,4]benzoxazepin-5,11-dione [(–)-(6)]**

Compound **27b** (0.20 g, 0.49 mmol) was dissolved in a mixture of trifluoroacetic acid/anisole, 1:1 (20 ml) at 0 °C. The mixture was then stirred at room temperature for 50 min. The volatiles were evaporated under vacuum and the residue was azeotropized several times with toluene to give essentially pure 2-[(1,3-thiazolidin-4-yl carbonyl)oxy]benzoic acid **28b** which was subjected to cyclization without further purification. A solution of the hydroxyacid **28b** (0.10 g, 0.39 mmol) in dry DMF (2 ml) was slowly added to a solution of PyBOP (0.20 g, 0.39 mmol) and DIEA (0.05 g, 0.39 mmol) in dry DMF (5 ml). The

mixture was stirred for 1 h and then the solvent was evaporated under vacuum. The residue obtained was partitioned between water and ethyl acetate and the organic layer was separated and washed with 1 N hydrochloric acid and water. After evaporation of the solvent, the oily residue was purified by column chromatography (ethyl acetate: hexanes, 1:6) to give pure compound (–)-**6** (70 mg, 75% yield) which shows identical data as above reported **6**, but  $[\alpha]_{\text{D}}^{20} = -111$  ( $\text{CHCl}_3$ ,  $c = 1$ ),  $ee = > 97\%$ .

## Pyrroloquinoxalinyacylhydrazide derivatives

### General procedure for the preparation of compounds 29-35

The preparation of compound **31** is reported as a representative example.

### 1-(*H*-Pyrrolo[1,2-*a*]quinoxalin-4-yl)hydrazine (**47**)

A solution of N-(2-aminophenyl)pyrrole **44** (2.00g, 1.26 mmol) in toluene (30 mL) and triphosgene was heated under reflux for 30 min. The solution was then allowed to come to room temperature and set aside for 24 hours. The heavy crystalline precipitate was filtered off and washed with light petrol to give compound **44** which was recrystallized from n-hexane. The lactame **44** was successively treated with phosphorus oxychloride under reflux for 4 hours. Crushed ice was added to the resultant solution and the chloro compound extracted with dichloromethane. Evaporation of the dried extract gave compound **45** which was recrystallized from dichloromethane/n-hexane. Such a material (1.13g, 6.25 mmol) was dissolved in DMF (25 mL) and to this was added hydrazine monohydrate (25 mL). The mixture was stirred at room temperature for 24 hours. The solvent was evaporated, and the residue was partitioned between ethyl acetate and water. The organic layer was separated, shaken with brine and dried over MgSO<sub>4</sub>. The resulting residue was crystallized from dichloromethane/ petroleum ether to give the title compound **47** (45% yield for the entire process). mp 160-161 °C. <sup>1</sup>H NMR (DMSO-*d*<sub>6</sub>) δ (ppm): 8.70 (bs, 1 H), 8.13- 8.04 (d, 1 H, *J* = 7.6 Hz), 7.61-7.53 (d, 1 H, *J* = 7.6 Hz), 7.37-7.23 (dt, 3 H, *J* = 7.0, 16.8), 7.02 (s, 1 H), 6.79-6.20 (t, 1 H, *J* = 3.1 Hz), 4.56 (bs, 2 H). MS (CI) *m/z* 199 (MH<sup>+</sup>). Anal. C<sub>11</sub>H<sub>10</sub>N<sub>4</sub> (C, H, N).

### **1*H*-Indole-2-carboxylic acid *N*'-pyrrolo[1,2-*a*]quinoxalin-4-yl-hydrazide (31)**

To a stirred solution of EDC (94 mg, 0.49 mmol) and DMAP (cat.) in ethyl acetate (15 mL), 1-(*H*-pyrrolo[1,2-*a*]quinoxalin-4-yl)hydrazine **47** (77 mg, 0.39 mmol) and 2-indolecarboxylic acid (63 mg, 0.39 mmol) were added portionwise within 15 minutes. The resulting mixture was stirred at room temperature for 24 h, then shaken with sodium bicarbonate saturated solution and water. Evaporation of the dried extract gave a residue, which was crystallized to give **31** as a white solid (82 mg, 62% yield); mp 186°C (dichloromethane/light petroleum); IR (KBr) 3255, 1680 cm<sup>-1</sup>; <sup>1</sup>H NMR (DMSO-*d*<sub>6</sub>) δ (ppm): 11.80 (bs, 1 H), 10.65 (bs, 1 H), 9.55 (bs, 1 H), 8.35 (s, 1 H), 8.10 (m, 1 H), 7.65 (m, 1 H), 7.40 (m, 3 H), 7.20 (m, 4 H), 7.05 (m, 1 H), 6.75 (s, 1 H). MS (CI) *m/z* 342 (MH<sup>+</sup>). Anal. (C<sub>20</sub>H<sub>15</sub>N<sub>5</sub>O) C, H, N.

### **1*H*-Indole-5-carboxylic acid *N*'-pyrrolo[1,2-*a*]quinoxalin-4-yl-hydrazide (32)**

Following the procedure identical to that described for **31**, but using 2-indolecarboxylic acid (63 mg, 0.39 mmol), **32** was obtained as a white solid (69 mg, 52% yield); mp 160°C (dichloromethane/light petroleum); IR (KBr) 3250, 1680 cm<sup>-1</sup>; <sup>1</sup>H NMR (acetone-*d*<sub>6</sub>) δ (ppm): 11.45 (bs, 1 H), 10.70 (bs, 1H), 9.60 (bs, 1 H), 8.39 (s, 1 H), 8.20 (m, 1 H), 8.03 (m, 1 H), 7.85 (d, 1 H, *J* = 8.5 Hz), 7.51 (m, 3 H), 7.29 (m, 2 H), 7.23 (d, 1 H, *J* = 3.6 Hz), 6.75 (t, 1 H, *J* = 3.6 Hz), 6.60 (d, 1H, *J* = 3.6 Hz). MS (CI) *m/z* 342 (MH<sup>+</sup>). Anal. (C<sub>20</sub>H<sub>15</sub>N<sub>5</sub>O) C, H, N.



**1*H*-Indole-6-carboxylic acid *N'*-pyrrolo[1,2-*a*]quinoxalin-4-yl-hydrazide (33)**

Following a procedure identical to that described for **31**, but using 6-indolecarboxylic acid (63 mg, 0.39 mmol), **33** was obtained as a white solid (17 mg, 13% yield); mp 198.5 °C (dichloromethane/light petroleum); IR (KBr) 3245, 1685 cm<sup>-1</sup>; <sup>1</sup>H NMR (acetone-*d*<sub>6</sub>) δ (ppm): 11.51 (bs, 1 H), 10.55 (bs, 1 H), 9.44 (bs, 1 H), 8.70 (m, 2 H), 8.39 (m, 1 H), 8.15 (s, 1 H), 7.60 (d, 1 H, *J* = 8.1 Hz), 7.45 (m, 1 H), 7.48 (m, 3 H), 7.28 (m, 1 H), 6.85 (m, 1 H), 6.55 (m, 1H). MS (CI) *m/z* 342 (MH<sup>+</sup>). Anal. (C<sub>20</sub>H<sub>15</sub>N<sub>5</sub>O) C, H, N.

**1*H*-Indole-3-carboxylic acid *N'*-pyrrolo[1,2-*a*]quinoxalin-4-yl-hydrazide (34)**

Following a procedure identical to that described for **31**, but using 3-indolecarboxylic acid (63 mg, 0.39 mmol), **34** was obtained as a white solid (42 mg, 32% yield); mp 162.5 °C (dichloromethane/light petroleum); IR (KBr) 3250, 1685 cm<sup>-1</sup>; <sup>1</sup>H NMR (CDCl<sub>3</sub>) δ (ppm): 11.60 (bs, 1 H), 10.25 (bs, 1 H), 9.20 (bs, 1 H), 8.30 (m, 1 H), 8.11 (s, 1 H), 8.10 (m, 1 H), 7.90 (m, 2 H), 7.58 (m, 1H), 7.48 (m, 1 H), 7.30-7.60 (m, 4 H), 7.08 (d, 1 H, *J* = 3.2 Hz), 6.90 (t, 1 H, *J* = 3.3 Hz), 6.80 (m, 1 H). MS (CI) *m/z* 342 (MH<sup>+</sup>). Anal. (C<sub>20</sub>H<sub>15</sub>N<sub>5</sub>O) C, H, N.

**2-Methoxy-*N'*-(*H*-pyrrolo[1,2-*a*]quinoxalin-4-yl)benzohydrazide (35)**

Following a procedure identical to that described for **31**, but using 2-methoxybenzoic acid (60 mg, 0.39 mmol), **35** was obtained as a white solid (98 mg, 75% yield); mp 204.5°C (dichloromethane/light petroleum); IR (KBr) 3200, 1675 cm<sup>-1</sup>; <sup>1</sup>H NMR (DMSO-*d*<sub>6</sub>) δ (ppm): 10.30 (bs, 1 H), 9.75 (bs, 1 H), 8.25 (bs, 1 H), 8.00 (m, 1 H), 7.75 (m, 1 H), 7.45 (m,

2 H), 7.15 (m, 5 H), 6.70 (m, 1 H), 3.90 (s, 3H). MS (CI)  $m/z$  333 ( $MH^+$ ). Anal. ( $C_{19}H_{16}N_4O_2$ ) C, H, N.

### **Thiazolidine-4-carboxylic acid *N'*-pyrrolo[1,2-*a*]quinoxalin-4-yl- hydrazide (29)**

Starting from *N-boc*-thiazolidine-4-carboxylic acid (90 mg, 0.39 mmol), *tert*-butyl 4-[(2-pyrrolo[1,2-*a*]quinoxalin-4-ylhydrazino)carbonyl]-1,3-thiazolidine-3-carboxylate was obtained as a solid, after crystallization (hexanes). The solid obtained was added to a stirred mixture of TFA (2 mL) and anisole (2 mL) at 0°C. The reaction mixture was allowed to reach to room temperature and stirred for a further 50 minutes. Evaporation of the volatiles by azeotropization with toluene (3 x 3 mL) gave **29** as a pale yellow solid (66 mg, 55% yield based on compound **47**). mp 162 °C (ethyl acetate/hexanes); IR (KBr) 3255, 1690  $cm^{-1}$ ;  $^1H$  NMR (methanol- $d_4$ )  $\delta$  (ppm): 11.20 (bs, 1 H), 10.40 (bs, 1 H), 8.38 (m, 1 H), 8.09 (d, 1 H,  $J = 9.3$  Hz), 7.71 (d, 1 H,  $J = 7.4$  Hz), 7.41 (m, 3 H), 6.92 (m, 1 H), 4.45 (dd, 1 H,  $J = 7.1, 4.9$  Hz), 4.25 (0.5 of ABq, 1 H,  $J = 9.7$  Hz), 4.11 (0.5 of ABq, 1 H,  $J = 9.7$  Hz), 3.30 (dd, 1 H,  $J = 10.9, 7.1$  Hz), 3.15 (dd, 1 H,  $J = 10.9, 4.9$ ). MS (CI)  $m/z$  314 ( $MH^+$ ). Anal. ( $C_{15}H_{15}N_5OS$ ) C, H, N.

### **3-Amino-propionic acid *N'*-pyrrolo[1,2-*a*]quinoxalin-4-yl-hydrazide (30)**

Following a procedure identical to that described for compound **29**, but using *N-boc*-*R*-alanine (74 mg, 0.39 mmol), **30** was obtained as a white solid (92 mg, 88% yield based on compound **47**). mp 164.5°C (dichloromethane/light petroleum); IR (KBr) 3255, 1680  $cm^{-1}$ ;  $^1H$  NMR (DMSO- $d_6$ )  $\delta$  (ppm): 11.25 (bs, 1 H), 10.70 (bs, 1 H), 8.60 (m, 1 H), 8.30 (m, 1 H), 7.95 (m, 2 H), 7.50 (m, 2 H), 7.05 (m, 1 H), 3.20 (m, 2 H), 2.80 (m, 2 H). MS (CI)  $m/z$  270 ( $MH^+$ ). Anal. ( $C_{14}H_{15}N_5O$ ) C, H, N.

## General procedure for the preparation of compounds 36-43

The preparation of compound **36** is reported as a representative example.

### Fluoro-4-chloropyrrolo[1,2-*a*]quinoxaline (**51**)

To a solution of 2,4-difluoroaniline **48** (1.00 g, 7.70 mmol) in glacial acetic acid (5 mL) was slowly added 2,5-dimethoxytetrahydrofuran (1.0 mL, 7.80 mmol). The reaction mixture was refluxed for 1 hour, cooled and evaporated to afford an oily residue (1.05 g, 5.90 mmol) which was chromatographed (EtOAc) to give the corresponding pyrrolo derivative as a colorless oil, which was successively added to a cooled (-5 °C) mixture of anhydrous *N,N*-dimethylformamide (0.48 mL, 6.20 mmol) and oxalyl chloride (0.54 mL, 6.20 mmol) in anhydrous 1,2-dichloroethane (15 mL). The reaction mixture was allowed to stirred at room temperature for 4 hours, and then a warm solution of hydroxylamine hydrochloride (0.43 g, 6.20 mmol) and dry sodium acetate (0.51 g, 6.20 mmol) in anhydrous *N,N*-dimethylformamide (10 mL) was slowly added. After the mixture was refluxed for 20 hours, acetic anhydride (2.30 mL, 24.40 mmol) was added and the solution was refluxed for 4 h. The cooled mixture was treated with 10% sodium carbonate solution until pH 8, diluted with water, and extracted with ethyl acetate. The organic layer was washed with brine, dried, and concentrated. The residue was chromatographed (EtOAc) to give 0.65 g of nitrile derivative **49** as colorless prisms. Successively, a suspension of **49** (0.2 g, 1.0 mmol) and 85% potassium hydroxide (0.2 g, 4.0 mmol) in of *tert*-butyl alcohol (8 mL) was heated at 80 °C for 2 hours under argon. The mixture was then cooled, poured into crushed ice, and extracted with ethyl acetate. The organic layer was washed with brine, dried, and concentrated. The residue was chromatographed (ethyl acetate) to afford 0.18 g of lactame **50** as a white solid. Finally, a mixture of **50** and phosphorus oxychloride (4 mL) was refluxed for 4 hours under argon, cooled, poured into crushed ice and extracted with dichloromethane. The organic layers were washed with brine, dried and concentrated to give a white solid which was recrystallized from CH<sub>2</sub>CL<sub>2</sub>/ petroleum ether to give 0.31 g of **51** as colorless prisms. mp = 190-191°C. IR (CHCl<sub>3</sub>) 3320 cm<sup>-1</sup>; <sup>1</sup>H NMR (CDCl<sub>3</sub>) δ (ppm):

7.95-7.86 (m, 1H), 7.81-7.73 (dd, 1 H,  $J = 8.5, 6.2$  Hz), 7.62-7.53 (dd, 1 H,  $J = 5.5, 6.2$  Hz), 7.30-7.43 (m, 1 H), 7.11-7.00 (m, 1 H), 6.90-6.82 (m, 1 H). Anal. ( $C_{11}H_6ClFN_2$ ) C, H, N.

### **7-Fluoro-4-hydrazinopyrrolo[1,2-*a*]quinoxaline (52)**

A mixture of 7-fluoro-4-chloropyrrolo[1,2-*a*]quinoxaline **51** (100 mg, 0.45 mmol) and hydrazine monohydrate (5 mL) in DMF (2 mL) was heated at 70-80 °C for one hour. Crushed ice was then added and the mixture was extracted with ethyl acetate. The organic layer was separated and shaken with water and brine successively. After evaporation of the solvents, compound **2** was obtained as a solid (84 mg, 86% yield) and used in the subsequent step without further purification. An analytical sample was obtained by crystallization (dichloromethane/light petroleum); mp 158 °C; IR (KBr) 3300  $cm^{-1}$ ;  $^1H$  NMR ( $DMSO-d_6$ )  $\delta$  (ppm): 8.87 (bs, 1 H), 8.15 (s, 1 H), 8.02 (dd, 1 H,  $J = 8.9, 5.6$  Hz), 7.18 (dd, 1 H,  $J = 10.6, 2.7$  Hz), 7.03 (m, 2 H), 6.66 (t, 1 H,  $J = 3.2$  Hz), 4.56 (bs, 2 H). Anal. ( $C_{11}H_9FN_4$ ) C, H, N.

## ***N'*-(7-Fluoropyrrolo[1,2-*a*]quinoxalin-4-yl)pyrazine-2-carbohydrazide (36)**

### **(Method A)**

To a stirred suspension of 2-pyrazinecarboxylic acid (0.62 g, 0.50 mmol) in dry dichloromethane (2mL) were added, portion-wise, within one hour, triphenylphosphine (0.26 g, 1.00 mmol) and 2,2'-dipyridyl disulfide (0.22 g, 1.00 mmol). When the starting material disappeared a solution of 7-fluoro-4-hydrazinopyrrolo[1,2 *a*]quinoxaline (0.11 g, 0.50 mmol), in the same solvent (6 mL) was added and the resulting mixture was stirred at room temperature overnight. The solvent was removed and the residue was partitioned between ethyl acetate and water. The organic layer was separated, shaken with brine and dried over MgSO<sub>4</sub>. The resulting residue was purified by flash-chromatography (chloroform:methanol:ammonium hydroxide, 89:10:1) to afford **36** as a pale yellow solid (56 mg, 35 % yield); (methanol/ethyl acetate); mp 195 °C; IR (KBr) 3255, 1690 cm<sup>-1</sup>; <sup>1</sup>H NMR (DMSO-*d*<sub>6</sub>) δ (ppm): 11.67 (bs, 1 H), 9.22 (s, 1 H), 8.94 (d, 1 H, *J* = 2.7 Hz), 8.82 (m, 1 H), 3.75 (bs, 1 H), 6.96 (m, 1 H), 7.35 (t, 1 H, *J* = 8.7 Hz), 7.68 (m, 2 H), 8.30 (dd, 1 H, *J* = 8.7, 4.8 Hz), 8.60 (s, 1 H). MS (MALDI, TOF/TOF) *m/z* 323 (MH<sup>+</sup>) Anal. (C<sub>16</sub>H<sub>11</sub>FN<sub>6</sub>O) C, H, N.

### **(Method B)**

A mixture of 7-fluoro-4-chloropyrrolo[1,2-*a*]quinoxaline (0.20 g, 0.90 mmol) and pyrazine-2-carbohydrazide (0.12 mg, 0.90 mmol) in EtOH (2 mL) was refluxed for 5 hours and then chilled overnight. The product was collected by filtration, washed with cold EtOH, and dried *in vacuo* to give pure **36·HCl** (0.26 mg, 80 % yield). mp 282 °C (dec.) (methanol/ethyl acetate); IR (KBr) 3255, 1690 cm<sup>-1</sup>; <sup>1</sup>H NMR (DMSO-*d*<sub>6</sub>) δ (ppm): 11.67 (bs, 1 H), 9.22 (s, 1 H), 8.94 (d, 1 H, *J* = 2.7 Hz), 8.82 (m, 1 H), 8.60 (s, 1 H), 8.30 (dd, 1 H, *J* = 8.7, 4.8 Hz), 7.68 (m, 2 H), 7.35 (t, 1 H, *J* = 8.7 Hz), 6.96 (m, 1 H), 3.75 (bs, 1 H). MS (CI) *m/z* 323 (MH<sup>+</sup>). Anal. (C<sub>16</sub>H<sub>12</sub>ClFN<sub>6</sub>O) C, H, N.

***N'*-(7-Fluoropyrrolo[1,2-*a*]quinoxalin-4-yl)pyridine-2-carbohydrazide hydrochloride (37·HCl)**

Following the same procedure described for compound **36·HCl**, but using picolinohydrazide (0.12 g, 0.90 mmol), **37·HCl** was obtained as a yellow solid (0.26 g; 82% yield). mp > 280 °C (dec.) (ethanol/ethyl acetate); IR (KBr) 3245, 1750 cm<sup>-1</sup>; <sup>1</sup>H-NMR (CD<sub>3</sub>OD) δ (ppm): 8.80 (dd, 2H *J* = 6.2, 1.4 Hz); 8.45 (m, 1H); 8.18 (dd, 1H *J* = 9.2, 4.9 Hz); 8.03 (d, 2H, *J* = 6.0); 7.60 (m, 1H); 7.47 (dd, 1H, *J* = 9.2, 2.7 Hz); 7.28 (m, 1H); 7.0 (dd, 1H *J* = 4.2, 2.8 Hz). MS (CI) *m/z* 322 (MH<sup>+</sup>). Anal. (C<sub>17</sub>H<sub>13</sub>ClFN<sub>5</sub>O) C, H, N.

***N'*-(9-Fluoropyrrolo[1,2-*a*]quinoxalin-4-yl)pyrazine-2-carbohydrazide hydrochloride (38·HCl)**

Following the same procedure described for compound **36·HCl**, but using 4-chloro-9-fluoropyrrolo[1,2-*a*]quinoxaline (0.20 g, 0.90 mmol), **38·HCl** was obtained as a yellow solid (0.30 g; 94% yield). mp 248 °C (dec.) (ethanol/ethyl acetate); IR (KBr) 3250, 1680 cm<sup>-1</sup>; <sup>1</sup>H-NMR (DMSO-*d*<sub>6</sub>) δ (ppm): 10.90 (bs, 1H); 9.80 (bs, 1H); 9.20 (s, 1H); 8.90 (s, 1H); 8.80 (s, 1H); 8.10 (m, 1H); 7.20 (m, 5H); 6.80 (s, 1H). MS (CI) *m/z* 323 (MH<sup>+</sup>). Anal. (C<sub>16</sub>H<sub>12</sub>ClFN<sub>6</sub>O) C, H, N.

***N'*-(7-Fluoropyrrolo[1,2-*a*]quinoxalin-4-yl)nicotinyl hydrazide hydrochloride (39·HCl)**

Following the same procedure described for compound **36·HCl**, but using nicotinohydrazide (0.12 g, 0.90 mmol), **39·HCl** was obtained as a white solid (0.23 g; 72% yield). mp > 250 °C (dec.) (ethanol/ethyl acetate); IR (KBr) 3200, 1750 cm<sup>-1</sup>; <sup>1</sup>H-NMR (DMSO-*d*<sub>6</sub>) δ (ppm): 10.90 (bs, 1H); 9.80 (bs, 1H); 9.12 (s, 1H); 8.77 (s, 1H); 8.32 (m, 2H); 8.15 (m, 1H); 7.59 (m, 1H); 7.15 (m, 2H); 6.77 (s, 1H); 4.10 (m, 2H). MS (CI) *m/z* 322 (MH<sup>+</sup>). Anal. (C<sub>17</sub>H<sub>13</sub>ClFN<sub>5</sub>O) C, H, N.

### **N'-(7-Fluoropyrrolo[1,2-*a*]quinoxalin-4-yl)2'-fluoro-benzoylhydrazide hydrochloride (40·HCl)**

Following the same procedure described for compound **36·HCl**, but using 2-fluorobenzohydrazide (0.14 g; 0.90 mmol), **40·HCl** was obtained as a white solid (0.22 g; 66% yield). mp= 247°C (dec.) (ethanol/ethyl acetate); IR (KBr) 3250, 1675 cm<sup>-1</sup>; <sup>1</sup>H-NMR (DMSO-*d*<sub>6</sub>) δ (ppm): 10.45 (bs, 1H); 9.75 (bs, 1H); 8.30 (s, 1H); 8.15 (m, 1H), 7.80 (m, 1H); 7.60 (m, 1H); 7.35 (m, 2H); 7.20 (m, 2H); 6.78 (m, 1H); 4.09 (m, 2H). MS (CI) *m/z* 339 (MH<sup>+</sup>). Anal.(C<sub>18</sub>H<sub>13</sub>ClFN<sub>4</sub>O) C, H, N.

### **N'-(7-Fluoropyrrolo[1,2-*a*]quinoxalin-4-yl)thiophene-2-carbohydrazide hydrochloride (41·HCl)**

Following the same procedure described for compound **36·HCl**, but using thiophene-2-carbohydrazide (0.13 g; 0.90mmol), **41·HCl** was obtained as a white solid (0.25 g; 77% yield). mp= 261°C (dec.) (ethanol/ethyl acetate); IR (KBr) 3245, 1680 cm<sup>-1</sup>; <sup>1</sup>H-NMR (CD<sup>3</sup>OD) δ (ppm): 8.41 (m, 1H); 8.18 (dd, 1H, *J* = 9.3, 5.0 Hz); 7.89 (dd, 1H, *J* = 3.8, 1.1 Hz); 7.82 (d, 1H, *J* = 4.9); 7.57 (m, 1H); 7.49 (dd, 1H, *J* = 9.3, 2.8); 7.28 (m, 1H); 7.21 (dd, 1H, *J* = 4.9, 3.8); 6.98 (dd, 1H, *J* = 4.2, 2.8 Hz). MS (CI) *m/z* 327 (MH<sup>+</sup>). Anal. (C<sub>16</sub>H<sub>12</sub>ClFN<sub>4</sub>SO) C, H, N.

### **N'-(7-Fluoropyrrolo[1,2-*a*]quinoxalin-4-yl)furan-2-carbohydrazide hydrochloride (42·HCl)**

Following the same procedure described for compound **36·HCl**, but using furan-2-carbohydrazide (0.11 g; 0.90mmol), **42·HCl** was obtained as a pale yellow solid (0.24 g; 78% yield). mp= 256°C (dec.) (ethanol/ethyl acetate); IR (KBr) 3240, 1700 cm<sup>-1</sup>; <sup>1</sup>H-NMR (CD<sub>3</sub>OD) δ (ppm): 8.48 (m, 1H); 8.25 (m, 1H); 7.85 (m, 1H); 7.65 (dd, 1H *J* = 4.3, 1.2 Hz); 7.55 (dd, 1H *J* = 9.2, 2.7 Hz); 7.35 (m, 2H); 7.05 (m, 1H); 6.73 (m, 1H). MS (CI) *m/z* 311 (MH<sup>+</sup>). Anal.(C<sub>16</sub>H<sub>12</sub>ClFN<sub>4</sub>O<sub>2</sub>) C, H, N.

**N'-(7-Fluoropyrrolo[1,2-*a*]quinoxalin-4-yl)quinoxaline-2-carbohydrazide hydrochloride (43·HCl)**

Following the same procedure described for compound **36·HCl**, but using quinoxaline-2-carbohydrazide (0.17 g; 0.90mmol), **43·HCl** was obtained as a pale yellow solid (0.33 g; 89% yield). mp= 280°C (dec.) (ethanol/ethyl acetate); IR (KBr) 3255, 1750 cm<sup>-1</sup>; <sup>1</sup>H-NMR (CD<sub>3</sub>OD) δ (ppm): 9.55 (s, 1H); 8.47 (m, 1H); 8.28 (m, 1H); 8.20 (m, 2H); 7.97 (m, 2H); 7.68 (dd, 1H, *J* = 4.5, 1.2); 7.44 (dd, 1H, *J* = 9.3, 2.5); 7.32 (m, 1H); 7.04 (dd, 1H, *J* = 4.2, 2.5). MS (CI) *m/z* 373 (MH<sup>+</sup>). Anal. (C<sub>20</sub>H<sub>14</sub>ClFN<sub>6</sub>O) C, H, N.



# **GENERAL EXPERIMENTAL BIOLOGY**

## **Integrase assays**

To determine the extent of 3'-processing and strand transfer, wild-type IN was preincubated at a final concentration of 200nM with the inhibitor in reaction buffer (50mM NaCl, 1mM HEPES, pH7.5, 50 μM EDTA, 50 μM dithiothreitol, 10% glycerol (w/v), 7.5mM MnCl<sub>2</sub>, 0.1 mg/mL bovine serum albumin, 10mM 2-mercaptoethanol, 10% dimethyl sulfoxide, and 25mM MOPS, pH 7.2) at 30 °C for 30 min. Then, 20nM of the 50-end <sup>32</sup>P-labeled linear oligonucleotide substrate was added, and incubation was continued for an additional one hour. Reactions were quenched by the addition of an equal volume (16 μL) of loading dye (98% deionized formamide, 10mM EDTA, 0.025% xylene cyanol, and 0.025% bromophenol blue). An aliquot (5 μL) was electrophoresed on a denaturing 20% polyacrylamide gel (0.09M tris-borate pH8.3, 2mM EDTA, 20% acrylamide, 8M urea). Gels were dried, exposed in a PhosphorImager cassette, and analyzed using a Typhoon 8610 Variable Mode Imager (Amersham Biosciences) and quantitated using ImageQuant 5.2. The IC<sub>50</sub> values were determined by plotting the logarithm of drug concentration versus percent inhibition to obtain concentration that produced 50% inhibition.

## Cell Culture

### Cell lines

- Human breast cancer cells: MDA-MB-435;
- Colon cancer cell: HT29 (p53 mutant); HCT116 p53<sup>+/+</sup> and HCT116 p53<sup>-/-</sup>;
- Human prostate cancer cells: hLN-CaP.

Cells were maintained as monolayer cultures in RPMI 1640 media supplemented with 10% fetal bovine serum (Gemini-Bioproducts, Woodland, CA) and 2 mmol/L L-Glutamine at 37°C in a humidified atmosphere of 5% CO<sub>2</sub>. To remove the adherent cells from the flask for passaging and counting, cells were washed with PBS without calcium or magnesium, incubated with a small volume of 0.25% trypsin-EDTA solution (Sigma-Aldrich, St. Louis, MO) for 5-10 minutes, and washed with culture medium and centrifuged. All experiments were performed using cells in exponential growth. Cells were routinely checked for mycoplasma contamination using a PCR-based assay.

### Drugs

A 10 mM stock solutions of all compounds were prepared in DMSO and stored at -20 °C. Further dilutions were freshly made in PBS or cell-culture media.

## **Cytotoxicity assays**

### **3-(4,5-Dimethylthiazol-2-yl)-2,5-diphenyltetrazoliumbromide (MTT) assay**

Cytotoxicity was assessed by a (MTT) assay. Cells were seeded in 96-well microtiter plates and allowed to attach. Cells were subsequently treated with a continuous exposure to the corresponding drug for 72 hours. A MTT solution (at a final concentration of 0.5 mg/mL) was added to each well and cells were incubated for 4 hours at 37°C. After removal of the medium, DMSO was added and the absorbance was read at 570 nm.

All assays were done in triplicate. The IC<sub>50</sub> was then determined for each drug from a plot of log (drug concentration) versus percentage of cell kill.

### **Colony formation assay**

Cells were plated in 6-well plates at a density of 100 cells/well and allowed to attach. Next day, serial dilutions of the corresponding compounds were added for 24 hours. After exposure, cells were washed in PBS and cultured in free media until colonies were formed (8 to 10 days). Cells were subsequently washed, fixed with a glutaraldehyde 1% solution for 30 min and stained with a solution of crystal violet (2%) for 30 minutes. After staining, cells were thoroughly washed with water. Colonies were imaged on the VersaDoc Imaging System (BioRad) and counted using the Quantity One quantitation software package (BioRad). The data reported represent the mean of a minimum of three independent experiments.

## **Cell Cycle Analysis**

Cell cycle perturbations were analyzed by propidium iodide DNA staining. Briefly, exponentially growing cells were treated with different doses of the drug for various times. At the end of each treatment time, cells were collected and washed with PBS after a gentle centrifugation at 200x g for 5 minutes. Cells were thoroughly resuspended in 0.5 mL of PBS and fixed in 70% ethanol for at least 2 hours at 4°C. Ethanol-suspended cells were then centrifuged at 200xg for 5 minutes and washed twice in PBS to remove residual ethanol. For cell cycle analysis, the pellets were suspended in 1 mL of PBS containing 0.02 mg/mL of propidium iodide, 0.5 mg/mL of DNase-free RNase A and 0.1% of Triton X-100 and incubated at 37°C for 30 minutes. Cell cycle profiles were obtained using a FACScan flow cytometer (Becton Dickinson, San Jose, CA) and data were analyzed by ModFit LT software (Verity Software House, Inc., Topsham, ME).

## **Apoptosis Assay**

To quantify drug-induced apoptosis, cells were stained with annexin V/propidium iodide and counted by flow cytometry. Briefly, after drug treatments (IC<sub>80</sub> for each drug for 72 hours), both floating and attached cells were combined and subjected to annexin V/propidium iodide staining using annexin V-FITC apoptosis detection kit (Oncogene Research Products, San Diego, CA) according to the protocol provided by the manufacturer. Untreated control cells (24–72 hours) were maintained in parallel to the drug-treated group. In cells undergoing apoptosis, annexin V binds to phosphatidylserine, which is translocated from the inner to the outer leaflet of the cytoplasmic membrane. Double staining is used to distinguish between viable, early apoptotic, and necrotic or late apoptotic cells.<sup>16</sup> The resulting fluorescence (FLH-1 channel for green fluorescence and FLH-2 channel for red fluorescence) was measured by flow cytometry using a FACScan flow cytometer (Becton Dickinson).

## **In vivo studies**

### **Animals**

50 female virgin athymic nude (*nu/nu*) mice (Charles River Laboratories, Wilmington, MA) were used for *in vivo* testing. The animals were fed *ad libitum* and kept in airconditioned rooms at  $20 \pm 2$  °C with a 12 hour light-dark period. Animal care and manipulation were in agreement with the University of Southern California (USC) institutional guidelines, which are in accordance with the Guidelines for the Care and Use of Laboratory Animals.

### **In vivo Xenograft Studies**

Human breast MDA-MB-435 cells in logarithmic phase growth from *in vitro* cell culture were inoculated s.c. in both flanks of athymic nude mice ( $2 \times 10^6$  cells/flank) under aseptic conditions. Tumor growth was assessed by biweekly measurement of tumor diameters with a Vernier caliper (length x width). Tumor weight was calculated according to the formula:

$$TW \text{ (mg)} = \text{tumor volume (mm}^3\text{)} = d^2 \times D/2$$

where *d* and *D* are the shortest and longest diameters, respectively. Tumors were allowed to grow to an average volume of 100 mm<sup>3</sup>. Animals were then randomly assigned to control and treatment groups, to receive control vehicle or compound **36** (0.3, 0.8 and 4 mg/Kg, dissolved in sesame oil) via i.p injections once a day for 5 days. Treatment of each animal was based on individual body weight. After 5-days treatment, the tumor volumes in each group were measured once a week for four weeks. Treated animals were checked daily for treatment toxicity/mortality. The percentage of tumor growth inhibition was calculated as  $T/C \% = 100 \times (\text{mean TW of treated group}) / (\text{mean TW of control group})$ .

## REFERENCES

- [1] Coffin, J.; Haase, A.; Levy, J. A.; Montagnier, L.; Oroszlan, S.; Teich, N.; Temin, H.; Toyoshima, K.; Varmus, H.; Vogt, P.; et al. What to call the AIDS virus? *Nature*, 1986, 321, 10.
- [2] UNAIDS. Report on the global AIDS epidemic 2006 [www.unaids.org](http://www.unaids.org), 2006.
- [3] Joint United Nations Programme on HIV/AIDS (2006).
- [4] Louie, M.; Markowitz, M. Goals and milestones during treatment of HIV-1 infection with antiretroviral therapy: a pathogenesis-based perspective. *Antiviral Res*, 2002, 55, 15-25.
- [5] Yerly, S.; Kaiser, L.; Race, E.; Bru, J. P.; Clavel, F.; Perrin, L. Transmission of antiretroviral-drug-resistant HIV-1 variants. *Lancet*, 1999, 354, 729-33.
- [6] LaFemina, R. L.; Schneider, C. L.; Robbins, H. L.; Callahan, P. L.; LeGrow, K.; Roth, E.; Schleif, W. A.; Emini, E. A. Requirement of active human immunodeficiency virus type 1 integrase enzyme for productive infection of human T-lymphoid cells. *J Virol*, 1992, 66, 7414-9.
- [7] Buchbinder, S. P.; Katz, M. H.; Hessol, N. A.; O'Malley, P. M.; Holmberg, S. D. Long-term HIV-1 infection without immunologic progression. *Aids*, 1994, 8, 1123-8.
- [8] Nielsen, M. H.; Pedersen, F. S.; Kjems, J. Molecular strategies to inhibit HIV-1 replication. *Retrovirology*, 2005, 2, 10.
- [9] Dragic, T.; Litwin, V.; Allaway, G. P.; Martin, S. R.; Huang, Y.; Nagashima, K. A.; Cayanan, C.; Maddon, P. J.; Koup, R. A.; Moore, J. P.; Paxton, W. A. HIV-1 entry into CD4+ cells is mediated by the chemokine receptor CC-CKR-5. *Nature*, 1996, 381, 667-73.
- [10] Deng, H.; Liu, R.; Ellmeier, W.; Choe, S.; Unutmaz, D.; Burkhart, M.; Di Marzio, P.; Marmon, S.; Sutton, R. E.; Hill, C. M.; Davis, C. B.; Peiper, S. C.; Schall, T. J.; Littman, D. R.; Landau, N. R. Identification of a major co-receptor for primary isolates of HIV-1. *Nature*, 1996, 381, 661-6.
- [11] Feng, Y.; Broder, C. C.; Kennedy, P. E.; Berger, E. A. HIV-1 entry cofactor: functional cDNA cloning of a seven-transmembrane, G protein-coupled receptor. *Science*, 1996, 272, 872-7.
- [12] Cocchi, F.; DeVico, A. L.; Garzino-Demo, A.; Arya, S. K.; Gallo, R. C.; Lusso, P. Identification of RANTES, MIP-1 alpha, and MIP-1 beta as the major HIV-suppressive factors produced by CD8+ T cells. *Science*, 1995, 270, 1811-5.
- [13] Bridger, G.; Skerlj, R.; Kaller, A.; Harwig, C.; Bogucki, D.; Wilson, T. R.; Crawford, J.; McEachern, E. J.; Atsma, B.; Nan, S.; Zhou, Y. S., D.; Smith, C. D.; Di Fluri, R. M. WO0222599, 2002.
- [14] Leonard, J. T.; Roy, K. The HIV entry inhibitors revisited. *Curr Med Chem*, 2006, 13, 911-34.
- [15] Seibert, C.; Sakmar, T. P. Small-molecule antagonists of CCR5 and CXCR4: a promising new class of anti-HIV-1 drugs. *Curr Pharm Des*, 2004, 10, 2041-62.
- [16] Cervia, J. S.; Smith, M. A. Enfuvirtide (T-20): a novel human immunodeficiency virus type 1 fusion inhibitor. *Clin Infect Dis*, 2003, 37, 1102-6.

- [17] Zheng, Y. H.; Lovsin, N.; Peterlin, B. M. Newly identified host factors modulate HIV replication. *Immunol Lett*, 2005, 97, 225-34.
- [18] Hiscott, J.; Kwon, H.; Genin, P. Hostile takeovers: viral appropriation of the NF-kappaB pathway. *J Clin Invest*, 2001, 107, 143-51.
- [19] Pollard, V. W.; Malim, M. H. The HIV-1 Rev protein. *Annu Rev Microbiol*, 1998, 52, 491-532.
- [20] Gelderblom, H. R.; Ozel, M.; Pauli, G. Morphogenesis and morphology of HIV. Structure-function relations. *Arch Virol*, 1989, 106, 1-13.
- [21] Daniel, R.; Katz, R. A.; Skalka, A. M. A role for DNA-PK in retroviral DNA integration. *Science*, 1999, 284, 644-7.
- [22] Daniel, R.; Katz, R. A.; Merkel, G.; Hittle, J. C.; Yen, T. J.; Skalka, A. M. Wortmannin potentiates integrase-mediated killing of lymphocytes and reduces the efficiency of stable transduction by retroviruses. *Mol Cell Biol*, 2001, 21, 1164-72.
- [23] De Clercq, E.; Schols, D. Inhibition of HIV infection by CXCR4 and CCR5 chemokine receptor antagonists. *Antivir Chem Chemother*, 2001, 12 Suppl 1, 19-31.
- [24] Andrade, M. D.; Skalka, A. M. Retroviral integrase, putting the pieces together. *J Biol Chem*, 1996, 271, 19633-6.
- [25] Burke, C. J.; Sanyal, G.; Bruner, M. W.; Ryan, J. A.; LaFemina, R. L.; Robbins, H. L.; Zeff, A. S.; Middaugh, C. R.; Cordingley, M. G. Structural implications of spectroscopic characterization of a putative zinc finger peptide from HIV-1 integrase. *J Biol Chem*, 1992, 267, 9639-44.
- [26] Cai, M.; Zheng, R.; Caffrey, M.; Craigie, R.; Clore, G. M.; Gronenborn, A. M. Solution structure of the N-terminal zinc binding domain of HIV-1 integrase. *Nat Struct Biol*, 1997, 4, 567-77.
- [27] Pluymers, W.; De Clercq, E.; Debyser, Z. HIV-1 integration as a target for antiretroviral therapy: a review. *Curr Drug Targets Infect Disord*, 2001, 1, 133-49.
- [28] Craigie, R. HIV integrase, a brief overview from chemistry to therapeutics. *J Biol Chem*, 2001, 276, 23213-6.
- [29] Asante-Appiah, E.; Skalka, A. M. Molecular mechanisms in retrovirus DNA integration. *Antiviral Res*, 1997, 36, 139-56.
- [30] Yi, J.; Arthur, J. W.; Dunbrack, R. L., Jr.; Skalka, A. M. An inhibitory monoclonal antibody binds at the turn of the helix-turn-helix motif in the N-terminal domain of HIV-1 integrase. *J Biol Chem*, 2000, 275, 38739-48.
- [31] Cannon, P. M.; Byles, E. D.; Kingsman, S. M.; Kingsman, A. J. Conserved sequences in the carboxyl terminus of integrase that are essential for human immunodeficiency virus type 1 replication. *J Virol*, 1996, 70, 651-7.
- [32] Lodi, P. J.; Ernst, J. A.; Kuszewski, J.; Hickman, A. B.; Engelman, A.; Craigie, R.; Clore, G. M.; Gronenborn, A. M. Solution structure of the DNA binding domain of HIV-1 integrase. *Biochemistry*, 1995, 34, 9826-33.
- [33] Dayam, R.; Deng, J.; Neamati, N. HIV-1 integrase inhibitors: 2003-2004 update. *Med Res Rev*, 2006, 26, 271-309.



- [34] Adesokan, A. A.; Roberts, V. A.; Lee, K. W.; Lins, R. D.; Briggs, J. M. Prediction of HIV-1 integrase/viral DNA interactions in the catalytic domain by fast molecular docking. *J Med Chem*, 2004, 47, 821-8.
- [35] Dayam, R.; Sanchez, T.; Neamati, N. Diketo acid pharmacophore. 2. Discovery of structurally diverse inhibitors of HIV-1 integrase. *J Med Chem*, 2005, 48, 8009-15.
- [36] Koehn, F. E.; Carter, G. T. The evolving role of natural products in drug discovery. *Nat Rev Drug Discov*, 2005, 4, 206-20.
- [37] Singh, S. B.; Felock, P.; Hazuda, D. J. Chemical and enzymatic modifications of integrase and HIV-1 integrase inhibitory activity. *Bioorg Med Chem Lett*, 2000, 10, 235-8.
- [38] Singh, S. B.; Zink, D. L.; Heimbach, B.; Genilloud, O.; Teran, A.; Silverman, K. C.; Lingham, R. B.; Felock, P.; Hazuda, D. J. Structure, stereochemistry, and biological activity of integramycin, a novel hexacyclic natural product produced by *Actinoplanes* sp. that inhibits HIV-1 integrase. *Org Lett*, 2002, 4, 1123-6.
- [39] Mazumder, A.; Neamati, N.; Sommadossi, J. P.; Gosselin, G.; Schinazi, R. F.; Imbach, J. L.; Pommier, Y. Effects of nucleotide analogues on human immunodeficiency virus type 1 integrase. *Mol Pharmacol*, 1996, 49, 621-8.
- [40] Mazumder, A.; Uchida, H.; Neamati, N.; Sunder, S.; Jaworska-Maslanka, M.; Wickstrom, E.; Zeng, F.; Jones, R. A.; Mandes, R. F.; Chenault, H. K.; Pommier, Y. Probing interactions between viral DNA and human immunodeficiency virus type 1 integrase using dinucleotides. *Mol Pharmacol*, 1997, 51, 567-75.
- [41] Este, J. A.; Cabrera, C.; Schols, D.; Cherepanov, P.; Gutierrez, A.; Witvrouw, M.; Pannecouque, C.; Debyser, Z.; Rando, R. F.; Clotet, B.; Desmyter, J.; De Clercq, E. Human immunodeficiency virus glycoprotein gp120 as the primary target for the antiviral action of AR177 (Zintevir). *Mol Pharmacol*, 1998, 53, 340-5.
- [42] Carteau, S.; Mouscadet, J. F.; Goulaouic, H.; Subra, F.; Auclair, C. Effect of topoisomerase inhibitors on the in vitro HIV DNA integration reaction. *Biochem Biophys Res Commun*, 1993, 192, 1409-14.
- [43] Wang, Y. X.; Neamati, N.; Jacob, J.; Palmer, I.; Stahl, S. J.; Kaufman, J. D.; Huang, P. L.; Huang, P. L.; Winslow, H. E.; Pommier, Y.; Wingfield, P. T.; Lee-Huang, S.; Bax, A.; Torchia, D. A. Solution structure of anti-HIV-1 and anti-tumor protein MAP30: structural insights into its multiple functions. *Cell*, 1999, 99, 433-42.
- [44] Mazumder, A.; Wang, S.; Neamati, N.; Nicklaus, M.; Sunder, S.; Chen, J.; Milne, G. W.; Rice, W. G.; Burke, T. R., Jr.; Pommier, Y. Antiretroviral agents as inhibitors of both human immunodeficiency virus type 1 integrase and protease. *J Med Chem*, 1996, 39, 2472-81.
- [45] Eich, E.; Pertz, H.; Kaloga, M.; Schulz, J.; Fesen, M. R.; Mazumder, A.; Pommier, Y. (-)-Arctigenin as a lead structure for inhibitors of human immunodeficiency virus type-1 integrase. *J Med Chem*, 1996, 39, 86-95.
- [46] Zhuang, L.; Wai, J. S.; Embrey, M. W.; Fisher, T. E.; Egbertson, M. S.; Payne, L. S.; Guare, J. P., Jr.; Vacca, J. P.; Hazuda, D. J.; Felock, P. J.; Wolfe, A. L.; Stillmock, K. A.; Witmer, M. V.; Moyer, G.; Schleif, W. A.; Gabryelski, L. J.; Leonard, Y. M.; Lynch, J. J., Jr.; Michelson, S. R.; Young, S. D. Design and synthesis of 8-hydroxy-[1,6]naphthyridines as novel inhibitors of HIV-1 integrase in vitro and in infected cells. *J Med Chem*, 2003, 46, 453-6.

- [47] Zhang, X.; Pais, G. C.; Svarovskaia, E. S.; Marchand, C.; Johnson, A. A.; Karki, R. G.; Nicklaus, M. C.; Pathak, V. K.; Pommier, Y.; Burke, T. R. Azido-containing aryl beta-diketo acid HIV-1 integrase inhibitors. *Bioorg Med Chem Lett*, 2003, 13, 1215-9.
- [48] Wai, J. S.; Egbertson, M. S.; Payne, L. S.; Fisher, T. E.; Embrey, M. W.; Tran, L. O.; Melamed, J. Y.; Langford, H. M.; Guare, J. P., Jr.; Zhuang, L.; Grey, V. E.; Vacca, J. P.; Holloway, M. K.; Naylor-Olsen, A. M.; Hazuda, D. J.; Felock, P. J.; Wolfe, A. L.; Stillmock, K. A.; Schleif, W. A.; Gabryelski, L. J.; Young, S. D. 4-Aryl-2,4-dioxobutanoic acid inhibitors of HIV-1 integrase and viral replication in cells. *J Med Chem*, 2000, 43, 4923-6.
- [49] Jones, K. S.; Coleman, J.; Merkel, G. W.; Laue, T. M.; Skalka, A. M. Retroviral integrase functions as a multimer and can turn over catalytically. *J Biol Chem*, 1992, 267, 16037-40.
- [50] Hong, H.; Neamati, N.; Wang, S.; Nicklaus, M. C.; Mazumder, A.; Zhao, H.; Burke, T. R., Jr.; Pommier, Y.; Milne, G. W. Discovery of HIV-1 integrase inhibitors by pharmacophore searching. *J Med Chem*, 1997, 40, 930-6.
- [51] Neamati, N.; Hong, H.; Mazumder, A.; Wang, S.; Sunder, S.; Nicklaus, M. C.; Milne, G. W.; Proksa, B.; Pommier, Y. Depsides and depsidones as inhibitors of HIV-1 integrase: discovery of novel inhibitors through 3D database searching. *J Med Chem*, 1997, 40, 942-51.
- [52] Nicklaus, M. C.; Neamati, N.; Hong, H.; Mazumder, A.; Sunder, S.; Chen, J.; Milne, G. W.; Pommier, Y. HIV-1 integrase pharmacophore: discovery of inhibitors through three-dimensional database searching. *J Med Chem*, 1997, 40, 920-9.
- [53] Neamati, N.; Hong, H.; Sunder, S.; Milne, G. W.; Pommier, Y. Potent inhibitors of human immunodeficiency virus type 1 integrase: identification of a novel four-point pharmacophore and tetracyclines as novel inhibitors. *Mol Pharmacol*, 1997, 52, 1041-55.
- [54] Deng, J.; Sanchez, T.; Neamati, N.; Briggs, J. M. Dynamic pharmacophore model optimization: identification of novel HIV-1 integrase inhibitors. *J Med Chem*, 2006, 49, 1684-92.
- [55] Neamati, N.; Turpin, J. A.; Winslow, H. E.; Christensen, J. L.; Williamson, K.; Orr, A.; Rice, W. G.; Pommier, Y.; Garofalo, A.; Brizzi, A.; Campiani, G.; Fiorini, I.; Nacci, V. Thiazolothiazepine inhibitors of HIV-1 integrase. *J Med Chem*, 1999, 42, 3334-41.
- [56] Aiello, F.; Brizzi, A.; Garofalo, A.; Grande, F.; Ragno, G.; Dayam, R.; Neamati, N. Synthesis of novel thiazolothiazepine based HIV-1 integrase inhibitors. *Bioorg Med Chem*, 2004, 12, 4459-66.
- [57] Wolfe, S.; Militello, G.; Ferrari, C.; Hasan, S. K.; Lee, S. L. Conversion of amino hydroxyacids to oxazolidine-4-carboxylic acids, oxazolidine-5-carboxylic acids and tetrahydrooxazine-4-carboxylic acids. *Tetrahedron Lett.*, 1979, 20, 3913-3916.
- [58] Bergeron, R. J.; Wiegand, J.; Wollenweber, M.; McManis, J. S.; Algee, S. E.; Ratliff-Thompson, K. Synthesis and biological evaluation of naphthyl-desferrithiocin iron chelators. *J Med Chem*, 1996, 39, 1575-81.
- [59] Magnus, P.; Kreisberg, J. D. Synthesis of benzofuranones related to diazonamide via an intramolecular Pummerer reaction. *Tetrahedron Lett.*, 1999, 40, 451-454.
- [60] Saigo, K.; Usui, M.; Kikuchi, K.; Shimada, E.; Mukaiyama, T. New method for the preparation of carboxylic esters. *Bull. Chem. Soc. Jpn.*, 1977, 50, 1863-1866.
- [61] Sun, Y.; Lu, G.; Tam, J. P. A thioester ligation approach to amphipathic bicyclic peptide library. *Org Lett*, 2001, 3, 1681-4.

- [62] T. Rückle; P. de Lavallaz; M. Keller; P. Dumy; Mutter., M. *Tetrahedron*, 1999, 55, 11281-11288.
- [63] B. Castro; G. Evin; C.Selve; Seyer, R. *Synthesis.*, 1977, 6, 413.
- [64] Long, Y. Q.; Jiang, X. H.; Dayam, R.; Sanchez, T.; Shoemaker, R.; Sei, S.; Neamati, N. Rational design and synthesis of novel dimeric diketoacid-containing inhibitors of HIV-1 integrase: implication for binding to two metal ions on the active site of integrase. *J Med Chem*, 2004, 47, 2561-73.
- [65] Jemal, A.; Ward, E.; Hao, Y.; Thun, M. Trends in the leading causes of death in the United States, 1970-2002. *Jama*, 2005, 294, 1255-9.
- [66] Jemal, A.; Murray, T.; Ward, E.; Samuels, A.; Tiwari, R. C.; Ghafoor, A.; Feuer, E. J.; Thun, M. J. Cancer statistics, 2005. *CA Cancer J Clin*, 2005, 55, 10-30.
- [67] Neamati, N.; Barchi, J. J., Jr. New paradigms in drug design and discovery. *Curr Top Med Chem*, 2002, 2, 211-27.
- [68] Cattley, R. C.; Radinsky, R. R. Cancer therapeutics: understanding the mechanism of action. *Toxicol Pathol*, 2004, 32 Suppl 1, 116-21.
- [69] Dean, N. M. Functional genomics and target validation approaches using antisense oligonucleotide technology. *Curr Opin Biotechnol*, 2001, 12, 622-5.
- [70] Taylor, D. L.; Woo, E. S.; Giuliano, K. A. Real-time molecular and cellular analysis: the new frontier of drug discovery. *Curr Opin Biotechnol*, 2001, 12, 75-81.
- [71] Hunt, D. F. Personal commentary on proteomics. *J Proteome Res*, 2002, 1, 15-9.
- [72] Patel, D.; Gordon, E. Applications of small-molecule combinatorial chemistry to drug discovery. *Drug Discovery Today*, 1996, 1, 134-144.
- [73] Lipinski, C. A. Chris Lipinski discusses life and chemistry after the Rule of Five. *Drug Discov Today*, 2003, 8, 12-6.
- [74] Testa, B.; Carrupt, P. A.; Gaillard, P.; Billois, F.; Weber, P. Lipophilicity in molecular modeling. *Pharm Res*, 1996, 13, 335-43.
- [75] Plasencia, C.; Dayam, R.; Wang, Q.; Pinski, J.; Burke, T. R., Jr.; Quinn, D. I.; Neamati, N. Discovery and preclinical evaluation of a novel class of small-molecule compounds in hormone-dependent and -independent cancer cell lines. *Mol Cancer Ther*, 2005, 4, 1105-13.
- [76] Rice, P.; Craigie, R.; Davies, D. Retroviral integrases and their cousins. *Current Opinion in Structural Biology*, 1996, 6, 76-83.
- [77] Neamati, N.; Marchand, C.; Pommier, Y. HIV-1 integrase inhibitors: past, present, and future. *Adv Pharmacol*, 2000, 49, 147-65.
- [78] Kim, D. R.; Dai, Y.; Mundy, C. L.; Yang, W.; Oettinger, M. A. Mutations of acidic residues in RAG1 define the active site of the V(D)J recombinase. *Genes Dev*, 1999, 13, 3070-80.
- [79] Landree, M. A.; Wibbenmeyer, J. A.; Roth, D. B. Mutational analysis of RAG1 and RAG2 identifies three catalytic amino acids in RAG1 critical for both cleavage steps of V(D)J recombination. *Genes Dev*, 1999, 13, 3059-69.

- [80] Fesen, M. R.; Kohn, K. W.; Leteurtre, F.; Pommier, Y. Inhibitors of human immunodeficiency virus integrase. *Proc Natl Acad Sci U S A*, 1993, 90, 2399-403.
- [81] Melek, M.; Jones, J. M.; O'Dea, M. H.; Pais, G.; Burke, T. R., Jr.; Pommier, Y.; Neamati, N.; Gellert, M. Effect of HIV integrase inhibitors on the RAG1/2 recombinase. *Proc Natl Acad Sci U S A*, 2002, 99, 134-7.
- [82] Neamati, N.; Hong, H.; Owen, J. M.; Sunder, S.; Winslow, H. E.; Christensen, J. L.; Zhao, H.; Burke, T. R., Jr.; Milne, G. W.; Pommier, Y. Salicylhydrazine-containing inhibitors of HIV-1 integrase: implication for a selective chelation in the integrase active site. *J Med Chem*, 1998, 41, 3202-9.
- [83] Neamati, N.; Lin, Z.; Karki, R. G.; Orr, A.; Cowansage, K.; Strumberg, D.; Pais, G. C.; Voigt, J. H.; Nicklaus, M. C.; Winslow, H. E.; Zhao, H.; Turpin, J. A.; Yi, J.; Skalka, A. M.; Burke, T. R., Jr.; Pommier, Y. Metal-dependent inhibition of HIV-1 integrase. *J Med Chem*, 2002, 45, 5661-70.
- [84] Campiani, G.; Aiello, F.; Fabbrini, M.; Morelli, E.; Ramunno, A.; Armaroli, S.; Nacci, V.; Garofalo, A.; Greco, G.; Novellino, E.; Maga, G.; Spadari, S.; Bergamini, A.; Ventura, L.; Bongiovanni, B.; Capozzi, M.; Bolacchi, F.; Marini, S.; Coletta, M.; Guiso, G.; Caccia, S. Quinoxalinylolethylpyridylthioureas (QXPTs) as potent non-nucleoside HIV-1 reverse transcriptase (RT) inhibitors. Further SAR studies and identification of a novel orally bioavailable hydrazine-based antiviral agent. *J Med Chem*, 2001, 44, 305-15.
- [85] Plasencia C; Grande F; Oshima T; Sanchez T; Aiello F; Garofalo A; N., N. Discovery of SC144, a Novel Small-Molecule Compound with Broad Spectrum of Anticancer Activity. *J. Med. Chem*, under review.
- [86] Fand, T. I.; Spoerri, P. E. preparation and thermal decomposition of pyrazinoic benzenesulphonhydrazide. *J Am Chem Soc*, 1952, 74, 1345.
- [87] Grande, F.; Aiello, F.; Grazia, O. D.; Brizzi, A.; Garofalo, A.; Neamati, N. Synthesis and antitumor activities of a series of novel quinoxalinhydrazides. *Bioorg Med Chem*, 2006.
- [88] Mosmann, T. Rapid colorimetric assay for cellular growth and survival: application to proliferation and cytotoxicity assays. *J Immunol Methods*, 1983, 65, 55-63.
- [89] Ferrari, M.; Fornasiero, M. C.; Isetta, A. M. MTT colorimetric assay for testing macrophage cytotoxic activity in vitro. *J Immunol Methods*, 1990, 131, 165-72.
- [90] Munshi, A.; Hobbs, M.; Meyn, R. E. Clonogenic cell survival assay. *Methods Mol Med*, 2005, 110, 21-8.